The human archaeome and its implications for human health

Submitted by

Rokhsareh Mohammadzadeh

for the Academic Degree of

Doctor of Philosophy

(PhD)

at the

Medical University of Graz

Diagnostics and Research Institute of Hygiene, Microbiology, and Environmental Medicine

under the Supervision of

Prof. Dr. Christine Moissl-Eichinger

2026

Declaration

“I hereby confirm that the present diploma thesis is the result of my own independent scholarly work. I also confirm that in all cases, where material from the work of others (in books, articles, essays, dissertations, and on the internet) is acknowledged, quotations and paraphrases are clearly indicated. No material other than that cited in the reference list has been used. I have read and understood the Medical University’s regulations and procedures concerning plagiarism.

Furthermore, I acknowledge the use of the AI language model ChatGPT (https://chatgpt.com/, OpenAI, GPT-5) as a writing and editing support tool during the preparation of this dissertation. The AI was provided with the prompt: “Optimize the following paragraphs of a dissertation according to clarity and readability”, after which sections of text were submitted for optimization. All AI- generated output was critically reviewed, assessed for accuracy, and rewritten or adapted where necessary. The scientific content, data interpretation, and conclusions presented in this work are entirely my own, and the AI was not used to generate, alter, or fabricate experimental results or references.”

Rokhsareh Mohammadzadeh

Graz, 28.04.2026

Disclosures

Parts of the introduction, materials and methods, results and discussion are already published in and contain the verbatim text of:

Rokhsareh Mohammadzadeh, et al. (2022). Archaeal key-residents within the human microbiome: characteristics, interactions and involvement in health and disease. *Current Opinion in Microbiology.* https://doi.org/10.1016/j.mib.2022.102146 (1).

Mohammadzadeh, et al. (2025a). Age-related dynamics of predominant methanogenic archaea in the human gut microbiome. *BMC Microbiology*. https://doi.org/10.1186/s12866-025-03921-9 (2).

Mohammadzadeh, et al. (2026). Cross-domain metabolic interactions link Methanobrevibacter smithii to colorectal cancer microbial ecosystems. *Nature Communications.* https://doi.org/10.1038/s41467-026-69711-7 (3).

- Permission for re-use of figures and text from these publications has been given with the Open-Access-Publication Agreements of the respective publishing groups (Creative Commons Attribution license CC-BY 4.0).

Disclosures

All co-authors gave their approval to reuse the published manuscript within this thesis:

Chapter 1: **Archaeal key-residents within the human microbiome: characteristics, interactions and involvement in health and disease (1).**

Rokhsareh Mohammadzadeh[1], Alexander Mahnert[1], Stefanie Duller[1], Christine Moissl-Eichinger[1,2].*

[1]Diagnostic and Research Institute of Hygiene, Microbiology and Environmental Medicine, Medical University of Graz, Neue Stiftingtalstraße 6, 8010 Graz, Austria

[2]BioTechMed, 8010 Graz, Austria

*Corresponding author

- **Rokhsareh Mohammadzadeh** wrote the manuscript.
- **Alexander Mahnert** provided critical discussion and corrected the final draft.
- **Stefanie Duller** provided the electron microscopy pictures.
- **Christine Moissl-Eichinger** supervised the literature research and wrote parts of the manuscripts.

Chapter 2: **Age-related dynamics of predominant methanogenic archaea in the human gut microbiome (2).**

Rokhsareh Mohammadzadeh[1], Alexander Mahnert[1], Tejus Shinde[1], Christina Kumpitsch[1], Viktoria Weinberger[1], Helena Schmidt [2], Christine Moissl-Eichinger[1,3]

[1] Diagnostic and Research Institute of Hygiene, Microbiology and Environmental Medicine, Medical University of Graz, Neue Stiftingtalstraße 6, 8010 Graz, Austria

[2]Division of Molecular Biology and Biochemistry, Medical University of Graz, Graz, Austria

[3]BioTechMed, 8010 Graz, Austria

- **Rokhsareh Mohammadzadeh** did the DNA extraction and data analysis, produced most of the figures and wrote the manuscript.
- **Alexander Mahnert** co-designed the study.
- **Tejus Shinde** supported data analysis.
- **Christina Kumpitsch** performed sampling.
- **Viktoria Weinberger** contributed to figure preparations.
- **Helena Schmidt** performed sampling.
- **Christine Moissl-Eichinger** supervised all activities, and wrote parts of the manuscript.

Chapter 3: **Cross-domain metabolic interactions link *Methanobrevibacter smithii* to colorectal cancer microbial ecosystems (3)**.

Rokhsareh Mohammadzadeh[1], Alexander Mahnert[1], Tamara Zurabischvili[1], Lisa Wink[1], Christina Kumpitsch[1], Hansjoerg Habisch[2], Jannik Sprengel[3,4], Klara Filek[1], Polona Mertelj[1], Dominique Pernitsch[5], Kerstin Hingerl[5], Marija Durdevic[6,7], Gregor Gorkiewicz[6,12], Christian Diener[1], Alexander Loy[8], Dagmar Kolb[5], Christoph Trautwein[3,4,9,10,11], Tobias Madl[2, 12], Christine Moissl-Eichinger[1,12]*

[1] Diagnostic and Research Institute of Hygiene, Microbiology and Environmental Medicine, Medical University of Graz, 8010 Graz, Austria
[2] Otto Loewi Research Center, Medicinal Chemistry, Medical University of Graz, Graz, Austria
[3] Core Facility Metabolomics, Medical Faculty University of Tübingen, Tübingen, Germany
[4] M3 Research Center for Malignome, Metabolome & Microbiome, Medical Faculty University of Tübingen, Tübingen, Germany
[5] Core Facility Ultrastructure Analysis, Medical University of Graz, Graz, Austria
[6] Institute of Pathology, Medical University of Graz, Graz, Austria
[7] Core Facility Computational Bioanalytics, Center for Medical Research, Medical University of Graz, Graz, Austria
[8] Division of Microbial Ecology, Centre for Microbiology and Environmental Systems Science, University of Vienna, Vienna, Austria
[9] Department of Preclinical Imaging and Radiopharmacy, Werner Siemens Imaging Center, University Hospital Tübingen, Tübingen, Germany
[10] Cluster of Excellence CMFI (EXC 2124) "Controlling Microbes to Fight Infections", Eberhard Karls University of Tübingen, Tübingen, Germany
[11] Cluster of Excellence iFIT (EXC 2180) "Image Guided and Functionally Instructed Tumor Therapies", University of Tübingen, Tübingen, Germany
[12] BioTechMed, Graz, Austria

- **Rokhsareh Mohammadzadeh** designed the study, collected data, performed bioinformatics, data analysis, plotting, and drafted the manuscript.
- **Alexander Mahnert** co-designed the study.
- **Tamara Zurabischvili** and **Lisa Wink** performed sample cultivation.
- **Christina Kumpitsch** performed qPCR.
- **Hansjoerg Habisch** and **Tobias Madl** performed NMR metabolomics.
- **Jannik Sprengel** and **Christoph Trautwein** performed MS metabolomics.
- **Klara Filek** contributed to one figure preparation in Mohammadzadeh *et al.,* 2025b.
- **Polona Mertelj** performed *E. coli* isolation and confirmation.
- **Dominique Pernitsch**, **Kerstin Hingerl**, and **Dagmar Kolb** performed SEM.
- **Marija Durdevic** performed Machine Learning.
- **Christian Diener** helped with data analysis.

- **Gregor Gorkiewicz** and **Alexander Loy** assisted with sample preparation.
- **Christine Moissl-Eichinger** provided critical discussions, and valuable help regarding all methods, revised the manuscript, and helped in the development of the experimental design.

Rokhsareh Mohammadzadeh was involved in the following publications during her PhD time, which were not directly related to this thesis:

- Torben Kühnast, Christina Kumpitsch, Rokhsareh Mohammadzadeh, Thomas Weichhart, Christine Moissl-Eichinger, Holger Heine (2024). **Exploring the human archaeome: its relevance for health and disease, and its complex interplay with the human immune system.** https://doi.org/10.1111/febs.17123.

- Stefanie Duller, Simone Vrbancic, Łukasz Szydłowski, Alexander Mahnert, Marcus Blohs, Michael Predl, Christina Kumpitsch, Verena Zrim, Christoph Högenauer, Tomasz Kosciolek, Ruth A Schmitz, Anna Eberhard, Melanie Dragovan, Laura Schmidberger, Tamara Zurabischvili, Viktoria Weinberger, Adrian Mathias Moser, Dagmar Kolb, Dominique Pernitsch, Rokhsareh Mohammadzadeh, Torben Kühnast, Thomas Rattei, Christine Moissl-Eichinger (2024). **Targeted isolation of Methanobrevibacter strains from fecal samples expands the cultivated human archaeome.** *Nature Communications.* https://doi.org/10.1038/s41467-024-52037-7.

- Charlotte J Neumann, Rokhsareh Mohammadzadeh, Pei Yee Woh, Tanja Kobal, Manuela-Raluca Pausan, Tejus Shinde, Victoria Haid, Polona Mertelj, Eva-Christine Weiss, Vassiliki Kolovetsiou-Kreiner, Alexander Mahnert, Christina Kumpitsch, Evelyn Jantscher-Krenn, Christine Moissl-Eichinger (2025). **First-year dynamics of the anaerobic microbiome and archaeome in infants' oral and gastrointestinal systems**. *mSystems*. https://doi.org/10.1128/msystems.01071-24.

- Viktoria Weinberger, Rokhsareh Mohammadzadeh, Marcus Blohs, Kerstin Kalt, Alexander Mahnert, Sarah Moser, Marina Cecovini, Polona Mertelj, Tamara Zurabishvili, Bhawna Arora, Jacqueline Wolf, Tejus Shinde, Tobias Madl, Hansjörg Habisch, Dagmar Kolb, Dominique Pernitsch, Kerstin Hingerl, William Metcalf, Christine Moissl-Eichinger (2025). Expanding the cultivable human archaeome: **Methanobrevibacter intestini sp. nov. and strain Methanobrevibacter smithii 'GRAZ-2' from human faeces**. *International Journal of Systematic and Evolutionary Microbiology*. https://doi.org/10.1099/ijsem.0.0067.

- Pei Yee Woh, Yehao Chen, Christina Kumpitsch, Rokhsareh Mohammadzadeh, Laura Schmidt, Christine Moissl-Eichinger (2025). **Reevaluation of the gastrointestinal methanogenic archaeome in multiple sclerosis and its association with treatment**. *Microbiology spectrum*. https://doi.org/10.1128/spectrum.02183-24.

- Viktoria Weinberger, Barbara Darnhofer, Himadri B Thapa, Polona Mertelj, Régis Stentz, Emily Jones, Gerlinde Grabmann, Rokhsareh Mohammadzadeh, Tejus Shinde, Christina Karner, Jennifer Ober, Rokas Juodeikis, Dominique Pernitsch, Kerstin Hingerl, Tamara Zurabishvili, Christina Kumpitsch, Torben Kuehnast, Beate Rinner, Heimo Strohmaier, Dagmar Kolb, Kathryn Gotts, Thomas Weichhart, Thomas Köcher, Harald Köfeler, Simon R Carding, Stefan Schild, Christine Moissl-Eichinger. (2025). **Proteomic and metabolomic profiling of extracellular vesicles produced by human gut archaea**. *Nature Communications*. https://doi.org/10.1038/s41467-025-60271-w.

- Tejus Shinde, Christina Kumpitsch, Yancong Zhang, Eric A. Franzosa, Rokhsareh Mohammadzadeh, Viktoria Weinberger, Tomas Mikal Eagan, Curtis Huttenhower, Vasile Foris, Christine Moissl-Eichinger (2025). **Pan-microbiome analysis along the human respiratory axis reveals an ecological continuum in health and collapse in disease**. *bioRxiv*. https://doi.org/10.1101/2025.09.04.674.

Quote

“Never was my heart denied the quest to know,

Few were the secrets left I did not probe.

Seventy-two years I thought, both night and day

At last, I learned: nothing is known, anyway.”

Omar Khayyam

Acknowledgments

First and foremost, I would like to express my deepest and most sincere gratitude to my supervisor, **Christine Moissl-Eichinger**. You were not only a PhD supervisor to me, but also a guide through life. You created a healthy and supportive working environment where I felt safe to grow, to make mistakes, and to learn from them. You trusted me, gave me independence, and supported me in moments when I needed it most. You truly made this PhD journey possible. I am deeply and sincerely grateful for everything.

Next, I would like to thank my PhD buddies and my sanity anchors, **Viktoria Weinberger** and **Tejus Shinde** who made this journey not only possible but meaningful! I am so lucky to have had you two by my side! We survived and grew (also age-wise :D) through this PhD together. We had our strategic "Fita" moments, and we had the moments where we just kept going anyway. Now… it is time for a tattoo!!!

Viktoria, you helped me with settling into life here, and you were always so selfless and kind. Throughout this challenging yet beautiful PhD journey, you were my sunshine, helping me overcome both academic and personal challenges.

Tejus, thank you for reminding me that a PhD is not just about working, but also about spending time with peers, taking breaks and caring for my health. Thank you for sharing your knowledge with me, both scientific and beyond.

I would also like to thank **Charlotte Neumann**. Your kindness always touched my heart. Thank you to **Alexander Mahnert** for all your ideas throughout my projects. I am truly grateful. A big thank you to **Christina Kumpitsch**, my patient teacher at the beginning of my PhD.

Thank you to **Lisa Wink**, who guided me in the beginning and showed me how things work at MedUni and in the lab. Special thanks go to **Tamara Zurabishvili** and **Polona Mertelj**, who were a constant source of support in the lab.

Thank you to **Klara Filek**. You inspired me in so many different aspects of life. Thanks to **Marcus Blohs** for showing me how things work at MedUni at the beginning.

Thanks to **Bhawna Arora**, whose smile always made everything brighter, and to **Eliska Sedlackova**, who constantly brought us together in her home in different ways. Thanks to **Gal Mlaker** and **Luna Groon**, who were patient with me during the last months of my PhD.

And thank you to every current or previous member of **MEL** and **Diener lab** for their support, kindness, and happy times we spent together. I always felt so lucky to have met all of you and always consider you as my family in Austria!

I would also like to thank my thesis committee members, **Barbara Obermayer-Pietsch**, **Alexander Loy**, and **Gregor Gorkiewicz**, for your guidance and constructive criticism throughout my PhD. A special thanks to Alexender Loy for hosting me in your lab as a visiting researcher. I also sincerely thank **Jeroen Raes** and **Arnau Vich Vila** for hosting me at KU Leuven. I learned so much from you and your lab.

Thank you to **Thomas Vogl**, **Guillaume Meric**, and **Sabine Wagner-Lichtenegger** for agreeing to assess my thesis and for your time and support.

I gratefully acknowledge the **Medical University of Graz** and the PhD Program in **Molecular Medicine (MolMed)** for their financial support and the education provided which made this journey possible.

To all the **friends** I made **in Belgium**: thank you for the parties, the laughter, and the unforgettable memories.

To **Sahar** and **Ali**, thanks a lot for making my move from Iran to Graz way easier!

A very special thank you to my partner in crime, **Farzad**. You have been like a brother to me, supporting me through every high and low. I cannot imagine having gone through Graz without you by my side.

To **Arash**, you were my emotional anchor, the part of me I had left back home that somehow kept me together when I felt broken. I am so grateful to have you here by my side now. I honestly do not know how I would do life without you.

I owe my deepest gratitude to **my parents**.

بابا جون، مامان! مرسی که در همه سختی ها کنارم بودین و تو هر شرایطی نذاشتین آب تو دلم تکون بخوره. بدون فداکاری های شما من هیچ وقت به اینجا نمیرسیدم. هیچ وقت نمیتونم خوبی هاتون رو جبران کنم و بابت دور بودن ازتون همیشه دلگیرم، ولی همیشه و تا ابد قدردان زحمتایی که برای من کشیدین هستم و خواهم بود. امیدوارم که بتونم همیشه باعث سربلندیتون باشم.

I carry with me the roots you gave me, which I hold with pride. I come from **Iran**, a land of rich culture and profound traditions. I sincerely hope for peace and brighter days for its people.

Finally, as I promised **myself** to do so if I make it this far:

Table of content

Table of content

Abbreviations

AD – Alzheimer's disease

AEVs – Archaeal extracellular vesicles

ALPs – Adhesin-like proteins

BMI – Body mass index

CD – Crohn's disease

CENT – Centenarians

CRC – Colorectal cancer

GIT – Gastrointestinal tract

IBD – Irritable bowel disease

IBS – Irritable bowel syndrome

MS – Multiple sclerosis

OAs – Older adults

PD – Parkinson's disease

AD – Alzheimer's disease

SCFAs – Short-chain fatty acids

SCZ – Schizophrenia

T2D – Type 2 diabetes

TFB – Transcription factor B

TLR8 – Toll-like receptor 8

TMA – Trimethylamine

TMAO – Trimethylamine N-oxide

UHGG – Unified Human Gastrointestinal Genome

UTIs – Urinary tract infections

YAs – Young adults

Zusammenfassung

Durch drei komplementäre Publikationen beleuchtet diese Arbeit die Verteilung, Funktion und Krankheitsassoziationen human-assoziierter Archaeen und erweitert damit das Verständnis des menschlichen Archaeoms.

Kapitel 1 bietet einen umfassenden Überblick über die Vielfalt und Biologie der Archaeen im menschlichen Körper. Es fasst ihre einzigartigen metabolischen Eigenschaften, ökologischen Interaktionen und ihre Bedeutung für Gesundheit und Krankheit zusammen. Zudem werden zentrale Wissenslücken in der Archaeenforschung aufgezeigt, was die Notwendigkeit archaeom-inklusiver Ansätze in der Mikrobiomforschung unterstreicht, um mikrobielle und Wirtsinteraktionen besser zu verstehen.

Kapitel 2 untersucht altersabhängige Dynamiken des archaeelen Mikrobioms im menschlichen Darm in drei Altersgruppen – junge Erwachsene, ältere Erwachsene und Hundertjährige. Die Studie zeigt, dass methanogene Archaeen während des Alterns deutliche Zusammensetzungsänderungen erfahren. Während die archaeale Diversität insgesamt abnimmt, weisen Hundertjährige eine Gemeinschaftsstruktur auf, die jener jüngerer Personen ähnelt – angereichert mit *Methanobrevibacter smithii* und geprägt durch eine hohe archaeal-bakterielle Netzwerkverknüpfung. Funktionell sind ausgeprägte Methanogen-Phänotypen mit einer verstärkten Produktion kurzkettiger Fettsäuren über alternative Butyratwege assoziiert, was darauf hindeutet, dass Archaeen zur metabolischen Resilienz und Darmstabilität im hohen Alter beitragen könnten.

Kapitel 3 untersucht die krankheitsspezifische Rolle der Archaeen anhand einer groß angelegten Metaanalyse von Shotgun-Metagenomen über verschiedene Erkrankungen hinweg, darunter kolorektaler Krebs. Die Studie zeigt eine konsistente Anreicherung von *M. smithii* bei kolorektaler Krebs. Integrative metabolische Modellierungen, Ko-Kultur-Experimente und Metabolom-Analysen belegen, dass *M. smithii* mit CRC-assoziierten Bakterien wie *Fusobacterium nucleatum* über Metaboliten wie Succinat, Aminosäuren und Polyaminvorstufen interagiert und so zur Bildung eines metabolisch aktiven, krebsassoziierten Mikrobioms beiträgt. Diese Arbeit liefert den ersten mechanistischen Nachweis, der archaeelle Aktivität mit der kolorektalen Karzinogenese in Verbindung bringt, und definiert Archaeen als aktive metabolische Regulatoren statt als passive mikrobielle Mitbewohner.

Abstract

Through three complementary publications, this work focuses on the distribution, function, and disease associations of human-associated archaea. Chapter 1 provides a comprehensive overview of archaeal diversity and biology across the human body. It summarizes their unique metabolic features, ecological interactions, and relevance to health and disease. The review also highlights major knowledge gaps in archaeal research, emphasizing the need for archaeome-inclusive approaches in microbiome studies to better understand microbe–microbe and microbe–host interactions.

Chapter 2 explores age-related archaeal dynamics in the human gut across three age groups (young adults, older adults, and centenarians). The study reveals significant compositional shifts of methanogenic archaea during aging. While overall archaeal diversity declines with age, centenarians display a community structure similar to that of younger individuals, enriched in *Methanobrevibacter smithii* and characterized by strong archaeal–bacterial network connectivity. Functionally, high methanogen phenotypes are associated with enhanced short-chain fatty acid metabolism through alternative butyrate pathways, suggesting that archaea may contribute to metabolic resilience and microbiome stability in extreme aging.

Chapter 3 investigates the disease-specific role of archaea through a large-scale meta-analysis of shotgun metagenomes across multiple disorders, including colorectal cancer (CRC). The study identifies a consistent enrichment of *M. smithii* in CRC. Integrative metabolic modeling, co-culture experiments, and metabolomic profiling show that *M. smithii* engages in metabolic interactions with CRC-associated bacteria such as *Fusobacterium nucleatum*. Through cross-feeding of metabolites including succinate, amino acids, and polyamine precursors, *M. smithii* influences bacterial metabolism and promotes the formation of a metabolically active, cancer-associated microbiome. This work provides the first mechanistic evidence linking archaeal activity to colorectal carcinogenesis and redefines archaea as active metabolic regulators rather than passive microbial residents.

Introduction

Archaeal phylogeny

The domain Archaea represents one of the three fundamental branches of life, alongside Bacteria and Eukarya, a classification first proposed based on 16S rRNA phylogenetic analyses by Carl Woese and George Fox in 1977 (4). Although initially thought to be confined to extreme environments, archaea are now known to inhabit a wide range of ecosystems, including mesophilic and host-associated habitats such as the human body (5). Phylogenetically, archaea are deeply divergent from bacteria despite superficial similarities in cellular structure (e.g., lack of nucleus and organelles).

The archaeal domain is currently divided into several major phyla, including: Methanobacteriota, Halobacteriota, Thermoproteota (formerly part of the TACK super-phylum), Nitrososphaerota, Thermoplasmatota, Microcaldota, Promethearchaeota, and Nanobdellota as well as several phyla proposed based on genomic or metagenomic data, which are not cultured yet and have not been validly published under the formal rules of nomenclature, including *Candidatus* Parvarchaeota, *Candidatus* Iainarchaeota, *Candidatus* Korarchaeota, *Candidatus* Aenigmatarchaeota, *Candidatus* Nanohalarchaeota, *Candidatus* Augarchaeota.

Modern archaeal phylogeny is now primarily reconstructed using concatenated marker gene sets and whole-genome phylogenomic approaches, which have uncovered previously unrecognized diversity and evolutionary relationships. In particular, genome-resolved metagenomics has greatly expanded the known tree of life, revealing hundreds of novel archaeal lineages, some of which inhabit the human gut, oral cavity, and skin (6).

Structural, molecular, and metabolic characteristics of archaea

Archaea possess unique biochemical and structural features that not only reflect their evolutionary lineage but also enable their survival in diverse and often extreme environments. Unlike bacteria, archaeal cell walls do not contain peptidoglycan. Instead, some species synthesize pseudomurein, while others utilize proteinaceous S-layers that form paracrystalline surface structures. These S-layers may serve multiple roles, including protection, adhesion, and immune evasion (7, 8). Some archaeal species, such as *Ignicoccus*, possess a unique outer cellular membrane that may maintain an electrochemical gradient and facilitate interaction with

symbionts like another archaeal species called *Nanoarchaeum equitans* (9), through facilitating metabolic exchange and energy sharing between the two partners. This organization is rare among Archaea and makes *Ignicoccus* cell architecture quite unique. Classical double membranes, resembling those in Gram-negative bacteria, have also been identified in *Methanomassiliicoccus luminyensis* and *Candidatus* Altiarchaeum hamiconexum (10). The presence of double membranes in these lineages suggests that the last common ancestor of Archaea might have been more structurally diverse, or that double membranes evolved multiple times independently (11). It is suspected that more archaea have such double membranes, but detecting them remains technically challenging, since standard electron microscopy techniques often lack the resolution to clearly separate two closely spaced membranes, and sample preparation can create artifacts (12). Moreover, archaea lack established outer-membrane markers, so there are no molecular signatures to confirm a second membrane (13).

One of the most defining characteristics of archaea lies in the composition of their cell membranes. In contrast to the ester-linked fatty acids of bacterial and eukaryotic membranes, archaeal membranes are composed of ether-linked isoprenoid chains bound to L-glycerol (14). This lipid architecture provides exceptional chemical and thermal stability, enabling survival in extreme environments and supporting metabolic flexibility in diverse habitats. The major archaeal lipids include archaeol, caldarchaeol, and cyclic archaeol, accompanied by membrane-associated sugars such as glucose, fructose, rhamnose, ribose, and xylose. Importantly, synthetic vesicles made from these lipids, known as archaeosomes, display remarkable stability and immunostimulatory activity, engaging innate immune receptors such as CLEC4E.

Archaea also exhibit distinct mechanisms of motility and adhesion. Their motility apparatus, called the archaellum, is structurally more similar to bacterial type IV pili than to bacterial flagella, reflecting convergent functional adaptation rather than shared ancestry. In addition, archaea express a range of surface appendages, including pili and hami, the latter which are grappling-hook-like filaments that are involved in adhesion to both abiotic surfaces and host cells (15-17). Interestingly, many host-associated archaea encode adhesins or adhesin-like proteins (ALPs), which are often highly glycosylated and thought to mediate host colonization and interspecies interactions. These surface proteins, particularly well-characterized in *Methanobrevibacter* and *Methanosphaera* species, may also influence host immune recognition through their glycan structure (18). Interestingly, research has revealed that *M. smithii* and *M.*

stadtmanae dedicate a remarkably high portion of their genomes (~10%) to encoding ALPs, which is significantly more than typical bacteria (19). Furthermore, archaeal species are capable of forming biofilms, a trait that supports persistence in complex microbial communities such as the human gut (20).

An additional characteristic of archaeal physiology is the production of extracellular vesicles, specifically archaeal extracellular vesicles (AEVs). While many archaeal lineages are capable of releasing such vesicles, AEV production has also been observed in human-associated methanogens like *Methanobrevibacter smithii*, *M. intestini*, and *Methanosphaera stadtmanae*, which are morphologically similar to bacterial extracellular vesicles, with diameters typically ranging from 87 to 198 nanometers. AEVs are enriched in putative adhesins and a range of small metabolites, including glutamic acid, aspartic acid, and choline glycerophosphate. Notably, these vesicles can be internalized by human macrophages in vitro and trigger species-specific immune responses, including the induction of chemokines such as IL-8 and CX3CL1 in immune and epithelial cells. Moreover, one study on *M. smithii* demonstrated that its extracellular vesicles also carry DNA (including extrachromosomal circular DNA and proviral DNA), and biogenesis appears to occur via budding from the cytoplasmic membrane, with vesicles initially trapped between the membrane and cell-wall (peptidoglycan) layers before release. It is considered that AEVs may serve as a novel mechanism of host-microbe and microbe-microbe communication within the gut ecosystem (21).

Interestingly, recent structural bioinformatics (AlphaFold2) has identified gut-specific proteins involved in N-linked and O-glycosylation, suggesting that *M. smithii* may decorate its surface to mimic the host's intestinal glycan landscape to evade the immune system (22).

Internally, archaeal DNA is usually wrapped around histone proteins, forming compact, nucleosome-like structures that help stabilize and organize the genome, a feature rarely found in bacteria (23, 24). These simple histones are thought to represent evolutionary ancestors of eukaryotic chromatin. In addition, many of the molecular systems that control transcription and translation in Archaea are similar to those in eukaryotes. Their RNA polymerase closely resembles eukaryotic RNA polymerase II, and transcription initiation relies on TATA-binding protein and transcription factor B (TFB), parallels to eukaryotic TFII factors (25). Similarly, the DNA replication machinery and ribosomal proteins of Archaea show greater similarity to eukaryotic than to bacterial components, highlighting their **c**entral position in the evolutionary

bridge between prokaryotes and eukaryotes (13, 26). Some archaeal species employ translational recoding mechanisms, enabling them to incorporate non-canonical amino acids such as pyrrolysine (27).

Although archaea are not typically considered spore-forming organisms, recent genomic analyses have revealed the presence of sporulation-associated genes, such as *SpoVAE* and *SpoVAD*, in *M. smithii*. These genes, likely acquired via horizontal gene transfer from Firmicutes like *Clostridium*, are expressed in fecal samples, though their functional capacity for sporulation has not yet been experimentally demonstrated (28).

Metabolically, the best-characterized archaea in the human gut are methanogens, particularly species within the genera *Methanobrevibacter* and *Methanosphaera*. *Methanobrevibacter* species, such as *M. smithii*, rely primarily on hydrogen and carbon dioxide to produce methane, though they are also capable of utilizing formate. This metabolic strategy enables them to thrive in the anoxic niches of the gastrointestinal tract (GIT). Other archaeal taxa, particularly members of the Methanomassiliicoccales (e.g., *Methanomassiliicoccus luminyensis*), can utilize trimethylamine (TMA) as a substrate for hydrogen-dependent methanogenesis, converting TMA into methane. Through this process, these methanogens may modulate host metabolism by consuming TMA, a microbial degradation product of dietary choline, carnitine, and betaine. As TMA serves as the direct precursor of trimethylamine N-oxide (TMAO), which is a a metabolite implicated in **c**ardiovascular disease, atherosclerosis, and metabolic dysfunction, archaeal activity may indirectly influence TMAO accumulation and thereby contribute to host metabolic health (29, 30). Moreover, while traditionally viewed as hydrogenotrophic, the discovery of acetoclastic pathways in monogastric hosts (like swine *Methanomassiliicoccales*) in 2023 represents a major shift in understanding archaeal energy acquisition in the gut (31).
M. stadtmanae differs from other methanogens by utilizing methanol as an electron acceptor, reduced by hydrogen to produce methane. The methanol–hydrogen pathway of *M. stadtmanae* represents a highly specialized adaptation to the human gut, where methanol arises from the degradation of dietary pectins and methylated compounds by other microbes (32, 33).

A critical ecological role of methanogens lies in their syntrophic relationships with hydrogen-producing bacteria, a process known as interspecies hydrogen transfer. During the fermentation

of carbohydrates, many gut bacteria release hydrogen as a metabolic by-product. Accumulation of hydrogen increases the partial pressure within the gut lumen, which can thermodynamically inhibit further bacterial fermentation. Methanogens consume this hydrogen, using it to reduce carbon dioxide or other one-carbon substrates to methane. By maintaining low hydrogen partial pressure, they shift bacterial metabolism toward more complete oxidation of substrates, thereby enhancing energy extraction from complex polysaccharides and promoting the production of short-chain fatty acids (SCFAs) such as acetate, propionate, and butyrate, which are essential energy sources for colonocytes and beneficial for host health (33).

This syntrophic relationship is particularly important in fiber-rich diets, where fermentation rates are high and efficient hydrogen removal is critical. A well-characterized example is the partnership between *M. smithii* and *Christensenella minuta*, first demonstrated using co-culture and microscopy analyses. *C. minuta* forms flocculated aggregates that physically associate with *M. smithii*, enabling direct interspecies hydrogen transfer and minimizing diffusion losses. This interaction supports archaeal methanogenesis and simultaneously alters the bacterial fermentation profile, shifting *C. minuta*'s metabolic end-products from butyrate toward acetate, thereby modifying the gut SCFA pool and potentially influencing host energy balance (34).

In addition to cooperative interactions, methanogens also compete with other hydrogen-utilizing microbes, such as homoacetogens (e.g., *Blautia hydrogenotrophica*) and sulfate-reducing bacteria, shaping gut redox balance and community composition. The outcome of this competition depends on environmental conditions such as hydrogen concentration (35).

Diversity and distribution of human-associated Archaea

While Archaea exhibit remarkable structural and metabolic diversity across ecosystems, only a limited number of lineages thrive within the human host. The GIT remains the most prominent habitat for archaea in the human body, where methanogenic archaea are particularly prevalent. These organisms correspond to an average of approximately 1.2% of the total microbial community (36).

Among the dominant archaeal species in the gut, *M. smithii* is the most commonly detected, with a prevalence exceeding 90% and an average abundance of 0.56% (37). Other frequent gut colonizers include *M. oralis*, found in nearly 44% of Chinese subjects, and *M. stadtmanae*, present in approximately one-third of samples (38). Additional members of the gut archaeome

include methanogens from the orders Methanomassiliicoccales (e.g., *Methanomassiliicoccus luminyensis*, *Candidatus* Methanomassiliicoccus intestinalis, *Candidatus* Methanomethylophilus alvus), as well as species from Methanomicrobiales, Methanosarcinales, and Methanococcales (38, 39). Interestingly, archaeal groups not traditionally associated with the human body, such as Halobacteriales, Desulfurococcales, Sulfolobales, Thermoproteales, and Nitrososphaerales, have also been detected in the gut (40-44). Signatures of *Methanobacterium*, previously unreported in the human GIT, have been identified in biopsy samples from the ileum and left colon (45). A recent large-scale catalog of 1,167 archaeal genomes from human GIT samples revealed a number of novel taxa, including *M. intestini*, a species formerly misclassified under *M. smithii*. Compared to other anatomical sites, the gut archaeome exhibits relatively high diversity (39).

The skin also harbors a distinct archaeal community, primarily composed of Thermoproteota (former phylum Thaumarchaeota) closely related to ammonia-oxidizing *Ca.* Nitrosocosmicus (46). These archaea can constitute up to 10% of the skin microbiome and may participate in ammonia turnover, potentially influencing skin pH and odor. In addition to ammonia-oxidizing Archaea, skin samples have revealed the presence of Euryarchaeota, including Methanobacteriaceae, Halobacteriaceae, Woesearchaeota, and Aenigmarchaeota. Archaeal abundance on the skin tends to increase with age, particularly in individuals younger than 12 or older than 60 years, suggesting a possible link between skin maturation and archaeal colonization (47).

In the oral cavity, the archaeal community is dominated by the genus *Methanobrevibacter*, especially *M. oralis* and *M. smithii*. Other methanogens such as *M. stadtmanae*, as well as non-methanogenic archaea from Thermoplasmata, Thaumarchaeota, and halophilic Euryarchaeota, have also been identified (29). A 2024 study in Tunisia provided the first detailed data on methanogens in North African adults, confirming their universal presence in the oral cavity across diverse geographic populations (48). Moreover, *Methanomassiliicoccus massiliense* was recently identified and cultivated from infected dental pulps, showing a symbiotic relationship with specific bacteria like *Pyramidobacter piscolens* (49).

Archaeal sequences have also been recovered from the human respiratory tract, including both nasal and pulmonary samples. In the lungs, Woesearchaeota, a member of the DPANN superphylum, have emerged as the dominant archaeal taxa, with their presence in the human microbiome first reported only recently. The nasal cavity harbors a combination of

methanogens and Thermoproteota, with *M. smithii* and *M. oralis* detected consistently. However, the functional roles and precise taxonomy of respiratory archaea remain largely unknown (50).

The urogenital tract also supports archaeal colonization. In the vaginal microbiome, *M. smithii* is frequently identified and appears to be the predominant archaeal species. Its presence has been linked to maintaining pH balance by mitigating excessive acidification. In the urinary tract, *M. smithii* has been detected in individuals with urinary tract infections (UTIs), suggesting a potential role in urogenital pathophysiology (51, 52). Importantly, characterization of the *M. smithii* genome (strain U29) from the urinary tract has revealed that contains unique viral sequences that may facilitate its colonization and persistence in this environment (53).

Several factors influence the diversity and distribution of archaea across individuals and populations. Archaea are not typically detected at birth, and evidence for in utero colonization remains unsubstantiated. Archaeal signatures, primarily belonging to *M. smithii*, begin to appear during the first months of life, coinciding with the establishment of anaerobic gut conditions and the onset of breastfeeding. Longitudinal analyses have shown that *M. smithii* is rare or absent in the neonatal period but becomes detectable by 1–3 months, with prevalence and abundance increasing throughout infancy and early childhood (54, 55). Archaeal abundance and diversity tend to increase with age in various human populations. For instance, *M. luminyensis* has been particularly associated with older individuals, while certain halophiles such as *Haloarcula marismortui* and *Halorubrum lacusprofundi* are also found in greater abundance beyond the age of 50 (56-58).

Geographical origin, ethnicity, lifestyle, and dietary patterns also significantly shape archaeal communities. Comparative studies have revealed striking differences across populations. For example, Methanomassiliicoccales are generally absent in Chinese cohorts but prevalent in Western populations, reflecting considerable transnational variation (59). Certain archaeal taxa are enriched in specific ethnic groups. Urbanization has also been associated with archaeal depletion: individuals living in rural areas tend to harbor a more diverse and archaeal-rich microbiota, with taxa such as *M. oralis*, *Methanobrevibacter sp_87_7*, *Methanobrevibacter olleyae*, and several *Halococcus* species enriched compared to urban residents. This trend may reflect higher hygiene standards and reduced environmental exposure in urban settings (39, 59).

Dietary habits further modulate archaeal colonization. High-carbohydrate diets as well as diets rich in fiber have been associated with increased detection of *M. smithii*, likely reflecting the

greater availability of fermentation-derived hydrogen that supports methanogenesis (60, 61). On the other hand, higher vitamin B_{12} intake has been linked to reduced number of methanogens. Mechanistically, vitamin B_{12} deficiency alters bacterial one-carbon metabolism, leading to the accumulation of formate and molecular hydrogen, which are key substrates for hydrogenotrophic methanogens such as *M. smithii*. This shift in redox balance and substrate availability promotes methanogenic activity and methane emission, linking low B_{12} status to enhanced archaeal metabolism in the gut (61).

Finally, host genetics also influences archaeal colonization. Twin studies have shown that *M. smithii* abundance is more similar in identical (monozygotic) twins than in fraternal (dizygotic) pairs, indicating a heritable component to archaeal establishment (62). Follow-up analyses identified a single-nucleotide variant (rs2304130) in a long non-coding RNA locus associated with *M. smithii* levels (63). Although the function of this locus remains unclear, it may affect immune or metabolic regulation, creating a host environment that favors methanogen persistence. Recent genome-wide studies have confirmed that human genetic variation contributes to archaeal community structure, linking archaeal abundance to host genes involved in lipid metabolism, bile acid turnover, and redox balance (64).

Interaction of Archaea with the human immune system

Archaea interact with the human immune system in diverse and species-specific ways, shaping host responses through whole cells, extracellular vesicles, and their metabolic products. Among gut-associated methanogens, *M. stadtmanae* and *M. smithii* have been the most intensively studied, revealing striking differences in their immunogenicity. Both species can activate human dendritic cells, yet *M. stadtmanae* consistently elicits a markedly stronger pro-inflammatory response. Upon exposure to *M. stadtmanae*, dendritic cells produce high levels of TNF-α, IL-1β, and IL-6, and upregulate maturation markers such as CD86 and CCR7, indicating robust activation. This inflammatory signalling depends on phagocytosis and phagolysosomal acidification, demonstrating that archaeal components must be internalized and recognized within endosomal compartments. Supporting this mechanism, *M. stadtmanae* RNA has been shown to activate Toll-like receptor 8 (TLR8), which triggers downstream production of pro-inflammatory cytokines and type I/III interferons. In contrast, *M. smithii* induces only weak dendritic cell activation, with lower cytokine levels and reduced surface

maturation markers (65, 66). These observations mirror its ecological role as a dominant gut commensal with limited pathogenic potential.

Beyond whole cells, AEVs represent an additional layer of host–microbe interaction. AEVs are produced by several human-associated methanogens and carry a diverse cargo of proteins and small metabolites capable of modulating immune responses. In intestinal epithelial HT-29 cells, AEVs derived from *M. intestini* induce strong secretion of IL-8, whereas vesicles from *M. smithii* or *M. stadtmanae* trigger minimal IL-8 release. Nonetheless, all tested AEVs stimulate high levels of CX3CL1 (fractalkine), suggesting a shared ability among archaeal species to activate epithelial chemokine signalling. In macrophages, AEVs produce more nuanced, species-specific patterns of cytokine expression. Exposure of THP-1 macrophages to AEVs results in differential induction of chemokines such as CXCL9 and CXCL11, indicative of a Th1-skewing immune environment. Again, *M. intestini* AEVs shows the strongest pro-inflammatory effect, underscoring substantial interspecies variability. Importantly, these vesicle-driven responses require cellular uptake, pointing to intracellular recognition pathways, likely involving endosomal pattern-recognition receptors similar to those engaged by whole *M. stadtmanae* cells (21).

Archaea can also interact with the immune system through their intrinsic resistance to antimicrobial peptides. For example, *M. luminyensis* exhibits notable resilience against several mammalian antimicrobial peptides, including the human cathelicidin LL-37. Although LL-37 shows some effectiveness against *M. luminyensis*, this species remains more susceptible than *M. stadtmanae* or *M. smithii*, suggesting distinct membrane properties that differentially influence archaeal survival under host immune pressure (65, 67).

Moreover, *M. smithii* has the potential to mimic human mucus glycans through specific glycosyltransferases, allowing it to emulate eukaryotic surfaces and potentially evade host immune detection (22). Recent research using mouse models has also demonstrated that *M. smithii* specifically activates group 3 innate lymphoid cells, significantly augmenting the production of TNF-α, IL-22, and IL-17, which helps protect the intestinal mucosal barrier (68).

Finally, archaeal metabolism itself may influence host immunity. Methane, the major end-product of methanogenesis, has been proposed to exert immunomodulatory effects within the gut. Experimental evidence suggests that methane exposure can enhance IL-10 production

while suppressing the release of IL-6, TNF-α, and IL-1β, collectively indicating a potential anti-inflammatory role. Although the physiological relevance of methane-mediated immune modulation in vivo remains unclear, these findings raise the possibility that methanogenesis may indirectly contribute to shaping gut immune homeostasis (69, 70).

Challenges in detecting the human archaeome

The detection of archaea is often hindered by several technical and methodological constraints. Commonly used “universal” 16S rRNA primers capture only a limited portion of archaeal diversity, while standard DNA extraction protocols often fail to disrupt archaeal cell envelopes efficiently. The typically low archaeal-to-bacterial DNA ratio, together with incomplete reference databases, further contributes to underestimation and misclassification of archaeal sequences (71).

Recent large-scale metagenomic assessments have revealed that a substantial proportion of archaeal reads are lost during conventional sequence assembly and binning, resulting in systematic biases in community profiling. Approaches integrating long-read sequencing, hybrid genome assemblies, and archaea-specific marker gene sets markedly improve detection and genome recovery (37, 72). Together, these methodological refinements, including sample preparation, sequencing strategy, and bioinformatic analysis, are now essential for accurately reconstructing the human archaeome and understanding its role within complex microbial ecosystems (73). Furthermore, the field lacks sufficient metadata regarding dietary habits and bowel transit times, which are critical because methanogen growth is highly sensitive to the gut's redox balance and substrate availability. Mathematical modeling, specifically ordinary differential equation-based approaches, is now being used to supplement these gaps by tracking biomass fluctuations and nutrient competition over time (74).

Objectives and summary of the thesis

Chapter 1: **Archaeal key-residents within the human microbiome: characteristics, interactions and involvement in health and disease (1).**

Archaea represent an essential yet historically underexplored domain of life within the human microbiome. For a long time, research on the human microbiome has primarily focused on bacteria, while the archaeal community received comparatively little attention. However, accumulating evidence in recent years has demonstrated that archaea are regular and functionally relevant members of multiple human body sites, including the gastrointestinal tract, oral cavity, skin, and even the respiratory system. With this growing awareness, the need to better understand their biological roles, metabolic features, and interactions with other microorganisms and the human host has become increasingly evident. In this review, the available literature on human-associated archaea was systematically summarized to provide an overview of their current taxonomic landscape, ecological characteristics, and putative roles in health and disease. The main objectives were to:

- compile and compare the current knowledge on archaeal diversity, distribution, and abundance across different human body sites
- describe their physiological and genomic features that enable survival and adaptation in host-associated environments,
- highlight the ecological interactions between archaea and bacteria, including syntrophic and competitive relationships
- outline the potential implications of archaeal activity for host physiology, immunity, and pathophysiological processes, and
- identify existing knowledge gaps and future directions for archaeome research, including methodological challenges and analytical limitations.

This chapter provides an overview of the human archaeome, spanning from fundamental aspects of archaeal biology to their potential contributions in host-associated microbial ecosystems. Special attention is given to the methanogenic archaea, particularly *M. smithii*, which represents one of the most prevalent archaeal species in the human gut. Beyond its metabolic specialization in hydrogen consumption and methane production, its ecological and clinical relevance are discussed in the context of metabolic disorders, inflammatory diseases, and colorectal cancer.

Finally, this review highlights how the incorporation of archaea into microbiome research reshapes our understanding of the human holobiont. It underscores the necessity of archaeome-inclusive approaches in future studies aiming to decipher microbe–microbe and microbe–host interactions, ultimately contributing to a more comprehensive understanding of human health and disease.

Chapter 2: **Age-related dynamics of predominant methanogenic archaea in the human gut microbiome (2).**

Although the relationship between gut microbiota composition and aging has been extensively studied, information about the human gut archaeome and its contribution to longevity remains limited. In this study, we aimed to explore age-related dynamics of methanogenic archaea in the human gut and their potential association with microbial networks and functional metabolism. Shotgun metagenomic data from 247 individuals spanning three age groups of young adults (YAs) (19–59 years), older adults (OAs) (60–99 years), and centenarians (CENT) (100–109 years), were analyzed. Overall, archaeal diversity decreased with age, yet centenarians displayed an archaeal composition resembling that of YAs, marked by an increased relative abundance of *M. smithii* and a lower abundance of *M. intestini*, which dominated in OAs. The class Thermoplasmata, particularly Methanomethylophylaceae and Methanomassiliicoccaceae, increased in OAs but declined again in CENT.

Network analyses revealed that *M. smithii* and *M. intestini* co-existed and showed central roles in age-specific microbial co-occurrence networks. The complexity of archaeal–bacterial co-occurrences was highest in CENT, highlighting a stable and interconnected community. Both methanogens consistently co-occurred with health-associated taxa such as members of Oscillospiraceae and Christensenellaceae, while showing mutual exclusion with Lachnospiraceae and Streptococcaceae. Notably, Lachnospiraceae, typically major butyrate producers, decreases across aging, and Oscillospiraceae, another butyrate producer, appears to compensate for this decline, in samples with high methanogen phenotype.

Stratification by archaeal abundance revealed a clear increase in the prevalence of the high methanogen phenotype with age (25 % in young adults, 42 % in older adults, and nearly 60 % in centenarians). Individuals with high methanogen phenotype exhibited significantly higher microbial diversity and distinct community compositions compared to low methanogen phenotype, especially among YAs and OAs. In subjects with high methanogen phenotype, particularly in OAs and CENT, butyrate- and propionate-related genes, including those encoding butyrate kinase (K00929) and phosphate butyryltransferase (K00634), were significantly upregulated, suggesting enhanced potential for SCFA production, through butyrate kinase pathway, rather than butyryl-CoA:acetate CoA-transferase pathway. Correlation analyses further linked these genes to Oscillospiraceae rather than Lachnospiraceae, supporting

a syntrophic association between methanogens and alternative butyrate-producing taxa, which particularly produce butyrate through the butyrate kinase pathway.

Together, these findings indicate that methanogenic archaea, particularly *M. smithii* and *M. intestini,* are integral to the restructuring of the gut ecosystem during aging. Their co-occurrence with beneficial bacterial partners and enrichment of butyrate-related metabolic pathways may help maintain intestinal stability and metabolic resilience in extreme aging, emphasizing the archaeome's potential contribution to longevity.

Chapter 3: **Cross-domain metabolic interactions link *Methanobrevibacter smithii* to colorectal cancer microbial ecosystems (3)**.

The potential contribution of archaea to disease processes has remained largely unexplored. To systematically assess archaeal–disease associations, we conducted the first large-scale meta-analysis of the human gut archaeome across 19 independent metagenomic studies comprising 3,243 participants from 12 countries, covering CRC, IBD, including Crohn's disease (CD) and ulcerative colitis (UC), T2D, MS, pre-Alzheimer's disease (pre-AD), Schizophrenia (SCZ), and PD. Using a standardized Kraken2/Bracken workflow based on the Unified Human Gastrointestinal Genome (UHGG v2.0.1), archaeal and bacterial profiles were reconstructed and case-control samples were matched for age, sex, and body mass index (BMI) in individual studies, when the metadata was available. Samples of CRC, pre-AD, and PD (diseases with more than one study each), were pooled for each disease, separately as well to obtain the global trends of archaeome in these diseases, after correcting for batch effect, using MMUPHin. In the pooled dataset of PD, significant enrichment of Methanobrevibacter_A_smithii, Methanobrevibacter_A_smithii_A, Methanomassilicoccus_intestinalis, and Methanomassilicoccus_luminyensis were observed. However, these significant trends were not visible in individual studies after matching the case-control samples. On the other hand, CD and UC were characterized by archaeal depletion, indicating disease-specific archaeome signatures. The strongest and most consistent significant enrichment observed for Methanobrevibacter_A_smithii was in CRC patients across multiple datasets (Feng (75) and Gupta (76) cohorts, as well as the pooled dataset). Other archaeal taxa, including Methanobrevibacter_A_smithii_A (known as *Methanobrevibacter intestini*) and Methanobrevibacter_A_sp900766745, were also significantly elevated in these individual datasets. Moreover, in the Random Forest classification model distinguishing CRC patients from healthy controls, Methanobrevibacter_A_smithii ranked among the top discriminatory taxa, indicating that archaeal abundances contributed to the diagnostic signal captured by the model.

To investigate the mechanisms underlying the CRC-specific enrichment of Methanobrevibacter_A_smithii, genome-scale metabolic modeling (gapseq and PyCoMo) was performed for *M. smithii* alongside 12 CRC-associated bacterial species, including *Fusobacterium nucleatum*, *Escherichia coli*, and *Bacteroides fragilis*, which also showed co-

occurrence and co-abundance with *M. smithii* in the pooled dataset. The reconstructed models predicted extensive cross-feeding interactions, revealing that *M. smithii* can take up several amino acids—such as L-asparagine, L-glutamine, L-leucine, L-threonine, L-valine, L-lysine, L-serine, and L-arginine, many of which have been linked to CRC metabolism. Additionally, *M. smithii* was predicted to import succinate, a key signaling metabolite implicated in promoting CRC metastasis.

Co-culture experiments confirmed that *M. smithii* enhances growth and metabolic activity of CRC-associated bacteria, and specially *F. nucleatum*. Quantitative PCR revealed elevated bacterial 16S rRNA and archaeal *mcrA* gene copy numbers in co-cultures relative to mono-cultures, underscoring a synergistic relationship.

Untargeted metabolomic profiling by NMR and LC-MS further demonstrated that *M. smithii–F. nucleatum* co-cultures produced a distinct metabolite spectrum enriched in amino acid derivatives and small molecules with tumor-modulating potential, including polyamines, 4-hydroxyphenylacetate, and other aromatic compounds. Several of these metabolites have been previously linked to inflammation, epithelial proliferation, and altered immune signaling within the tumor microenvironment.

Collectively, this multi-omics and experimental study identifies *M. smithii* as a key archaeal contributor to CRC-associated microbiome shifts. By modulating bacterial metabolism and metabolite exchange, *M. smithii* acts not as a passive hydrogen scavenger but as an active trophic regulator of the cancer bacteriome. These findings reveal a previously unrecognized ecological and metabolic link between the human archaeome and colorectal carcinogenesis and underscore the importance of incorporating archaeal functions into future microbiome-oncology framework

Publications

1st publication: **Archaeal key-residents within the human microbiome: characteristics, interactions and involvement in health and disease (1).**

Rokhsareh Mohammadzadeh[1], Alexander Mahnert[1], Stefanie Duller[1], Christine Moissl-Eichinger[1,2].*

[1]Diagnostic and Research Institute of Hygiene, Microbiology and Environmental Medicine, Medical University of Graz, Neue Stiftingtalstraße 6, 8010 Graz, Austria

[2]BioTechMed, 8010 Graz, Austria

*Corresponding author

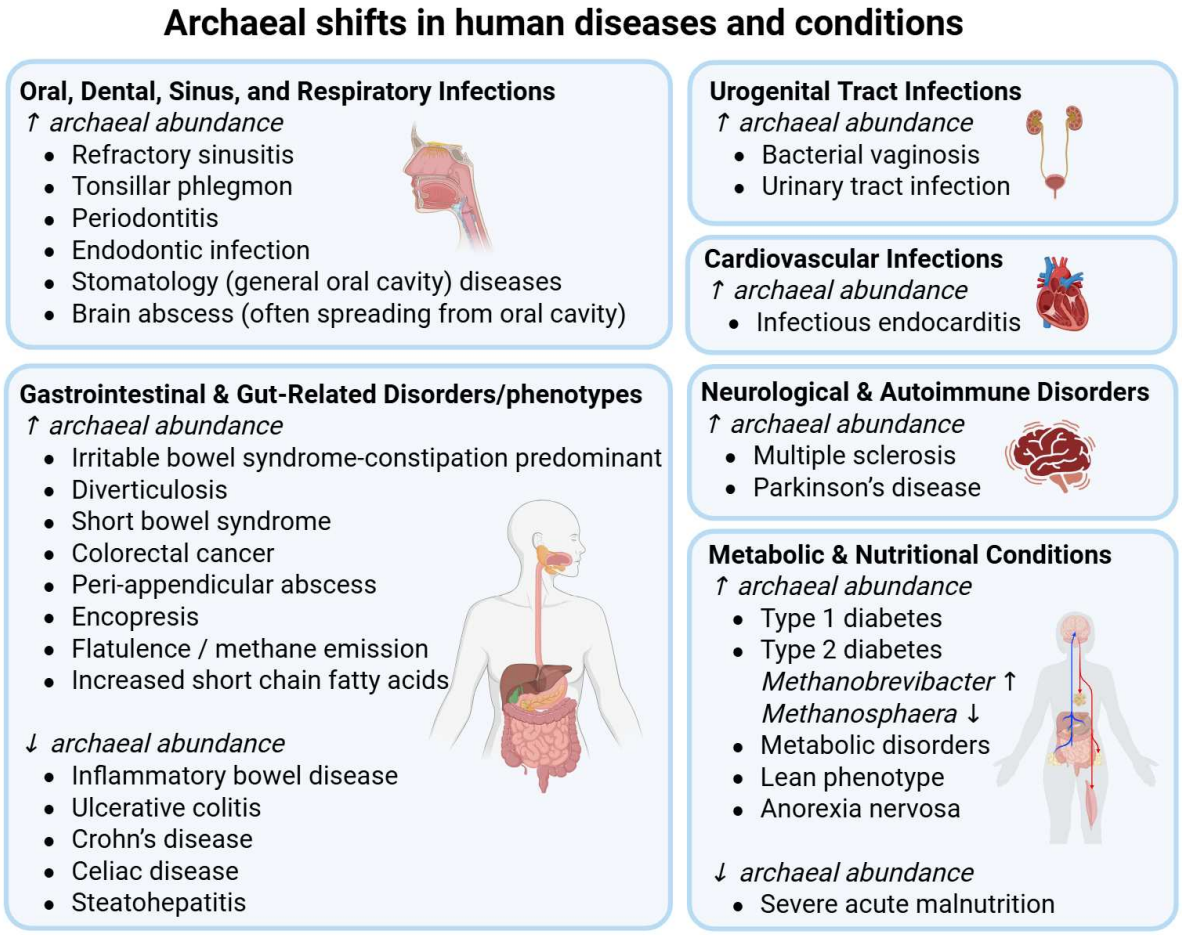

Figure 1. Graphical abstract of the major reported associations of Archaea with health and disease summarized in the 1st publication. Created in Biorender

Published in *Current Opinion in Microbiology* (April 2022)

2nd publication: **Age-related dynamics of predominant methanogenic archaea in the human gut microbiome (2).**

Rokhsareh Mohammadzadeh[1], Alexander Mahnert[1], Tejus Shinde[1], Christina Kumpitsch[1], Viktoria Weinberger[1], Helena Schmidt [2], Christine Moissl-Eichinger[1,3]

[1] Diagnostic and Research Institute of Hygiene, Microbiology and Environmental Medicine, Medical University of Graz, Neue Stiftingtalstraße 6, 8010 Graz, Austria

[2]Division of Molecular Biology and Biochemistry, Medical University of Graz, Graz, Austria

[3]BioTechMed, 8010 Graz, Austria

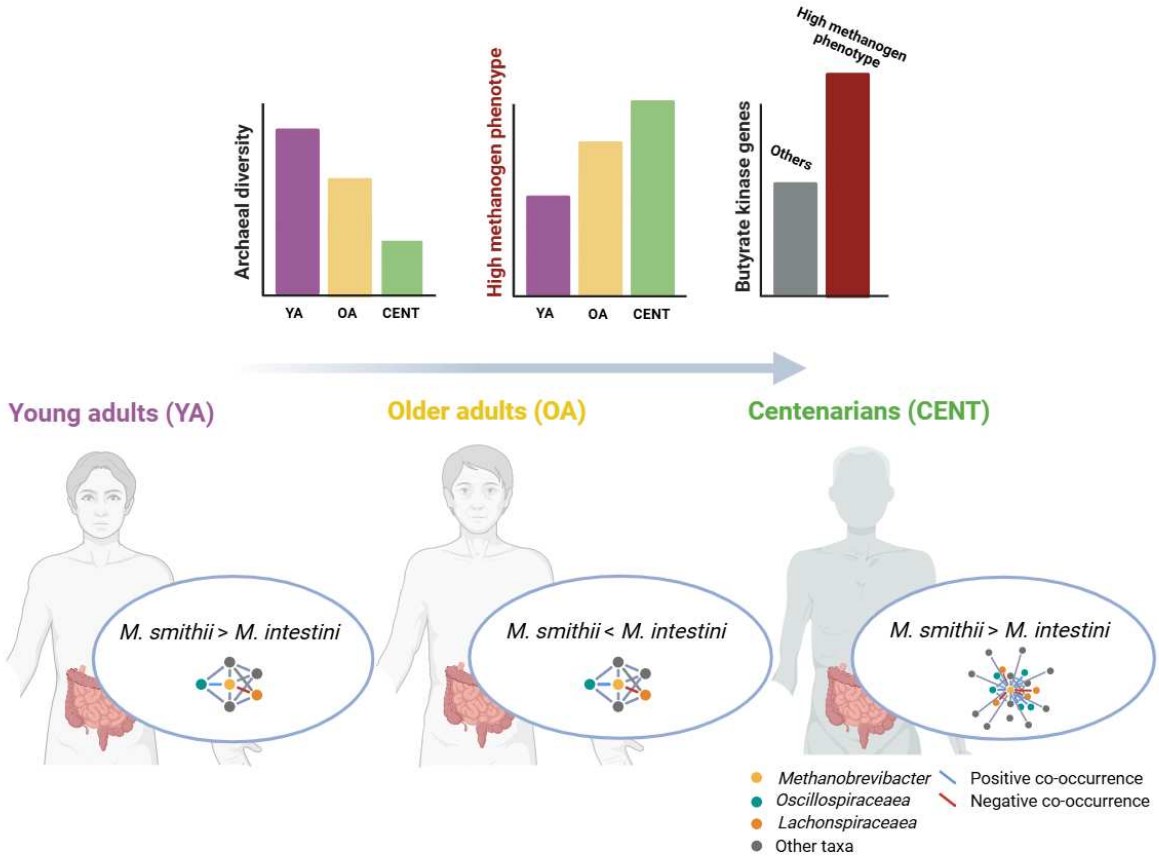

Figure 3. Graphical abstract of the major results of the 2nd publication. Created in Biorender.

Published in *BMC Microbiology* (April 2025)

3rd publication: **Cross-domain metabolic interactions link *Methanobrevibacter smithii* to colorectal cancer microbial ecosystems (3).**

Rokhsareh Mohammadzadeh[1], Alexander Mahnert[1], Tamara Zurabischvili[1], Lisa Wink[1], Christina Kumpitsch[1], Hansjoerg Habisch[2], Jannik Sprengel[3,4], Klara Filek[1], Polona Mertelj[1], Dominique Pernitsch[5], Kerstin Hingerl[5], Marija Durdevic[6,7], Gregor Gorkiewicz[6,12], Christian Diener[1], Alexander Loy[8], Dagmar Kolb[5], Christoph Trautwein[3,4,9,10,11], Tobias Madl[2, 12], Christine Moissl-Eichinger[1,12]*

[1] Diagnostic and Research Institute of Hygiene, Microbiology and Environmental Medicine, Medical University of Graz, 8010 Graz, Austria
[2] Otto Loewi Research Center, Medicinal Chemistry, Medical University of Graz, Graz, Austria
[3] Core Facility Metabolomics, Medical Faculty University of Tübingen, Tübingen, Germany
[4] M3 Research Center for Malignome, Metabolome & Microbiome, Medical Faculty University of Tübingen, Tübingen, Germany
[5] Core Facility Ultrastructure Analysis, Medical University of Graz, Graz, Austria
[6] Institute of Pathology, Medical University of Graz, Graz, Austria
[7] Core Facility Computational Bioanalytics, Center for Medical Research, Medical University of Graz, Graz, Austria
[8] Division of Microbial Ecology, Centre for Microbiology and Environmental Systems Science, University of Vienna, Vienna, Austria
[9] Department of Preclinical Imaging and Radiopharmacy, Werner Siemens Imaging Center, University Hospital Tübingen, Tübingen, Germany
[10] Cluster of Excellence CMFI (EXC 2124) "Controlling Microbes to Fight Infections", Eberhard Karls University of Tübingen, Tübingen, Germany
[11] Cluster of Excellence iFIT (EXC 2180) "Image Guided and Functionally Instructed Tumor Therapies", University of Tübingen, Tübingen, Germany
[12] BioTechMed, Graz, Austria

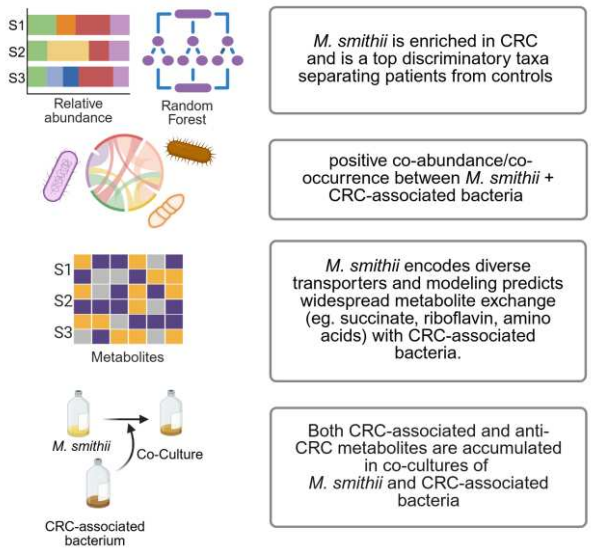

Figure 3. Graphical abstract of the major results of the 3rd publication. Created in Biorender.

Published in *Nature Communications* (February 2026)

Discussion

Chapter 1: **Archaeal key-residents within the human microbiome: characteristics, interactions and involvement in health and disease (1).**

This review (1) examined the emerging evidence on the human gut archaeome across a range of disease contexts and highlighted that our understanding of archaea in human health is still in its early stages. While the bacterial microbiome has been widely studied and clearly linked to host physiology, metabolism, immunity, and disease, archaea remain comparatively overlooked (77). The literature to date shows that archaeal signals in disease are not straightforward. Importantly, this review provides, for the first time, reliable quantitative estimates of the relative abundance of major archaeal taxa across studies, offering a clearer framework for interpreting archaeal signals in health and disease. Instead of showing a universal increase or decrease across all disorders, archaeal patterns appear to vary depending on the condition, the local gut environment, and methodological differences between studies (including DNA extraction protocols, primer choice, sequencing depth, and bioinformatic pipelines). This observation underscores that archaea cannot yet be treated simply as a parallel version of bacteria within the microbiome and should not be assumed to act as general indicators of dysbiosis.

Across available studies, methanogenic archaea, particularly *M. smithii* and *M. intestini*, were the most consistently reported gut archaea. However, their direction of change differed across diseases. Several studies reported enrichment of methanogens in colorectal cancer (CRC) and in some neurological disorders, while others found reductions in inflammatory bowel disease (IBD) (see more details on these aspects in Chapter 3) (78-81). Rather than representing conflicting results, these opposite trends likely reflect the fact that archaea are strongly influenced by the surrounding microbial and physiological environment. Methanogens thrive in fermentation-rich, anaerobic settings and benefit from slower intestinal transit and increased hydrogen production. In contrast, inflamed or oxygen-exposed environments, such as those in Crohn's disease (CD), or conditions with accelerated motility appear to be not ideal to their growth (82, 83). In this sense, archaeal abundance or prevalence seems to reflect ecological opportunity rather than being disease drivers.

In fact, archaea contribute to the gut microbiome community through metabolic interactions, particularly those linked to hydrogen disposal, fermentation efficiency, and redox balance. Their role appears to be more that of metabolic integrators within the gut ecosystem than direct pathogenic actors (78, 84). However, despite intriguing associations, definitive causal evidence remains limited.

A major challenge in interpreting the current archaeome literature is methodological variation. Differences in DNA extraction efficiency, sequencing depth, primer design, and bioinformatic reference databases can substantially affect archaeal detection. Many early studies relied on breath methane tests or 16S amplicon sequencing approaches that were not optimized for archaea (57, 73, 85). These limitations mean that some reported increases or absences of archaea may reflect technical factors rather than true biological differences. Confounding variables such as diet, medication use, antibiotic exposure, bowel transit time, and host physiology have also not been consistently accounted for (29, 86, 87). Together, these issues highlight the need for greater methodological consistency and archaeal-specific approaches in future work. In recognition of these challenges, chapters 2 and 3 included in this thesis were restricted to shotgun metagenomic sequencing datasets, which avoids many of the primer- and amplification-related biases inherent to 16S rRNA–based approaches and allows more reliable detection and quantification of archaeal taxa, and whenever possible, the effect of confounders were taken into consideration.

While variability in host and environmental factors cannot be fully resolved at the review level, this approach enabled a more consistent comparison of archaeal abundance across disease contexts and studies,

Overall, this review brings together the currently scattered evidence linking specific archaeal taxa to human disease and highlights recurring patterns, limitations, and open questions in how these associations are interpreted, suggesting that archaea should be understood as conditional and context-dependent members of the gut microbiome. Their influence appears to depend on the surrounding microbial community, substrate availability, and host physiology. As the field progresses, archaeome research will likely need to move beyond cataloguing species presence toward understanding metabolic flux, syntrophic interactions, spatial organization, and host responses. Such a shift will be essential for accurately defining when and how archaea

contribute to human disease and for evaluating their potential as therapeutic targets, diagnostic markers, or modulators of gut ecosystem resilience.

Chapter 2: **Age-related dynamics of predominant methanogenic archaea in the human gut microbiome (2).**

Understanding how the human gut microbiome evolves across the life course, and particularly in individuals who reach exceptional longevity, has become a central question in microbiome science. While bacterial dynamics during aging have been extensively studied, the archaeome remains comparatively unexplored. This study (2) provides a detailed characterization of archaeal signatures across three distinct age groups comprising young adults (YAs), older adults (OAs), and centenarians (CENT), based on whole-genome shotgun metagenomics. We used age categories rather than a continuous age scale to analyze archaeome changes across the lifespan. Although continuous models can increase statistical power, they were less suitable here because the datasets had an uneven age distribution, with few individuals at very old ages, which could skew results. To our knowledge, this is among the first studies to assess archaeome variation across the aging spectrum, including individuals over 100 years of age, with a particular focus on methanogenic archaea and their functional and ecological interactions.

Our findings demonstrated that gut archaeal diversity and richness tend to decline with advancing age, contrasting earlier 16S rRNA gene–based observations that suggested either stability or a moderate increase in diversity during aging (88, 89). By leveraging shotgun metagenomics rather than marker gene approaches, this study provides higher-resolution evidence that archaeal diversity decreases with age, refining and partially revising conclusions drawn from earlier 16S-based studies. To explore this further, we examined the compositional shifts of the archaeome across different age groups. Consistent with previous studies, we observed that methanogenic archaea, particularly members of the Methanobacteria, generally exhibited higher relative abundances with aging. Prior reports have also described an age-associated rise in members of Methanobacteria and even linked its abundance to pre-longevity stages (90-92).

Interestingly, however, our data indicate that the OAs in our cohort harbored higher relative levels of *M. intestini* rather than *M. smithii*, (*vice versa* to what was observed in YAs and CENT), suggesting a potential species-level replacement or ecological niche shift within the

Methanobrevibacter lineage during aging. Because our analysis is based on cross-sectional data, it remains possible that these patterns partly reflect differences in health or medication profiles between age groups rather than age *per se*. Longitudinal sampling of individuals will be essential to understand these effects.

Another archaeal lineage of interest is the Thermoplasmata, which are recurrently detected in the human gut and have been reported to increase in abundance among OAs (56). Similarly, in our dataset, Thermoplasmata showed elevated relative abundance in OAs, but notably declined again in CENT, approaching levels comparable to those of YAs. This non-linear trend may be ecologically meaningful. Certain Thermoplasmata members encode enzymes involved in the synthesis of potentially genotoxic or proinflammatory metabolites such as methylglyoxal, indole, and acetaldehyde. Thus, their depletion in exceptionally aged individuals might reflect a gut ecosystem more resistant to oxidative or metabolic stress, potentially contributing to healthier aging (88, 93).

Within the Thermoplasmata, functional diversity is considerable. Some members appear capable of metabolizing TMA, a precursor of trimethylamine N-oxide implicated in atherosclerosis, whereas others lack this capacity (94). This heterogeneity complicates the interpretation of their role in host metabolism. Of particular note, *Candidatus* Methanomassiliicoccus intestinalis has been found enriched in frail individuals, raising questions about whether its expansion is a consequence of altered intestinal motility or whether it may actively contribute to inflammatory states. Future studies integrating metatranscriptomic and immunological analyses are required to determine whether Methanomassiliicoccales primarily show protective effects through TMA removal or whether their impact on host physiology is more complex (95, 96). Moreover, as observed in chapter 3 (3) (see below), memebers of Thermoplasmata including *Methanomethylophilus alvus* showed a significant increase in the combined pre-Alzheimer's disease dataset, while *Methanomassiliicoccus intestinalis* and *Methanomassiliicoccus luminyensis* were significantly elevated in Parkinson's disease cohorts. These findings suggest that Thermoplasmatota may be associated with diseases which are mostly associated with old age.

Beyond compositional analysis, network analysis in our study revealed that both *M. smithii* and *M. intestini* consistently co-occurred with Christensenellaceae and Oscillospiraceae. These bacterial families are strongly associated with host genetics, leanness, fiber utilization, and healthy metabolic aging (96, 97). They have been repeatedly linked to longevity (98) and their stable co-presence with methanogens across age groups suggests an archaeal-bacterial metabolic axis or niche sharing likely based on hydrogen transfer and SCFA production.

Notably, CENT exhibited the highest archaeal network connectivity, suggesting that archaea may play a stabilizing role in the gut microbial ecosystem. In contrast, OAs showed the weakest network integration, potentially reflecting a transition phase marked by ecological imbalance or inflammaging (99, 100).

Stratifying individuals by high vs. low methanogen phenotype revealed that this phenotype was twice as prevalent in CENT as in YAs. In centenarians, where total caloric intake and metabolic rate are typically reduced (101), maintaining such cross-domain syntrophy (bacteria–archaea cooperation) may help sustain microbial energy yield and redox balance despite limited substrates. The high methanogen state could therefore act as a marker of a metabolically efficient and ecologically stable gut microbiome that continues to recycle available substrates effectively and resist oxidative or inflammatory stress.

Interestingly, the high methanogen phenotype was associated with reductions in Lachnospiraceae, yet increases in Oscillospiraceae, suggesting compensatory butyrate-producing networks that may buffer against age-associated depletion of core butyrate producers, i.e Lachnospiraceae. Considering the central role of butyrate in supporting intestinal barrier integrity and immune regulation, this compensation could have potential health relevance (102).

The metagenomic results reinforce this idea by showing that subjects with a high methanogen phenotype carry a broader set of genes involved in butyrate production. Although the abundance of these genes differed somewhat across age groups, the two main butyrate-producing routes (the butyryl-CoA:acetate-CoA and butyrate kinase pathways) remained active. Interestingly, genes encoding butyrate kinase (K00929) and phosphate butyryltransferase (K00634) were consistently more abundant in individuals with higher methanogen levels, suggesting that the butyrate kinase pathway may gain importance in supporting SCFA production as people age.

Moreover, the strong significant positive link between members of Oscillospiraceae and butyrate kinase genes, together with the decline of Lachnospiraceae, points to a shift in functional roles as alternative butyrate producers seem to step in and compensate for the loss of the Lachnospiraceae, as SCFA producers.

Overall, this study provides several novel contributions to the understanding of archaeal dynamics during human aging. Most importantly, it represents one of the first species-resolved, shotgun metagenomic investigations of the gut archaeome across the adult aging spectrum, including centenarians, a group rarely captured in archaeome-focused studies. By moving beyond marker gene–based approaches, the work offers new evidence for an age-associated decline in archaeal diversity accompanied by selective enrichment and restructuring of methanogenic archaea, thereby refining previous models of archaeal aging. A key new finding is the identification of a species-level shift within the *Methanobrevibacter* lineage, with differential dominance of *M. intestini* and *M. smithii* across age groups, a pattern that has not been previously reported. Finally, by integrating taxonomic, network, and functional gene analyses, this study newly demonstrates that methanogens act as central nodes in age-dependent microbial interaction networks and are associated with compensatory butyrate-producing pathways in late life, highlighting archaeal contributions to microbiome stability and metabolic organization during aging.

Despite the depth of our analysis, several considerations should be taken, while interpreting our findings. First, the cross-sectional nature of the cohorts provides only a snapshot of archaeal and microbial states at specific ages. As a result, we cannot distinguish true age-driven microbiome trends from cohort effects, lifestyle differences between generations, or individual variation. Longitudinal studies following individuals across the aging process, ideally with repeated biological sampling and detailed health monitoring, will be essential to establish causal links between archaeal dynamics and aging outcomes. Additionally, although the study populations were recruited from comparable European settings, metadata such as detailed diet information, medication history, bowel transit time, frailty measures, and immune phenotype were not uniformly available. These factors, which are strongly associated with microbiome structure in late life, could affect archaeal patterns and should be taken into consideration in future work to strengthen causal inference and to understand host–microbiome interactions (103-106).

Another limitation relates to the integration of three independently generated cohorts. While batch-effect control was applied and effectively reduced technical variation below the biological signals of interest, differences in sample handling, DNA extraction, storage, or sequencing depth cannot be entirely excluded. Harmonized cohorts would help confirm the reproducibility of archaeal aging signatures. Furthermore, although our results strongly suggest archaeal contributions to butyrate-associated pathways and syntrophic interactions, through shotgun metagenomics, direct functional validation is required. Future studies incorporating metatranscriptomics, and targeted metabolomics, including SCFA and methane measurements, will be critical to confirm whether archaeal pathways are transcriptionally and metabolically active across aging.

Finally, co-occurrence networks employed in this study capture ecological association rather than direct interaction, meaning that physical proximity, hydrogen exchange, and metabolic cross-feeding between archaea and bacterial partners remain inferred rather than demonstrated. Experimental validation through spatially resolved technologies such as advanced FISH platforms, imaging mass cytometry, and isotope tracing, alongside archaeal–bacterial co-culture and gnotobiotic models, will be essential to reveal the mechanistic basis of archaeal syntrophy and its potential role in maintaining metabolic resilience in longevity. As a whole, future research combining longitudinal sampling, harmonized metadata collection, multi-omics measurements, and experimental validation will enable a more definitive understanding of how archaea contribute to healthy aging and whether targeted dietary or microbiome-based approaches can modulate archaeal communities to support metabolic robustness in late life.

Chapter 3: Cross-domain metabolic interactions link *Methanobrevibacter smithii* to colorectal cancer microbial ecosystems (3).

By investigating stool metagenomes across diverse disease contexts which have been previously linked with archaea, this study (3) provides a unified view of archaeal dynamics in human health and disease. Previous work on the human archaeome has been limited by fragmented methodologies, 16S-based taxonomic constraints, and small cohort sizes, often leading to inconsistent or incomplete interpretations of archaeal behavior in disease settings (92, 107, 108), as discussed in chapter 1. By reprocessing shotgun data and covariate-aware case-control matching, our analysis clarifies when, where, and how archaeal shifts are

detectable and biologically meaningful, moving beyond scattered observations to a more consistent view across diseases.

While the bacterial microbiome exhibits well-documented disease-specific dysbiosis pattern (109-114), archaeal responses have been less consistent in the literature. This meta-analysis (3) represents one of the most comprehensive attempts so far to disentangle the role of Archaea across major human diseases, previously shown to be associated with archaeal shifts as reviewed in our study (Figure 1) (3) using shotgun metagenomic data. By integrating 2,959 samples from diverse cohorts (including CRC, type 2 diabetes (T2D), IBD, including CD and ulcerative colitis (UC), multiple sclerosis (MS), Alzeihmer's disease (AD), schizophrenia (SCZ), and parkinson's disease (PD)) and adjusting for confounders such as age, sex, and BMI for case-control samples, we aimed to move beyond the methodological fragmentation that has long hindered archaeome research. Despite differences in study design, sequencing platforms, and metadata resolution, our analysis uncovered reproducible, disease-associated shifts in archaeal community structure, highlighting that the human archaeome participates in disease-linked microbial reorganization.

Interestingly, these alterations were not universal but disease-specific, suggesting that archaea respond to particular ecological or physiological disturbances rather than showing a uniform pattern of change. In CD, for example, we observed a significant reduction in most *Methanobrevibacter* species, alongside enrichment of a single taxon, Methanobrevibacter_A_sp900766745. This inverse pattern within a single genus suggests that even closely related methanogens may differ in their environmental tolerance and syntrophic dependencies. CD is characterized by accelerated intestinal transit, altered substrate availability, and inflammatory stress. These factors disadvantage slow-growing methanogens like *M. smithii*, which rely on stable cross-feeding networks with hydrogen-producing bacteria (115). It is therefore plausible that inflammatory dysmotility selectively filters archaeal populations, allowing more resilient taxa to persist.

In contrast, SCZ showed a significant depletion of Methanobrevibacter_A_smithii. Although this association does not imply causation, it supports the idea that archaeal metabolism could be indirectly connected to host neurochemistry through its influence on fermentation end products and hydrogen balance (116, 117). Methanogens help stabilize microbial redox status by consuming hydrogen and formate, both of which affect SCFA production and intestinal pH

(118). A reduction in methanogenic activity might therefore shift metabolic fluxes in a way that modulates the gut–brain axis, since SCFAs are metabolites increasingly recognized as central mediators of the gut–brain axis, influencing neuroinflammation, neurotransmitter metabolism, and the integrity of the blood–brain barrier (119). While speculative, this link is intriguing in light of emerging evidence connecting gut redox potential and microbial metabolites to neurotransmission and inflammation in neuropsychiatric disorders.

In PD, our initial pooled analysis revealed an enrichment of methanogenic taxa, which was consistent with previous findings (79, 120). However, after stringent case-control matching for age, sex, and BMI, these differences no longer reached statistical significance within individual datasets. This pattern highlights one of the recurring challenges in archaeome research, which is the fragility of statistical signals to metadata handling and cohort structure.

Across disorders, the biggest challenge remains the limited metadata coverage. Important host-related variables such as medication use, antibiotic exposure, bowel transit time, diet, and inflammation status were rarely reported across studies. These factors are known to shape the gut microbiome and are particularly relevant for archaea, whose growth depends on specific substrate availability and redox balance (121-124). The absence of such information makes it difficult to distinguish true biological patterns from confounding environmental effects. Standardizing these metadata across future archaeome-focused studies will therefore be essential.

Among all diseases investigated, CRC exhibited the most consistent and biologically plausible archaeal signal. We observed a robust significant enrichment of Methanobrevibacter_A_smithii across pooled dataset as well as individual cohorts (i.e, Feng et al. (75), Gupta et al. (76)). Notably, when staging information was available, *M. smithii* abundance followed a non-linear trend: higher abundance at stage 0, reduced in early invasive cancer (stage I/II), and increased again in advanced or metastatic disease (stage III/IV), which was consistent with previous studies (125, 126). This pattern suggests that archaeal proliferation might not be an early initiating factor, but rather a secondary response to late-stage ecological remodeling within the tumor-altered gut. Such remodeling is consistent with increased mucin degradation, amino acid fermentation, and hydrogen accumulation observed in advanced CRC (127).

Finding this pattern across pooled dataset and independent cohorts, alongside identification of *M. smithii* as a top discriminatory feature in machine-learning models, indicates that methanogens may be integrated into CRC-specific ecological networks rather than responding solely to generalized gut disturbance. Importantly, this challenges prior assumptions that methanogens are uniformly beneficial by promoting fermentative efficiency and gut transit (128, 129); instead, our findings suggest a metabolic role within the tumor-altered colon. Mechanistic integration across correlation networks, in silico metabolic modeling, and anaerobic co-culture experiments revealed interesting metabolic cross-feeding patterns between *M. smithii* and CRC-associated bacteria.

While several studies have reported a loss of overall microbial co-occurrence in CRC as community structure becomes increasingly disordered (109, 110), our analysis reveals that specific archaeal–bacterial partnerships persist or even strengthen within this disrupted microbiome. In particular, Methanobrevibacter_A_smithii displayed positive co-occurrence with key CRC-associated bacteria including *F. nucleatum*, *B. fragilis*, and *E. coli*. This pattern was supported both by correlation analysis and binary presence/absence data.

Our metabolic modeling and experimental validation highlight *M. smithii* as an active metabolic partner within CRC-associated microbial networks rather than a passive hydrogen sink. In silico genome-scale metabolic reconstructions predicted a universal export of succinate by CRC-associated bacteria and its uptake by *M. smithii*. Succinate is a central intermediate in anaerobic metabolism and a known cross-fed metabolite in syntrophic communities (130). Elevated succinate levels have been repeatedly observed in the CRC tumor microenvironment, where they can function as signaling molecules, stabilize HIF-1α, and promote inflammation and tumor growth (131). Thus, the predicted succinate uptake by *M. smithii* suggests a potential role in buffering tumor-associated metabolite accumulation under hypoxic conditions.

Interestingly, *M. smithii* was also predicted to export riboflavin (vitamin B_2) and import several amino acids enriched in CRC metabolomes, including asparagine, glutamine, leucine, and arginine. These metabolites are central to cancer cell metabolism, supporting nucleotide synthesis, energy generation, and redox control (132, 133).

Experimental co-culture assays validated several of these predicted interactions. *M. smithii* growth increased significantly in the presence of *B. fragilis*, while *F. nucleatum* and *E. coli*

exhibited archaeon-induced early growth acceleration. These results support commensal or unidirectional relationships, where *M. smithii* supports bacterial partners through hydrogen or metabolite removal but gains little direct growth benefit. Notably, *B. fragilis* produces large amounts of succinate during carbohydrate fermentation (134), consistent with the enhanced *M. smithii* growth observed in their co-culture.

Untargeted metabolomics further confirmed elevated succinate levels in all co-cultures, supporting our genome-scale predictions. The *F. nucleatum–M. smithii* pairing showed the most extensive metabolic shift, with increased production of SCFAs (acetate, lactate, propionate, and butyrate) and several amino acids (alanine, valine, leucine, isoleucine, phenylalanine, proline, glycine). Many of these metabolites have been repeatedly associated with CRC progression and tumor metabolism (135-137).

Regarding the results on butyrate, findings from this chapter and those from chapter 2 highlight that the role of butyrate is highly context-dependent. In CENTs, an increased genetic potential for butyrate production aligns with a microbiome configuration associated with gut health, anti-inflammatory effects, and longevity. In contrast, in a CRC setting, butyrate emerges within microbial interactions, particularly involving *M. smithii* and *F. nucleatum*, that are linked to tumor-promoting metabolic environments. These seemingly opposing observations can be explained by the "butyrate paradox": while butyrate supports normal colon cell function and gut homeostasis, its effects change in cancer, where altered cellular metabolism can shift its role toward influencing tumor-related pathways. Overall, this suggests that butyrate should not be viewed as inherently beneficial or harmful, but rather as a metabolite whose impact depends on the surrounding microbial community and the physiological state of the host (138).

Beyond SCFAs and amino acid changes, several oncologically relevant metabolites were detected in the co-culture of *F. nucleatum–M. smithii*, including arginine derivatives (N-α-acetyl-L-arginine, N-acetyl-arginine, N-δ-acetylornithine), which feed into nitric oxide and polyamine biosynthetic pathways, both of which are involved in CRC proliferation and immune evasion (139). Other detected compounds such as hypoxanthine and indole-3-propionate (I3P) also link microbial metabolism to cancer metabolism and immune modulation (140).

Interestingly, some metabolites with potential tumor-suppressive properties, including γ-linolenic acid and 4E,8Z-sphingadiene, were also detected in *F. nucleatum–M. smithii* co-

cultures, both of which have been implicated in ferroptosis and apoptosis of cancer cells (141). These observations suggest that archaea might contribute not only to pro-tumor but also anti-tumor metabolic pools within the gut.

Together, our findings show *M. smithii* as a metabolically active member of CRC-associated microbial communities. Rather than functioning as a passive hydrogen consumer, *M. smithii* appears capable of shaping its surroundings through a network of cooperative metabolic exchanges. By engaging with key bacterial taxa, it may influence their growth dynamics and collectively contribute to a complex metabolic environment enriched in metabolites with both tumor-promoting and tumor-suppressive properties. Such bidirectional interactions suggest that *M. smithii* participates in maintaining, and possibly amplifying, metabolic cross-talk within the tumor microenvironment. Understanding how host conditions regulate the balance between beneficial and detrimental archaeal–bacterial interactions will be essential for clarifying whether *M. smithii* supports tumor-associated dysbiosis or contributes to microbial stability under stress. Finally, integrating archaeal metabolism into CRC models may open new perspectives on microbe-driven mechanisms of disease progression and opportunities for targeted therapeutic modulation.

Several important limitations should be acknowledged when interpreting these findings. First, our meta-analysis is cross-sectional in nature, which limits the ability to determine causality or the sequence of archaeal–bacterial changes during disease progression. Longitudinal studies following individuals over time will be essential to reveal whether archaeal expansion precedes disease onset or simply indicates downstream ecological shifts in a disturbed gut environment.

Second, despite consistent bioinformatic processing across datasets, absolute abundance data were not uniformly available, and many original studies might have not been optimized for archaeal detection during DNA extraction. This likely led to an underestimation of archaeal abundance and diversity. Future work will benefit from archaeal-inclusive extraction methods, and absolute quantification strategies that can more accurately capture archaeal contributions within complex microbial communities.

Third, host factors that shape archaeal ecology, including diet, medications, and bowel transit time were incompletely recorded across cohorts. Future studies should therefore integrate detailed clinical, lifestyle, and physiological metadata to more accurately investigate archaeal–

host interactions. Residual confounding remains an important consideration when interpreting the association between *M. smithii* and CRC. Among these factors, gut transit time likely plays the most prominent role. Because CRC is often accompanied by constipation, the resulting slow-transit environment may favor methanogen growth, meaning that part of the observed enrichment could reflect underlying gut physiology rather than a tumor-specific effect (142). However, the fact that the association persists even after accounting for transit-related measures suggests that it cannot be fully explained by this mechanism alone. Other factors, such as diet and medication or antibiotic use, are known to influence the gut archaeome, but their effects appear to be relatively modest and inconsistent, contributing more to variability than to systematic bias. Similarly, methodological differences across studies may affect how well archaea are detected, but are unlikely to drive the biological signal itself (78, 143, 144). These considerations suggest that improved standardization, particularly with respect to gut transit, would likely reduce the strength of the observed association, but not eliminate it entirely.

Fourth, while our results demonstrate a consistent enrichment of *M. smithii* in CRC across multiple cohorts, the directionality of this association remains unresolved and likely reflects a complex, context-dependent relationship. Notably, the observed nonlinear pattern across disease stages, characterized by enrichment in early lesions, reduction in intermediate stages, and re-enrichment in advanced CRC does not support a simple linear driver model.
An alternative interpretation is that CRC-associated changes in the gut environment, including altered substrate availability, inflammation, and intestinal transit dynamics, may create ecological conditions that favor the growth and persistence of methanogens such as *M. smithii*. Indeed, factors such as constipation and shifts in microbial fermentation have previously been linked to increased methanogen abundance, suggesting that enrichment may, at least in part, reflect a response to disease-associated environmental changes.
At the same time, our metabolic modeling and co-culture experiments indicate that *M. smithii* can actively participate in microbial cross-feeding networks, influencing the availability of metabolites such as succinate and amino acids that are relevant to tumor biology. This raises the possibility that *M. smithii* contributes to shaping the metabolic landscape of the CRC-associated microbiome once established.

Fifth, our *in vitro* co-culture system represents a controlled but simplified approximation of the colonic environment. While necessary to achieve comparable starting biomass, pre-enrichment

of *M. smithii* may bias ecological balance relative to natural systems. Moreover, these experiments were performed under nutrient-rich anaerobic conditions that cannot fully consider colonic nutrient gradients, mucin-rich matrices, immune pressures, or tumor-microenvironment complexity. Although the observed metabolic cross-feeding and morphological interaction signatures provide mechanistic insight, phenotypes *in vivo* are likely to be modulated by additional host and microbial factors. Future efforts should incorporate tumor-mimetic microfluidic systems, mucus scaffolds, and gnotobiotic mouse models to refine ecological interpretation. Moreover, although we used *M. smithii* strain ALI in our study which is a human gut-derived isolate, and supports its ecological relevance for modeling archaeal function in the intestinal environment, strain ALI represents a single strain and may not capture the full extent of strain-level heterogeneity within *M. smithii* populations (145). Accordingly, while ALI provides a biologically meaningful and experimentally tractable model, further strain-resolved studies with more strains obtained from human gut (e.g. *M. smithii* Graz 2) will be required to assess the generalizability of these findings.

Finally, although our combined observational, computational, and experimental evidence supports syntrophic coupling between *M. smithii* and CRC-associated bacteria such as *F. nucleatum*, direct *in situ* proof of physical co-localization remains scarce. Spatial ecology tools, including single-molecule FISH, spatial metabolomics, and imaging mass cytometry, will be critical to determine whether archaeal–bacterial interactions are structured within tumor-associated niche.

Conclusion

The review component establishes the current state of knowledge on human-associated archaea, highlighting both their widespread occurrence and the persistent methodological challenges that have limited their investigation. Although no archaeal pathogens have been identified to date, accumulating evidence indicates that methanogens, particularly members of the genus *Methanobrevibacter*, are metabolically active and tightly integrated into microbial networks through syntrophic interactions. It also shows that archaea should not be considered marginal components of the microbiome, but rather as organisms with the potential to influence microbial community structure and function.

Building on this conceptual framework, the aging-focused metagenomic analysis reveals pronounced age-related dynamics within the archaeal microbiome. While overall archaeal diversity decreases with age, the prevalence of methanogens and the frequency of a high-methanogen phenotype increase. Notably, centenarians exhibit an archaeal composition more similar to younger adults than to older adults, characterized by the co-occurrence of *Methanobrevibacter smithii* and *Methanobrevibacter intestini* within highly connected microbial networks. These findings suggest that specific archaeal–bacterial interactions may contribute to microbiome stability during extreme aging and potentially compensate for age-related losses of key bacterial taxa, particularly butyrate-producing lineages. Rather than reflecting a simple decline, the archaeome appears to undergo selective restructuring across the human lifespan.

The disease-oriented meta-analysis further demonstrates that archaeal alterations are visible across human diseases but highly heterogeneous. Among the conditions analyzed, colorectal cancer emerges as the most consistently associated with changes in the gut archaeome. Across multiple independent cohorts, *M. smithii* is reproducibly enriched in colorectal cancer (CRC) patients and integrated into disease-associated microbial networks. Mechanistic analyses indicate that this archaeon engages in extensive metabolic interactions with CRC–associated bacteria, including the exchange of metabolites with known relevance to tumor biology. These findings support the notion that archaea may participate in disease-associated microbiome configurations through indirect metabolic effects rather than through direct pathogenic mechanisms.

Despite these advances, several important questions remain unresolved. Methodological limitations continue to constrain archaeome research, including incomplete reference databases, primer coverage, and bioinformatic pipelines that are not optimized for archaeal detection. Future studies would benefit from standardized protocols specifically designed to capture archaeal diversity and activity, enabling more robust comparisons across cohorts and conditions.

From a biological perspective, most findings presented here are associative. Longitudinal studies and controlled experimental systems will be required to determine causality, particularly in the context of aging and CRC. Gnotobiotic models, defined microbial consortia, and targeted perturbation experiments could help clarify whether methanogens actively contribute to microbiome stability and disease progression or whether they primarily respond to ecological niches created by bacterial and host-derived factors.

The dual association of methanogens with both healthy aging and colorectal cancer highlights the importance of ecological context. Future research should focus on strain-level resolution, functional heterogeneity, and interaction specificity to determine under which conditions archaeal activity may be beneficial or detrimental to the host. Incorporating the archaeome into future studies will be essential for developing a more complete understanding of microbial ecology in human health, aging, and disease

References

1. Mohammadzadeh R, Mahnert A, Duller S, Moissl-Eichinger C. Archaeal key-residents within the human microbiome: characteristics, interactions and involvement in health and disease. Current Opinion in Microbiology. 2022;67.
2. Mohammadzadeh R, Mahnert A, Shinde T, Kumpitsch C, Weinberger V, Schmidt H, et al. Age-related dynamics of predominant methanogenic archaea in the human gut microbiome. BMC Microbiology. 2025;25(1).
3. Mohammadzadeh R, Mahnert A, Zurabishvili T, Wink L, Kumpitsch C, Habisch H, et al. Cross-domain metabolic interactions link
to colorectal cancer microbial ecosystems. Nature Communications. 2026;17(1).
4. Woese CR, Fox GE. Phylogenetic structure of the prokaryotic domain: The primary kingdoms. Proceedings of the National Academy of Sciences. 2011;74(11):5088-90.
5. Martiny JBH, Bohannan BJM, Brown JH, Colwell RK, Fuhrman JA, Green JL, et al. Microbial biogeography: putting microorganisms on the map. Nature Reviews Microbiology. 2006;4(2):102-12.
6. Almeida A, Mitchell AL, Boland M, Forster SC, Gloor GB, Tarkowska A, et al. A new genomic blueprint of the human gut microbiota. Nature. 2019;568(7753):499-504.
7. Albers S-V, Meyer BH. The archaeal cell envelope. Nature Reviews Microbiology. 2011;9(6):414-26.
8. McDougall M, Francisco O, Harder-Viddal C, Roshko R, Meier M, Stetefeld J. Archaea S-layer nanotube from a "black smoker" in complex with cyclo-octasulfur rings. Proteins. 2017;85(12):2209-16.
9. Heimerl T, Flechsler J, Pickl C, Heinz V, Salecker B, Zweck J, et al. A complex endomembrane system in the archaeon Ignicoccus hospitalis tapped by Nanoarchaeum equitans. Frontiers in Microbiology. 2017;8.
10. Kletzin A, Heimerl T, Flechsler J, van Niftrik L, Rachel R, Klingl A. Cytochromes c in Archaea: distribution, maturation, cell architecture, and the special case of Ignicoccus hospitalis. Frontiers in Microbiology. 2015;6.
11. Forterre P. The common ancestor of archaea and eukarya was not an archaeon. Archaea. 2013;2013:372396.
12. Reinhard R, Meyer C, Klingl A, Gürster S, Heimerl T, Wasserburger N, et al. Analysis of the ultrastructure of Archaea by Eelectron microscopy. Electron Microscopy of Model Systems. Methods in Cell Biology2010. p. 47-69.
13. Gribaldo S, Brochier-Armanet C. The origin and evolution of Archaea: a state of the art. Philosophical Transactions of the Royal Society B: Biological Sciences. 2006;361(1470):1007-22.
14. Koga Y, Morii H. Biosynthesis of ether-type polar lipids in archaea and evolutionary considerations. Microbiology and Molecular Biology Reviews. 2007;71(1):97-120.
15. Albers S-V, Jarrell KF. The archaellum: how archaea swim. Frontiers in Microbiology. 2015;6.
16. Perras AK, Daum B, Ziegler C, Takahashi LK, Ahmed M, Wanner G, et al. S-layers at second glance? Altiarchaeal grappling hooks (hami) resemble archaeal S-layer proteins in structure and sequence. Frontiers in Microbiology. 2015;6.
17. Hansen J, Mailand E, Swaminathan KK, Schreiber J, Angelici B, Benenson Y. Transplantation of prokaryotic two-component signaling pathways into mammalian cells. Proceedings of the National Academy of Sciences. 2014;111(44):15705-10.

18. Gupta AB, Seedorf H. Structural and functional insights from the sequences and complex domain architecture of adhesin-like proteins from Methanobrevibacter smithii and Methanosphaera stadtmanae. Frontiers in Microbiology. 2024;15.
19. Gupta AB, Seedorf H. Structural and functional insights from the sequences and complex domain architecture of adhesin-like proteins from Methanobrevibacter smithii and Methanosphaera stadtmanae. Front Microbiol. 2024;15:1463715.
20. Fröls S. Archaeal biofilms: widespread and complex. Biochemical Society Transactions. 2013;41(1):393-8.
21. Weinberger V, Darnhofer B, Thapa HB, Mertelj P, Stentz R, Jones E, et al. Proteomic and metabolomic profiling of extracellular vesicles produced by human gut archaea. Nature Communications. 2025;16(1).
22. Novikova PV, Bhanu Busi S, Probst AJ, May P, Wilmes P. Functional prediction of proteins from the human gut archaeome. ISME Communications. 2024;4(1).
23. Robertson CE, Harris JK, Spear JR, Pace NR. Phylogenetic diversity and ecology of environmental Archaea. Current Opinion in Microbiology. 2005;8(6):638-42.
24. Mattiroli F, Bhattacharyya S, Dyer PN, White AE, Sandman K, Burkhart BW, et al. Structure of histone-based chromatin in Archaea. Science. 2017;357(6351):609-12.
25. Bennett HM. Microbial genomes as cheat sheets. Nature Reviews Microbiology. 2013;11(5):302-.
26. Spang A, Saw JH, Jørgensen SL, Zaremba-Niedzwiedzka K, Martijn J, Lind AE, et al. Complex archaea that bridge the gap between prokaryotes and eukaryotes. Nature. 2015;521(7551):173-9.
27. Guo L-T, Amikura K, Jiang H-K, Mukai T, Fu X, Wang Y-S, et al. Ancestral archaea expanded the genetic code with pyrrolysine. Journal of Biological Chemistry. 2022;298(11).
28. Pasolli E, Asnicar F, Manara S, Zolfo M, Karcher N, Armanini F, et al. Extensive Unexplored Human Microbiome Diversity Revealed by Over 150,000 Genomes from Metagenomes Spanning Age, Geography, and Lifestyle. Cell. 2019;176(3):649-62.e20.
29. Gaci N, Borrel G, Tottey W, O'Toole PW, Brugère J-F. Archaea and the human gut: New beginning of an old story. World Journal of Gastroenterology. 2014;20(43).
30. Tang WHW, Wang Z, Levison BS, Koeth RA, Britt EB, Fu X, et al. Intestinal Microbial Metabolism of Phosphatidylcholine and Cardiovascular Risk. New England Journal of Medicine. 2013;368(17):1575-84.
31. Feehan B, Ran Q, Dorman V, Rumback K, Pogranichniy S, Ward K, et al. Novel complete methanogenic pathways in longitudinal genomic study of monogastric age-associated archaea. Anim Microbiome. 2023;5(1):35.
32. Fricke WF, Seedorf H, Henne A, Krüer M, Liesegang H, Hedderich R, et al. The genome sequence of Methanosphaera stadtmanae reveals why this human intestinal archaeon is restricted to methanol and H2 for methane formation and ATP synthesis. Journal of Bacteriology. 2006;188(2):642-58.
33. Samuel BS, Gordon JI. A humanized gnotobiotic mouse model of host–archaeal–bacterial mutualism. Proceedings of the National Academy of Sciences. 2006;103(26):10011-6.
34. Ruaud A, Esquivel-Elizondo S, de la Cuesta-Zuluaga J, Waters JL, Angenent LT, Youngblut ND, et al. Syntrophy via interspecies H2 transfer between Christensenella and Methanobrevibacter underlies their global cooccurrence in the human gut. mBio. 2020;11(1).
35. Wang T, Leibrock N, Plugge CM, Smidt H, Zoetendal EG. In vitro interactions between Blautia hydrogenotrophica, Desulfovibrio piger and Methanobrevibacter smithii under hydrogenotrophic conditions. Gut Microbes. 2023;15(2).

36. Minnebo Y, De Paepe K, Props R, Lacoere T, Boon N, Van de Wiele T. Methanogenic archaea quantification in the human gut microbiome with f420 autofluorescence-based flow cytometry. Applied Microbiology. 2024;4(1):162-80.
37. Duller S, Vrbancic S, Szydłowski Ł, Mahnert A, Blohs M, Predl M, et al. Targeted isolation of Methanobrevibacter strains from fecal samples expands the cultivated human archaeome. Nature Communications. 2024;15(1).
38. Bai X, Sun Y, Li Y, Li M, Cao Z, Huang Z, et al. Landscape of the gut archaeome in association with geography, ethnicity, urbanization, and diet in the Chinese population. Microbiome. 2022;10(1).
39. Chibani CM, Mahnert A, Borrel G, Almeida A, Werner A, Brugère J-F, et al. A catalogue of 1,167 genomes from the human gut archaeome. Nature Microbiology. 2021;7(1):48-61.
40. Coker OO, Wu WKK, Wong SH, Sung JJY, Yu J. Altered gut archaea composition and interaction with bacteria are associated with colorectal cancer. Gastroenterology. 2020;159(4):1459-70.e5.
41. Gill SR, Pop M, DeBoy RT, Eckburg PB, Turnbaugh PJ, Samuel BS, et al. Metagenomic analysis of the human distal gut microbiome. Science. 2006;312(5778):1355-9.
42. Rieu-Lesme F, Delbès C, Sollelis L. Recovery of partial 16s rdna sequences suggests the presence of crenarchaeota in the human digestive ecosystem. Current Microbiology. 2005;51(5):317-21.
43. Nam Y-D, Chang H-W, Kim K-H, Roh SW, Kim M-S, Jung M-J, et al. Bacterial, archaeal, and eukaryal diversity in the intestines of Korean people. The Journal of Microbiology. 2008;46(5):491-501.
44. Khelaifia S, Raoult D. Haloferax massiliensis sp. nov., the first human-associated halophilic archaea. New Microbes and New Infections. 2016;12:96-8.
45. Koskinen K, Pausan MR, Perras AK, Beck M, Bang C, Mora M, et al. First insights into the diverse human archaeome: specific detection of archaea in the gastrointestinal tract, lung, and nose and on skin. mBio. 2017;8(6).
46. Mahnert A, Dreer M, Perier Ü, Melcher M, Duller S, Lehnen A, et al. Molecular tracking and cultivation reveal ammonia oxidizing Archaea as integral members of the human skin microbiome. bioRxiv. 2025.
47. Moissl-Eichinger C, Probst AJ, Birarda G, Auerbach A, Koskinen K, Wolf P, et al. Human age and skin physiology shape diversity and abundance of Archaea on skin. Scientific Reports. 2017;7(1).
48. Bouzid F, Gtif I, Charfeddine S, Abid L, Kharrat N. Polyphasic molecular approach to the characterization of methanogens in the saliva of Tunisian adults. Anaerobe. 2024;85.
49. Pilliol V, Beye M, Terlier L, Balmelle J, Kacel I, Lan R, et al. Methanobrevibacter massiliense and Pyramidobacter piscolens Co-Culture Illustrates Transkingdom Symbiosis. Microorganisms. 2024;12(1).
50. Koskinen K, Pausan MR, Perras AK, Beck M, Bang C, Mora M, et al. First insights into the diverse human archaeome: specific detection of archaea in the gastrointestinal tract, lung, and nose and on skin. Mbio. 2017;8(6).
51. Belay N, Mukhopadhyay B, Demacario EC, Galask R, Daniels L. Methanogenic bacteria in human vaginal samples. J Clin Microbiol. 1990;28(7):1666-8.
52. Grine G, Drouet H, Fenollar F, Bretelle F, Raoult D, Drancourt M. Detection of Methanobrevibacter smithii in vaginal samples collected from women diagnosed with bacterial vaginosis. Eur J Clin Microbiol. 2019;38(9):1643-9.

53. Malat I, Bossi V, Drancourt M, Grine G, Ruimy R. Methanobrevibacter smithii strain U29 whole genome sequence delineates M. smithii intermediate cell variants. BMC Res Notes. 2025;18(1):414.
54. Neumann CJ, Mohammadzadeh R, Woh PY, Kobal T, Pausan MR, Shinde T, et al. First-year dynamics of the anaerobic microbiome and archaeome in infants' oral and gastrointestinal systems. Msystems. 2025;10(1).
55. Grine G, Boualam MA, Drancourt M. Methanobrevibacter smithii, a methanogen consistently colonising the newborn stomach. Eur J Clin Microbiol. 2017;36(12):2449-55.
56. Dridi B, Henry M, Richet H, Raoult D, Drancourt M. Age-related prevalence of Methanomassiliicoccus luminyensis in the human gut microbiome. Apmis. 2012;120(10):773-7.
57. Pausan MR, Csorba C, Singer G, Till H, Schöpf V, Santigli E, et al. Exploring the archaeome: detection of archaeal signatures in the human body. Frontiers in Microbiology. 2019;10.
58. Togo AH, Grine G, Khelaifia S, des Robert C, Brevaut V, Caputo A, et al. Culture of methanogenic archaea from human colostrum and milk. Scientific Reports. 2019;9(1).
59. Bai XW, Sun Y, Li Y, Li MJ, Cao ZR, Huang ZY, et al. Landscape of the gut archaeome in association with geography, ethnicity, urbanization, and diet in the Chinese population. Microbiome. 2022;10(1).
60. Pan C, Hoffmann C, Dollive S, Grunberg S, Chen J, Li H, et al. Archaea and fungi of the human gut microbiome: correlations with diet and bacterial residents. PLoS ONE. 2013;8(6).
61. Kumpitsch C, Fischmeister FPS, Mahnert A, Lackner S, Wilding M, Sturm C, et al. Reduced B12 uptake and increased gastrointestinal formate are associated with archaeome-mediated breath methane emission in humans. Microbiome. 2021;9(1).
62. Goodrich Julia K, Waters Jillian L, Poole Angela C, Sutter Jessica L, Koren O, Blekhman R, et al. Human genetics shape the gut microbiome. Cell. 2014;159(4):789-99.
63. Goodrich Julia K, Davenport Emily R, Beaumont M, Jackson Matthew A, Knight R, Ober C, et al. Genetic determinants of the gut microbiome in UK twins. Cell Host & Microbe. 2016;19(5):731-43.
64. Kurilshikov A, Medina-Gomez C, Bacigalupe R, Radjabzadeh D, Wang J, Demirkan A, et al. Large-scale association analyses identify host factors influencing human gut microbiome composition. Nature Genetics. 2021;53(2):156-65.
65. Foligne B, Bang C, Weidenbach K, Gutsmann T, Heine H, Schmitz RA. The intestinal archaea methanosphaera stadtmanae and methanobrevibacter smithii activate human dendritic cells. PLoS ONE. 2014;9(6).
66. Vierbuchen T, Bang C, Rosigkeit H, Schmitz RA, Heine H. The human-associated archaeon Methanosphaera stadtmanae is recognized through its RNA and induces TLR8-dependent NLRP3 inflammasome activation. Frontiers in Immunology. 2017;8.
67. Proost P, Bang C, Vierbuchen T, Gutsmann T, Heine H, Schmitz RA. Immunogenic properties of the human gut-associated archaeon Methanomassiliicoccus luminyensis and its susceptibility to antimicrobial peptides. Plos One. 2017;12(10).
68. Jin M, Hu J, Tian C, Wu H, Wang B, Wang Y, et al. Methanobrevibacter smithii activates immune microenvironment of intestinum tenue in a mouse model. Archives of Microbiology. 2026;208(4).
69. Zhang X, Li N, Shao H, Meng Y, Wang L, Wu Q, et al. Methane limit LPS-induced NF-κB/MAPKs signal in macrophages and suppress immune response in mice by enhancing PI3K/AKT/GSK-3β-mediated IL-10 expression. Scientific Reports. 2016;6(1).

70. Poles MZ, Juhász L, Boros M. Methane and inflammation - A review (fight fire with fire). Intensive Care Medicine Experimental. 2019;7(1).
71. Robinson NP, Mahnert A, Blohs M, Pausan M-R, Moissl-Eichinger C. The human archaeome: methodological pitfalls and knowledge gaps. Emerging Topics in Life Sciences. 2018;2(4):469-82.
72. Mirete S, Sánchez-Costa M, Díaz-Rullo J, González de Figueras C, Martínez-Rodríguez P, González-Pastor JE. Metagenome-Assembled Genomes (MAGs): advances, challenges, and ecological insights. Microorganisms. 2025;13(5).
73. Mahnert A, Blohs M, Pausan M-R, Moissl-Eichinger C. The human archaeome: methodological pitfalls and knowledge gaps. Emerging Topics in Life Sciences. 2018;2(4):469-82.
74. Adrian MA, Ayati BP, Mangalam AK. A mathematical model of Bacteroides thetaiotaomicron, Methanobrevibacter smithii, and Eubacterium rectale interactions in the human gut. Sci Rep. 2023;13(1):21192.
75. Feng Q, Liang S, Jia H, Stadlmayr A, Tang L, Lan Z, et al. Gut microbiome development along the colorectal adenoma–carcinoma sequence. Nature Communications. 2015;6(1):6528.
76. Gupta A, Dhakan DB, Maji A, Saxena R, Prasoodanan VPK, Mahajan S, et al. Association of Flavonifractor plautii, a flavonoid-degrading bacterium, with thegut microbiome of colorectal cancer patients in India. mSystems. 2019;4(6).
77. Baehren C, Buedding E, Bellm A, Schult F, Pembaur A, Wirth S, et al. The relevance of the bacterial microbiome, archaeome and mycobiome in pediatric asthma and respiratory disorders. Cells. 2022;11(8).
78. Li T, Coker OO, Sun Y, Li S, Liu C, Lin Y, et al. Multi-cohort analysis reveals altered Archaea in colorectal cancer fecal samples across populations. Gastroenterology. 2025;168(3):525-38.e2.
79. Wallen ZD, Demirkan A, Twa G, Cohen G, Dean MN, Standaert DG, et al. Metagenomics of Parkinson's disease implicates the gut microbiome in multiple disease mechanisms. Nature Communications. 2022;13(1).
80. Scanlan PD, Shanahan F, Marchesi JR. Human methanogen diversity and incidence in healthy and diseased colonic groups using mcrA gene analysis. BMC Microbiology. 2008;8(1).
81. Ghavami SB, Rostami E, Sephay AA, Shahrokh S, Balaii H, Aghdaei HA, et al. Alterations of the human gut Methanobrevibacter smithii as a biomarker for inflammatory bowel diseases. Microbial Pathogenesis. 2018;117:285-9.
82. Sahakian AB, Jee S-R, Pimentel M. Methane and the gastrointestinal tract. Digestive Diseases and Sciences. 2009;55(8):2135-43.
83. Riedel CU, Blais Lecours P, Marsolais D, Cormier Y, Berberi M, Haché C, et al. Increased prevalence of Methanosphaera stadtmanae in inflammatory bowel diseases. PLoS ONE. 2014;9(2).
84. Duller S, Moissl-Eichinger C. Archaea in the human microbiome and potential effects on human infectious disease. Emerg Infect Dis. 2024;30(8).
85. Ruden DM. The human archaeome: commensals, opportunists, or emerging pathogens? Pathogens. 2025;14(11).
86. Bresser LRF, de Goffau MC, Levin E, Nieuwdorp M. Gut microbiota in nutrition and health with a special focus on specific bacterial clusters. Cells. 2022;11(19).
87. Thomas CM, Desmond-Le Quéméner E, Gribaldo S, Borrel G. Factors shaping the abundance and diversity of the gut archaeome across the animal kingdom. Nature Communications. 2022;13(1).

88. Odamaki T, Kato K, Sugahara H, Hashikura N, Takahashi S, Xiao J-z, et al. Age-related changes in gut microbiota composition from newborn to centenarian: a cross-sectional study. BMC Microbiology. 2016;16(1).
89. Xu C, Zhu H, Qiu P. Aging progression of human gut microbiota. BMC Microbiology. 2019;19(1).
90. Mihajlovski A, Doré J, Levenez F, Alric M, Brugère JF. Molecular evaluation of the human gut methanogenic archaeal microbiota reveals an age-associated increase of the diversity. Environmental Microbiology Reports. 2010;2(2):272-80.
91. Vanderhaeghen S, Lacroix C, Schwab C, Margolles A. Methanogen communities in stools of humans of different age and health status and co-occurrence with bacteria. FEMS Microbiology Letters. 2015;362(13).
92. Kim JY, Whon TW, Lim MY, Kim YB, Kim N, Kwon M-S, et al. The human gut archaeome: identification of diverse haloarchaea in Korean subjects. Microbiome. 2020;8(1).
93. Cai M, Kandalai S, Tang X, Zheng Q, Xu ZZ. Contributions of human-associated archaeal metabolites to tumor microenvironment and carcinogenesis. Microbiology Spectrum. 2022;10(2).
94. Schmidt R, Cordovez V, de Boer W, Raaijmakers J, Garbeva P. Volatile affairs in microbial interactions. The ISME Journal. 2015;9(11):2329-35.
95. Borrel G, Fadhlaoui K, Ben Hania W, Gaci N, Pehau-Arnaudet G, Chaudhary PP, et al. Methanomethylophilus alvi gen. nov., sp. nov., a novel hydrogenotrophic methyl-reducing methanogenic archaea of the order Methanomassiliicoccales isolated from the human gut and proposal of the novel family Methanomethylophilaceae fam. nov. Microorganisms. 2023;11(11).
96. Xu Y, Wang Y, Li H, Dai Y, Chen D, Wang M, et al. Altered fecal microbiota composition in older adults with frailty. Frontiers in Cellular and Infection Microbiology. 2021;11.
97. Yang J, Li Y, Wen Z, Liu W, Meng L, Huang H. Oscillospira - a candidate for the next-generation probiotics. Gut Microbes. 2021;13(1).
98. Tseng CH, Wu CY. From dysbiosis to longevity: a narrative review into the gut microbiome's impact on aging. J Biomed Sci. 2025;32(1):93.
99. Zhang S-Y, Jouanguy E, Zhang Q, Abel L, Puel A, Casanova J-L. Human inborn errors of immunity to infection affecting cells other than leukocytes: from the immune system to the whole organism. Current Opinion in Immunology. 2019;59:88-100.
100. O'Toole PW, Jeffery IB. Gut microbiota and aging. Science. 2015;350(6265):1214-5.
101. Franceschi C, Ostan R, Santoro A. Nutrition and inflammation: are centenarians similar to individuals on calorie-restricted diets? Annual Review of Nutrition. 2018;38(1):329-56.
102. Siddiqui MT, Cresci GAM. The immunomodulatory functions of butyrate. J Inflamm Res. 2021;14:6025-41.
103. Ghosh TS, Das M, Jeffery IB, O'Toole PW. Adjusting for age improves identification of gut microbiome alterations in multiple diseases. eLife. 2020;9.
104. Wilmanski T, Gibbons SM, Price ND. Healthy aging and the human gut microbiome: why we cannot just turn back the clock. Nature Aging. 2022;2(10):869-71.
105. Valles-Colomer M, Bacigalupe R, Vieira-Silva S, Suzuki S, Darzi Y, Tito RY, et al. Variation and transmission of the human gut microbiota across multiple familial generations. Nature Microbiology. 2022;7(1):87-+.
106. Vandeputte D, De Commer L, Tito RY, Kathagen G, Sabino J, Vermeire S, et al. Temporal variability in quantitative human gut microbiome profiles and implications for clinical research. Nature Communications. 2021;12(1).

107. Dridi B. Laboratory tools for detection of archaea in humans. Clinical Microbiology and Infection. 2012;18(9):825-33.
108. Horz H-P. Archaeal lineages within the human microbiome: absent, rare or elusive? Life. 2015;5(2):1333-45.
109. Thomas AM, Manghi P, Asnicar F, Pasolli E, Armanini F, Zolfo M, et al. Metagenomic analysis of colorectal cancer datasets identifies cross-cohort microbial diagnostic signatures and a link with choline degradation. Nature Medicine. 2019;25(4):667-78.
110. Wirbel J, Pyl PT, Kartal E, Zych K, Kashani A, Milanese A, et al. Meta-analysis of fecal metagenomes reveals global microbial signatures that are specific for colorectal cancer. Nature Medicine. 2019;25(4):679-89.
111. Zeller G, Tap J, Voigt AY, Sunagawa S, Kultima JR, Costea PI, et al. Potential of fecal microbiota for early-stage detection of colorectal cancer. Molecular Systems Biology. 2014;10(11).
112. Lloyd-Price J, Arze C, Ananthakrishnan AN, Schirmer M, Avila-Pacheco J, Poon TW, et al. Multi-omics of the gut microbial ecosystem in inflammatory bowel diseases. Nature. 2019;569(7758):655-62.
113. Gilbert JA, Blaser MJ, Caporaso JG, Jansson JK, Lynch SV, Knight R. Current understanding of the human microbiome. Nature Medicine. 2018;24(4):392-400.
114. Hou K, Wu Z-X, Chen X-Y, Wang J-Q, Zhang D, Xiao C, et al. Microbiota in health and diseases. Signal Transduction and Targeted Therapy. 2022;7(1).
115. Hardy J, Bonin P, Lazuka A, Gonidec E, Guasco S, Valette C, et al. Similar methanogenic shift but divergent syntrophic partners in anaerobic digesters exposed to direct versus successive ammonium additions. Microbiology Spectrum. 2021;9(2).
116. Zhu F, Ju Y, Wang W, Wang Q, Guo R, Ma Q, et al. Metagenome-wide association of gut microbiome features for schizophrenia. Nature Communications. 2020;11(1).
117. Lyu N, Xing G, Yang J, Zhu X, Zhao X, Zhang L, et al. Comparison of inflammatory, nutrient, and neurohormonal indicators in patients with schizophrenia, bipolar disorder and major depressive disorder. Journal of Psychiatric Research. 2021;137:401-8.
118. Dirks B, Davis TL, Carnero EA, Corbin KD, Smith SR, Rittmann BE, et al. Methanogenesis associated with altered microbial production of short-chain fatty acids and human-host metabolizable energy. Isme J. 2025;19(1).
119. Cryan JF, O'Riordan KJ, Cowan CSM, Sandhu KV, Bastiaanssen TFS, Boehme M, et al. The microbiota-gut-brain axis. Physiological Reviews. 2019;99(4):1877-2013.
120. Kleine Bardenhorst S, Cereda E, Severgnini M, Barichella M, Pezzoli G, Keshavarzian A, et al. Gut microbiota dysbiosis in Parkinson disease: A systematic review and pooled analysis. European Journal of Neurology. 2023;30(11):3581-94.
121. Maier L, Pruteanu M, Kuhn M, Zeller G, Telzerow A, Anderson EE, et al. Extensive impact of non-antibiotic drugs on human gut bacteria. Nature. 2018;555(7698):623-8.
122. Langdon A, Crook N, Dantas G. The effects of antibiotics on the microbiome throughout development and alternative approaches for therapeutic modulation. Genome Medicine. 2016;8(1).
123. Bosco N, Noti M. The aging gut microbiome and its impact on host immunity. Genes & Immunity. 2021;22(5-6):289-303.
124. David LA, Maurice CF, Carmody RN, Gootenberg DB, Button JE, Wolfe BE, et al. Diet rapidly and reproducibly alters the human gut microbiome. Nature. 2013;505(7484):559-63.
125. Piccinno G, Thompson KN, Manghi P, Ghazi AR, Thomas AM, Blanco-Míguez A, et al. Pooled analysis of 3,741 stool metagenomes from 18 cohorts for cross-stage and strain-level reproducible microbial biomarkers of colorectal cancer. Nature Medicine. 2025;31(7):2416-29.

126. Yachida S, Mizutani S, Shiroma H, Shiba S, Nakajima T, Sakamoto T, et al. Metagenomic and metabolomic analyses reveal distinct stage-specific phenotypes of the gut microbiota in colorectal cancer. Nature Medicine. 2019;25(6):968-76.
127. Feng Q, Liang S, Jia H, Stadlmayr A, Tang L, Lan Z, et al. Gut microbiome development along the colorectal adenoma–carcinoma sequence. Nature Communications. 2015;6(1).
128. Triantafyllou K, Chang C, Pimentel M. Methanogens, methane and gastrointestinal motility. Journal of Neurogastroenterology and Motility. 2014;20(1):31-40.
129. Borrel G, Brugère J-F, Gribaldo S, Schmitz RA, Moissl-Eichinger C. The host-associated archaeome. Nature Reviews Microbiology. 2020;18(11):622-36.
130. Wei Y-h, Ma X, Zhao J-c, Wang X-q, Gao C-q. Succinate metabolism and its regulation of host-microbe interactions. Gut Microbes. 2023;15(1).
131. Tannahill GM, Curtis AM, Adamik J, Palsson-McDermott EM, McGettrick AF, Goel G, et al. Succinate is an inflammatory signal that induces IL-1β through HIF-1α. Nature. 2013;496(7444):238-42.
132. Sivanand S, Vander Heiden MG. Emerging roles for branched-chain amino acid metabolism in cancer. Cancer Cell. 2020;37(2):147-56.
133. Light SH, Su L, Rivera-Lugo R, Cornejo JA, Louie A, Iavarone AT, et al. A flavin-based extracellular electron transfer mechanism in diverse Gram-positive bacteria. Nature. 2018;562(7725):140-4.
134. Isar J, Agarwal L, Saran S, Saxena RK. Succinic acid production from Bacteroides fragilis: Process optimization and scale up in a bioreactor. Anaerobe. 2006;12(5-6):231-7.
135. Wang H, Wang L, Zhang H, Deng P, Chen J, Zhou B, et al. ^{1}H NMR-based metabolic profiling of human rectal cancer tissue. Molecular Cancer. 2013;12(1):121.
136. Liu YL, Lau HCH, Yu J. Microbial metabolites in colorectal tumorigenesis and cancer therapy. Gut Microbes. 2023;15(1).
137. Xie ZF, Zhu R, Huang XY, Yao F, Jin S, Huang QY, et al. Metabolomic analysis of gut metabolites in patients with colorectal cancer: Association with disease development and outcome. Oncology Letters. 2023;26(2).
138. Kalkan AE, BinMowyna MN, Raposo A, Ahmad MF, Ahmed F, Otayf AY, et al. Beyond the Gut: Unveiling Butyrate's Global Health Impact Through Gut Health and Dysbiosis-Related Conditions: A Narrative Review. Nutrients. 2025;17(8).
139. Blachier F, Selamnia M, Robert V, M'Rabet-Touil H, Duée P-H. Metabolism of l-arginine through polyamine and nitric oxide synthase pathways in proliferative or differentiated human colon carcinoma cells. Biochimica et Biophysica Acta (BBA) - Molecular Cell Research. 1995;1268(3):255-62.
140. Schütz B, Krause FF, Taudte RV, Zaiss MM, Luu M, Visekruna A. Modulation of host immunity by microbiome-derived indole-3-propionic acid and other bacterial metabolites. European Journal of Immunology. 2025;55(4).
141. Beatty A, Singh T, Tyurina YY, Tyurin VA, Samovich S, Nicolas E, et al. Ferroptotic cell death triggered by conjugated linolenic acids is mediated by ACSL1. Nature Communications. 2021;12(1).
142. Ghoshal UC, Srivastava D, Verma A, Misra A. Slow transit constipation associated with excess methane production and its improvement following rifaximin therapy: a case report. J Neurogastroenterol Motil. 2011;17(2):185-8.
143. Lin Y, Lau HC-H, Liu C, Ding X, Sun Y, Rong J, et al. Multi-cohort analysis reveals colorectal cancer tumor location-associated fecal microbiota and their clinical impact. Cell Host & Microbe. 2025;33(4):589-601.e3.

144. Tito RY, Raes J. Gut archaeal biomarkers in colorectal cancer prediction: a tale of opportunity and prudence. Gastroenterology. 2025;168(3):457-8.
145. Weinberger V, Mohammadzadeh R, Blohs M, Kalt K, Mahnert A, Moser S, et al. Expanding the cultivable human archaeome: Methanobrevibacter intestini sp. nov. and strain Methanobrevibacter smithii 'GRAZ-2' from human faeces. International Journal of Systematic and Evolutionary Microbiology. 2025;75(4).

Original Publications

Chapter 1: Archaeal key-residents within the human microbiome: characteristics, interactions and involvement in health and disease (1).

Chapter 2: Age-related dynamics of predominant methanogenic archaea in the human gut microbiome (2).

Chapter 3: Cross-domain metabolic interactions link *Methanobrevibacter smithii* to colorectal cancer microbial ecosystems (3).

Available online at www.sciencedirect.com

ScienceDirect

Current Opinion in Microbiology

Archaeal key-residents within the human microbiome: characteristics, interactions and involvement in health and disease

Rokhsareh Mohammadzadeh[1], Alexander Mahnert[1], Stefanie Duller[1] and Christine Moissl-Eichinger[1,2]

Since the introduction of Archaea as new domain of life more than 40 years ago, they are no longer regarded as eccentric inhabitants of extreme ecosystems. These microorganisms are widespread in various moderate ecosystems, including eukaryotic hosts such as humans.

Indeed, members of the archaeal community are now recognized as paramount constituents of human microbiome, while their definite role in disease or health is not fully elucidated and no archaeal pathogen has been reported. Here, we present a brief overview of archaea residing in and on the human body, with a specific focus on common lineages including *Methanobrevibacter, Methanosphaeraand* Methanomassilococcales.

Addresses
[1] Diagnostic and Research Institute of Hygiene, Microbiology and Environmental Medicine, Medical University of Graz, Neue Stiftingtalstraße 6, 8010 Graz, Austria

[2] BioTechMed, 8010 Graz, Austria

Corresponding author:
Moissl-Eichinger, Christine (christine.moissl-eichinger@medunigraz.at)

Current Opinion in Microbiology 2022, **67**:102146

This review comes from a themed issue on **Microbiota**

Edited by **Lindsay Hall** and **Melanie Schirmer**

For complete overview of the section, please refer to the article collection, "Microbiota"

Available online 12th February 2022

https://doi.org/10.1016/j.mib.2022.102146

1369-5274/© 2022 The Authors. Published by Elsevier Ltd. This is an open access article under the CC BY license (http://creativecommons.org/licenses/by/4.0/).

Archaea: history, distribution and diversity

Archaea were announced as a new domain of life in 1977 next to Bacteria and Eukaryotes [1]. Although first considered as being present only in extreme ecosystems, these microorganisms have been found in several moderate habitats including the human body [2–4]. To date, 20 different archaeal phyla, identified based on archaeal marker proteins, are listed within the Genome Taxonomy Database (GTDB) [5]. These include the Halobacteriota (with former Euryarchaeota class Methanomicrobiales), the Methanobacteriota (with former Euryarchaeota class Methanobacteriales), the Thermoplasmatota (including Methanomassiliicoccales) and the Thermoproteota phyla (with former Thaumarchaeota class Nitrososphaeria), into which most of the archaea associated with plant, animal and human hosts are placed [5]. However, a further expansion of archaeal diversity is to be expected [6].

Archaea have a unique biology, leading to a variety of drawbacks with respect to their detection: Many DNA extraction methods commonly used for bacteria might not be efficient due to the rigid, pseudomurein-containing cell wall, and universal primers used in standardized approaches cannot completely cover the archaeal lineages [7].

Nevertheless, the connection of archaea to eukaryotic hosts has been manifested over the recent years [8], resulting in a collection of more than 1000 unique archaeal genomes from the human gastrointestinal tract (GIT) [9••].

In this review, we focus merely on archaeal key species found in and on the human body (Figure 1a), to give a summary of the latest literature and briefly explain their physiology, specific characteristics, metabolism, interactions, and effects on human health status to facilitate the exploration of current understanding of these human-associated archaeal taxa.

However, in order to provide the broadest context for the readers, we include a comprehensive summary of previous reviews on human archaea and their main contexts in Table 1 (from 2015 onwards).

Methanobrevibacter — the ubiquitous archaeon in human gastrointestinal tract

The first isolation of *Methanobrevibacter* from a human fecal sample was reported by Nottingham and colleagues in 1968 [20]. *Methanobrevibacter* (Methanobacteriaceae) spp. have a coccobacillary shape and occur in single forms, but mostly in pairs or short chains (Figure 1b). They are considered as non-spore-forming, non-motile strict anaerobes with pseudomurein as their cell wall component [21]. All known *Methanobrevibacter* spp. in the human body share the genetic potential for formate and hydrogen/carbon dioxide utilization for methanogenesis [9••]. It has been indicated that by harboring the *mtaABC* genes, *Methanobrevibacter* spp. can additionally use alcoholic

Figure 1

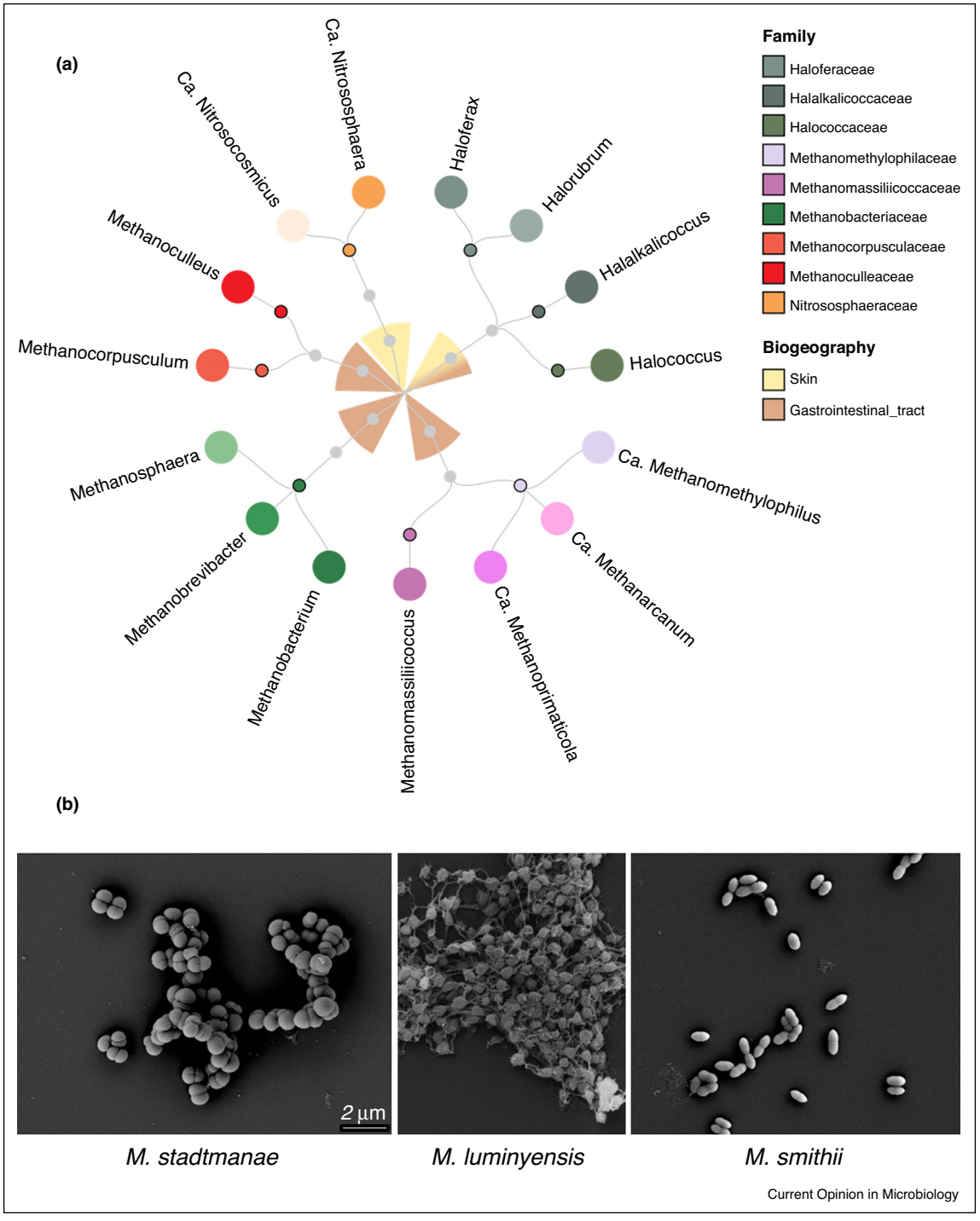

Diversity and phenotypes of human-associated Archaea.
(a) Overview of microbial genera that have been linked with the human skin and gastrointestinal tract microbiome (see also Ref. [8]). Dendrogram was prepared with RawGraphs2.0 beta [19]. **(b)** Scanning electron micrographs of archaeal isolates of the human gut microbiome. Bar: 2 μm, applies to all single displays. *M. stadtmanae: Methanosphaera stadtmanae. M. luminyensis: Methanomassiliicoccus luminyensis*. *M. smithii*: *Methanobrevibacter smithii.*

Table 1

Recent reviews on human-associated Archaea (2015 onwards)

Author	Publication year	Main contexts
Djemai *et al.* [10•]	2021	Commensal methanogens with respect to different body sites; presence of methanogens in different diseases due to alterations in microbial community; Bacteria-Archaea interactions in different pathological and physiological conditions.
Borrel *et al.* [8]	2020	Archaeal diversity and their potential associations with protists, plants, animals, and humans; methodological challenges in archaeome investigations; specific interactions between Archaea and other members of microbial community; roles of the archaeome in both health and disease; discussion on the pathogenicity of archaea.
Sereme *et al.* [11]	2019	Role of Archaea in the hemostasis between health and immune-associated conditions, specifically allergic and atopic disorders.
Sogodogo *et al.* [12]	2019	Archaeal components of microbiota in different body sites; detection methods of human-associated Archaea in the lab; involvement of Archaea in disease.
Bang *et al.* [13]	2019	Occurrence of Archaea in plants, animals, and humans; biofilm formation in Archaea; archaeal interaction with the immune system.
Mahnert *et al.* [7]	2018	Challenges in archaeome research; archaeal biogeographic patterns; archaeal role in human health status.
Moissl-Eichinger *et al.* [14]	2018	*In vivo* and *in vitro* interaction of Archaea with other microbial members; interaction of Archaea with living habitats, including plants, animals, and humans; occurrence of Archaea in biofilms; principles of archaeal interaction.
Nkamga *et al.* [15]	2017	Methods for investigation of methanogens within the human GIT; prevalence of methanogenic and non-methanogenic Archaea within the human digestive microbiota; diversity of methanogens with respect to age; association between human Archaea and diet; prospective role of human methanogens as probiotics; ecological interactions (i.e. hydrogen consumption, heavy metal transformation, and fecal pollution indication); implications of Archaea for human diseases.
Bang *et al.* [16]	2015	Archaeal prevalence in different mucosal surfaces; developments in the detection and quantification of human-linked Archaea; archaeal interactions with human innate and adaptive immune system; potential involvement of Archaea in human health or disease.
Lurie-Weinberger *et al.* [17]	2015	Prevalence of Archaea in different body site, including human gut, subgingival area, and skin; overview of the putative effect of Archaea on human health.
Horz *et al.* [18]	2015	Medical implications of the commonly found Archaea; challenges of detecting archaeal taxa in humans.

fermentation end-products, such as ethanol and methanol, a potential selective advantage for the human GIT environment [9••]. Additionally, acetate is used to feed into an assimilative incomplete reductive tricarboxylic acid cycle [22]. Notably, members of the genus *Methanobrevibacter* are generally not sensitive to antibiotics targeting bacterial RNA or protein synthesis, cell wall, and specific functions [23].

It has been established that a substantial proportion of the encoding genes of *Methanobrevibacter* have bacterial origin. Most of these genes are associated with the adaptations of archaea to their ecological niche and code for proteins involved in adhesion [8,22]. Although these genes most likely stem from the associated gut bacteriome, adaptation towards the human host was not reflected by a generally higher proportion of horizontal gene transfer (HGT) compared to environmental/animal-associated archaea [9••].

Methanobrevibacter and the GIT

With the relative abundance of up to 14% in metagenomic datasets from GIT, *Methanobrevibacter* spp. represent the most abundant methanogen in the human body [24]. This abundance could be explained by symbiotic cross-feeding, as they use bacterial fermentation end-products for methanogenesis. In fact, co-occurrence and syntrophy of *M. smithii* with human-associated bacteria namely *Bacteroides thetaiotaomicron* and *Christensenella* spp., as well as members of Ruminococcaceae have been established thus far [25••,26,27••]. Both detrimental and beneficial effects of *Methanobrevibacter*on human health have been reported thus far. In general, the association between methanogenesis within the human GIT and reduced bloating has been proposed as the overall pressure within this system is reduced through anaerobic respiration and production of one mole of methane by using four moles of hydrogen molecule and one mole of carbon dioxide, and interestingly, this hydrogen removal could enhance organic degradation and therefore promote digestion and fermentation [28]. *Methanobrevibacter* spp. have not been reported as pathogens; however, they have been associated with alterations in microbial composition and might contribute to certain medical conditions (Table 2).

Methanobrevibacter smithii is considered as the dominant methanogen in the human GIT with a high prevalence of >90% (Box 1). Reportedly, *M. smithii* comprise two species-level clades initially named smithii and smithii_A based on phylogenic relatedness [29] and later confirmed and named *M. smithii* and *Candidatus* M. intestini based on

Table 2

Overview of the studies indicating a possible link between human-associated archaea and medical conditions/host phenotypes. Only the studies published after 2019 and conducted on humans are included. For earlier references see Supplementary Table 1 (also available here: DOI: 10.17632/njn6x2kjhg.1)

Medical condition	Study type	Study size	Detection of	Methodology	Relevance to human health	Ref.
Tonsillar phlegmon	Case report	*n* = 1	*M. smithii*	Archaeal 16S rRNA gene amplification, amplicon sequencing analysis	Since *M. smithii* was detected in combination of different aerobic and anaerobic bacterial pathogens, this methanogen could possibly support their growth. The authors proposed that tonsillar phlegmon should be rather considered as a mixed infection and not just bacterial infection.	[43]
Irritable bowel syndrome (IBS)	Clinical case-control	*n* = 67 patients, *n* = 32 healthy subjects	*M. smithii*	PCR, breath test	High methane production by *M. smithii* could lead to abdominal pain and deficient bowel movement.	[44]
Vaginosis	Case-control	*n* = 33 patients with bacterial vaginosis, *n* = 92 controls	*M. smithii*	Microscopic examination, fluorescence *in situ* hybridization, PCR-sequencing, real-time PCR, isolation and cultivation	*M. smithii* is considered as a dominant methanogen in human gut and vaginosis is hypothesized to be associated with the transfer of feces to vagina, and therefore, the detection of this methanogen in vaginosis could support this hypothesis	[45]
Infectious endocarditis	Prospective	*n* = 7716 blood samples	*M. smithii*	Microscopy, PCR-based detection, cultivation	*M. smithii* was found to coincide with Enterobacteriaceae which have the potential to generate hydrogen, reinforcing the hypothesis that this methanogen could promote the growth of other bacteria that could be life-threatening. However, the exact involvement of methanogens in human pathology is not clear yet.	[46]
Urinary tract infections	Prospective	*n* = 383	*M. smithii*	Cultivation, PCR-based detection	The authors suggested that *M. smithii* is a constituent of urinary microbial community and together with enteric bacteria, it could lead to community-acquired urinary tract infection.	[47]
Severe malnutrition	Case-control	*n* = 143 cases, *n* = 110 controls	Absence of *M. smithii*	qPCR	The authors proposed that alterations in gut microbial community in cases with severe acute malnutrition represents a loss of *M. smithii*, thereby contradicting the immaturity hypothesis.	[48]
Stomatology diseases	Cohort	*n* = 31 patients	*M. smithii*, '*M. massiliense*' and *M. oralis*	Cultivation, Amplicon-sequencing, Fluorescence *in situ* hybridization (FISH)	This study suggests that the oral cavity is a host for a repertoire of methanogenic archaea irrespective of the geographical region.	[49]
Colorectal cancer	Cohort	*n* = 585 (184 CRC patients, 197 adenoma patients, 204 healthy subjects)	Increased abundance of *Halopelagius,* and absence of methanogens	Metagenomic analysis	The authors suggested that the increased abundance of halophilic archaea and the loss of methanogenic archaea (including *Methanosphaera, Methanococcoides, Methanocorpusculum, Methanocaldococcus,* and *Methanobacterium* species) are linked with colorectal cancer.	[50]

Table 2 (*Continued*)

Medical condition	Study type	Study size	Detection of	Methodology	Relevance to human health	Ref.
High methane emission	Cohort	n = 471	1000-fold increase in *M. smithii*	Amplicon-sequencing, qPCR, metagenomic analysis	A 1000 fold increase in *M. smithii* is linked to high methane emission in the breath of humans. Increased abundance is linked to diet, reduced B12 uptake, and increased formate levels in gut. *M. smithii* has the potential to push the microbiome function towards optimized fibre degradation and increased formate and acetate generation.	[32•]
Peri-appendicular abscesses	Case series	n = 4	*M. oralis* and *M. smithii*	PCR, Sanger sequencing, qPCR, electron microscopy	These methanogens were co-detected with other enterobacteria including *Enterococcus faecium*, *Escherichia coli*, and *Enterococcus avium*, suggesting the promotion of their growth by supporting their fermentation by hydrogen uptake. The authors also suggested to use of fusidic acid and metronidazole, which are both active against methanogens, for the treatment of per-appendicular abscesses	[51]
Orthopedic ProsthesisInfection	Case report	n = 1	*M. oralis*, *M. smithii*, and *M. wolinii*	PCR, autofluorescence, electron microscopy, culture, next-generation sequencing	Detection of methanogens in bones and joint samples of patients with bacterial infection (*Staphylococcus aureus*, *Staphylococcus epidermidis* and *Proteus mirabilis*) of these body sites suggests the possibility of co-occurrence of these methanogens with these pathogens	[52]
Sarcopenic cirrhosis	Case-control	n = 187 cirrhosis patients, n = 149 controls	Reduced abundance of *Methanobrevibacter*	Metabolomics, metagenomics	The human GIT microbiota of cirrhotic patients with sarcopenia showed poor *Methanobrevibacter* profile as well as *Prevotella* and *Akkermansia*, which are associated with physical function and the authors suggest the association between a healthy and physically active lifestyle with the increased abundance of these microorganisms.	[53]
Appendectomy	Cohort	n = 193 with appendectomy, n = 4784 without appendectomy	Reduced methane production	Breath test	This study suggested that appendectomy leads to the decreased levels of methane within breath and that appendix might be a reservoir of methanogens.	[54]
Parkinson's disease (PD)	Cohorts (reanalyzation of 10 available 16S microbiome database)	n = 681 patient, n = 530 control	*Methanobrevibacter*	16S sequencing	The increased abundance of *Methanobrevibacter* could be explained by the increased abundance of Christensenellaceae family in PD patients since these bacteria can support its proliferation through H_2 production.	[55]
Refractory sinusitis	Case series	n = 9	*M. smithii*, *M. oralis*, *M. massiliensis*	PCR, fluorescence in-situ hybridization, amplicon sequencing, culture	The authors suggested the presence of methanogens as a constituent of anaerobic microbiota in refractory sinusitis patients, and suggested the use of nitroimidazole derivate, which is also active against these microorganisms, to treat this condition.	[56]

Box 1 Abundance and prevalence of archaeal taxa in the human GIT

The human GIT archaeome is predominated by methanogenic archaea, that is, archaea capable of methane formation. Based on Bracken (Bayesian Reestimation of Abundance with Kraken), a highly accurate statistical method to compute the abundance of taxa in metagenomic gut datasets, we recently estimated the average (methano-) archaeal abundance to be 1.2% within the GIT microbiome, confirming previous estimations [9••].

For this approach, we screened 691 datasets (= individual samples) from various geographic locations (Europe, Asia, North/South America, Africa, and Oceania). The most prevalent archaeal species in the GIT are *Methanobrevibacter smithii* (0.56% average abundance, prevalent in 91.32% of analyzed datasets (n = 691); prevalence was counted positive only when >80% of the representative genome used for the mapping approach was covered (CoverM analysis, [9••]) and Candidatus *Methanobrevibacter intestini* (0.131% average abundance, prevalent in 90.01% of all samples). However, the *Methanobrevibacter* abundance correlates with methane breath content and is highly variable, ranging from 0.002 to 2% relative abundance in individuals with low and high methane emission, respectively [32•].

Also belonging to the Methanobacteriaceae, *Methanosphaera stadtmanae* revealed an average abundance of 0.028%, with a prevalence of 18.09% in the analyzed sample sets. The relative abundance of Methanomassiliicocacceae (with *Methanomassiliicoccus luminyensis*, and Methanomethylophilaceae (with *Methanomethylophilus alvus*) was estimated to be 0.043% and 0.145%, respectively. The prevalence of the mentioned species reached up to 6.95% in the analyzed datasets [9••]. These recent analyses confirmed the ubiquitous nature of *Methanobrevibacter* spp. in the human GIT despite their highly variable relative abundances [32•], whereas other methanogens, such as *Methanosphaera* and *Methanomethylophilus* representatives, appear only in a subset of samples, potentially indicating a more dedicated role in human development and health.

a unified archaeal protein catalogue, distant genome and *mcrA* gene sequence as well as other specific characteristics, including different gene sets for molybdate transport [9••].

It is still unclear at which age *Methanobrevibacter* establishes itself in the intestinal microbial community and available studies are often contradictory [30•,31]. However, *Methanobrevibacter* spp. have been suggested to be more abundant in the adult digestive tract compared to the infants [32•].

Methanobrevibacter in the oral cavity and other human niches

Methanobrevibacter oralis is considered as the predominant archaeon in the oral cavity, and has been linked to this location through ages of human evolution [32•]. Although this species is infrequently detected in healthy oral locations or healthy patients in general, it was found to be substantially linked with periodontal disorders [33] (prevalence in diseased locations: 45%; [34]). It has been suggested that *M. oralis* contributes to periodontal diseases through their syntrophy with sulfate-reducing and acetogenic bacteria such as *Desulfovibrio piger* and *Eubacterium limosum*, respectively [35]. Moreover, syntrophy between *Methanobrevibacter massiliense* and sulfate-reducing *Pyramidobacter piscolens* has been shown in severe cases of generalized periodontitis [36].

The first report on the detection of methanogens in the respiratory tract was achieved in 2017 where we revealed the occurrence of archaeal signatures in lung biopsies by targeted metagenomics [4]. In a more recent study, *M. oralis* and *M. smithii* were detected in bronchoalveolar lavages and sputum samples using culture and molecular-based methods as well as fluorescent *in situ* hybridization (FISH) [37]. Human skin is another potential habitat for *Methanobrevibacter* spp., but it remains unclear whether this archaeon is actively interacting with dermal epithelial cells or is only persisting in this niche [38].

Methanobrevibacter and the human immune system

It has been indicated that *Methanobrevibacter* interacts with human dendritic cells and is capable of inducing inflammatory cytokines and the subsequent recruitment of inflammatory cells [39]. Furthermore, *Methanobrevibacter*-derived archaeosomes are potential adjuvants for vaccines due to their distinctive lipid structure [40]. Notably, an increased abundance of *Methanobrevibacter* has been shown in multiple sclerosis (MS) patients and confirmed by increased breath methane contents [41]. Therein, a positive correlation between the expression of T-cell activation regulator TRAF5, which is known to be upregulated in MS patients, and *Methanobrevibacter* has also been suggested. In addition, the negative correlation between the abundance of this archaeal spp. and anti-inflammatory cytokine TNFAIP3, which is downregulated in MS patients, has been shown [41]. Furthermore, in a pilot study, MS children harboring *Methanobrevibacter* as a member of their microbiota, were shown to relapse faster [42].

Methanosphaera — a rare but important player in the human microbiome

Methanosphaera (Methanobacteriaceae) appears as irregular cocci organized either in single cells, pairs, or most commonly tetrads (Figure 1b), with pseudomurein-containing cell wall. Currently, two species of this archaeal genus, *M. stadtmanae* and *M. cuniculi*, have been reported from human GIT samples [9••,57]. *M. stadtmanae* is known for its different energy metabolism as it does not grow on CO_2. It uses acetate as the main carbon source and is dependent on methanol and hydrogen for generating methane. This different metabolism can be explained by the absence of molybdopterin cofactor and therefore, the absence of active formylmethanofuran dehydrogenase synthesis [58]. The host-specificity of this

archaeal genus can be attributed to variations of its genomic properties as shown by a larger number of different genotypes in ruminants and a smaller number of different genotypes in humans and monogastric animals [59]. The preferred niche for *M. stadtmanae* is mostly colonized by bacterial species within the Firmicutes and Bacteroidetes phyla. In fact, 73 ORFs have been detected in *M. stadtmanae* with high similarity to genes within bacteria or eukaryotes [58]. These genes mostly code for glycosyltransferase and are therefore involved in cell adhesion, indicating a remarkable inter-domain lateral gene transfer and the role of bacteria in the adaptation of this archaeon to host systems [60].

Despite the relevant prevalence of *Methanosphaera* in the digestive tract of most animals and humans [8], this archaeal genus remains poorly characterized and therefore, its involvement in health or disease is not clear yet. However, the increased abundance of *Methanosphaera* spp. has been indicated in subjects with inflammatory bowel disease (IBD) compared to healthy subjects [61]. On the other hand, *M. stadtmanae* has been associated with lower likelihood of asthma in children aged between 6–10 years old, suggesting the tolerogenicity of this archaeal species early in life [62].

The capability of *M. stadtmanae* to trigger immunological responses has been reported. *M. stadtmanae* is able to induce tumor necrosis factor-alpha (TNF-α) in high amounts by human peripheral blood mononuclear cells (PBMCs) [61]. Significant amounts of this cytokine as well as interleukin-1 beta (IL-1β) were also released after exposing monocyte-derived dendritic cells (moDCs) to *M. stadtmanae* in a concentration-dependent manner [39]. In addition, the activation of the immune cells and the subsequent cytokine release has been attributed to the rapid phagocytosis of this archaeal species and endosomal acidification. Notably, CD86 and CD197, which largely contribute to moDCs maturation and B-cell and T-cell activation, were upregulated after exposure to *M. stadtmanae*, indicating the induction of both innate and adaptive immune responses by this archaeal species [39]. Recently, the immunogenicity of *M. stadtmanae* has been assigned to its RNA component, where Toll-like receptors TLR7 and TLR8 were detected as the respective pattern recognition receptors for this molecule. Furthermore, a specific inflammasome activation pathway by this archaeal species has been suggested [63].

Methanomassilococcales — characteristics and interaction with the human host

Methanomassiliicoccales are frequently detected in soil and aquatic environments, as well as host systems [64•,65,66]. This order is split into two large clades, a free-living clade (Methanomassiliicoccaceae; including the isolates *Methanomassiliicoccus luminyensis* (Figure 1b) and *Ca.* M. intestinalis Issoire-Mx1) and a host-associated clade (*Ca.* Methanomethylophilaceae; including *Ca.* Methanomethylophilus alvus Mx1201). The host-associated clade shows several genomic adaptations, including the carriage of genes probably associated with shikimate pathway and bile resistance [67].

The isolation or enrichment of several Methanomassiliicocales members from human stool samples as well as subgingival plaques has been reported [67–70]. A specific association with elderly individuals has been suggested, whereas the representatives often remain undetected in young adults and infants [71,72].

The metabolism of the order Methanomassiliicoccales relies on H_2 as an electron donor and methyl-compounds for methanogenesis, and the genes contributing to the conventional CO_2-reduction/methyl-oxidation pathways are absent [73].

A different form of energy conservation has been shown in *M. luminyensis* compared to other methanogens as it uses different enzymatic compositions for electron transfer reactions, namely membrane-bound ferredoxin:heterodisulfide oxidoreductase system [74•]. Another distinct feature of these microorganisms is their capability to code for pyrrolysine (Pyl) amino acid, which seems to be related to a unique evolution [75]. This amino acid is essential for the activity of certain methyltransferase and confers this archaeal species the ability to produce methane using methylated amines: mono-methylamine, di-methylamine, and tri-methylamine (TMA). This metabolite is generated by the host gut microbiota through the consumption of dietary carnitine, lecithin, or choline and in the liver, it is oxidized into trimethylamine N-oxide (TMAO) through human flavin monooxygenases. A potential link between TMAO and cardiovascular events as well as chronic kidney diseases has been proposed, suggesting the contribution of Methanomassiliicoccales members in reducing the risk of these diseases [76,77]. Considering the potential positive impacts of these microorganisms on human health, an application as effective archaeobiotic has been proposed; however, further animal and clinical studies are required to validate its effectiveness [78].

Thus far, only one study has investigated the human immune response against *M. luminyensis*. Bang *et al.* showed the resistance of this strain against mammalian antimicrobial peptides, suggesting its adaptation to the intestinal environment. However, human cathelicidin LL37 (LL32) was effective against this archaeon and its effectiveness was stronger than that against *M. stadtmanae* and *M. smithii*. Furthermore, the moDCs activation by this Methanomassiliicoccales member was rarely observed and pro-inflammatory cytokines IL-1β and TNF-α were released only at very low levels, indicating its low immunogenicity and commensal nature in the human gut [79].

Thaumarchaeota on human skin

Thaumarchaeota, recently re-named as Thermoproteota (GTDB), comprise rod-shaped motile archaea with the ability to grow under various aerobic conditions, including the plant's phyllosphere or human and animal [7]. These archaea contain a specific tetraether membrane lipid with crenarchaeol and are mostly considered as autotrophs with the ability of CO_2 fixation; nevertheless, they sometimes depend on other bacteria or organic substrates for survival and growth [80]. Most representatives can oxidize ammonia to nitrite, however, some Thaumarchaeota lineages lack the *amoABC* genes and therefore are not dependent on ammonia for growth [81,82].

Strains of Thaumarchaeota were initially identified as common constituents of the human skin microbiota [38]. It was envisaged that these archaeal members could oxidize the ammonium from sweat, which is especially elevated during physical activity, and consequently decrease the skin pH, thereby supporting a healthy skin and removing the bad sweat odor. A potential association with age has also been indicated as <12 year-old or >60 year-old subjects had a more diverse and abundant thaumarchaeome compared to those in their middle age [83]. Moreover, the effect of sex on the presence of Thaumarchaeota has been reported as the continuous sampling of the male palm showed transient presence of this archaeal member, while its presence was persistent in female cases, which could be explained by different steroid productions [84]. The presence of these archaea, although in low abundance (less than 0.01% of all samples), has also been reported in dental caries [85] as well as nasal samples [4].

Conclusion/Outlook

Our knowledge on host-associated archaeal diversity and specifically human-associated archaea is still in its infancy. In addition to the abovementioned archaeal genera, many others may play a role in and on the human body. This includes genera like *Methanocorpusculum* or *Methanobacterium*, as well as a broad variety of unknown Methanomassiliicoccales, whose signatures were detected in metagenome-based approaches [9••]. Another frequently found archaeal signature in skin, fecal and mucosal samples with unknown role is assignable to haloarchaea. However, genomes binned from metagenomic datasets (*Haloferax, Halorubrum*) did not reveal any GIT-specific adaptations [9••], and the presence of haloarchaea had been previously linked with transient high salt concentrations on skin, the consumption of salt-fermented diet, and pre-endoscopic lavage solutions, respectively [83,86,87]. Nevertheless, a recent study reported a high abundance and prevalence of haloarchaea in Korean subjects [88], indicating a potential geographic allocation.

Evidently, the list of the human-associated archaea has only recently expanded and our understanding of the human archaeome is restricted mostly due to the biased methodologies towards bacteria. Identification and dedicated investigation on human-associated archaeal species could lead to a new insight on their potential links with pathological states. Those analyses could involve specific clinical studies, combined with multi-omic approaches, extended cultivation strategies and the use of (artificial) models in order to enlighten mechanistic connections.

Conflict of interest statement

Nothing declared.

Acknowledgements

The authors thank Guillaume Borrel for proof-reading and scientific input. We gratefully acknowledge the funding by the Austrian Science Fund FWF (P 32697, P 30796), and the financial support by the PhD program MolMed, Medical University of Graz. We thank Dagmar Kolb and her team from the ZMF core facility 'Ultrastructure Analysis' for the support in preparation of microbial cultures and SEM imaging.

Appendix A. Supplementary data

Supplementary material related to this article can be found, in the online version, at doi:https://doi.org/10.1016/j.mib.2022.102146.

References and recommended reading

Papers of particular interest, published within the period of review, have been highlighted as:

- • of special interest
- •• of outstanding interest

1. Woese CR, Fox GE: **Phylogenetic structure of the prokaryotic domain: the primary kingdoms**. *Proc Natl Acad Sci U S A* 1977, **74**:5088-5090.

2. Truu M, Nõlvak H, Ostonen I, Oopkaup K, Maddison M, Ligi T, Espenberg M, Uri V, Mander U, Truu J: **Soil bacterial and archaeal communities and their potential to perform N-cycling processes in soils of boreal forests growing on well-drained peat**. *Front Microbiol* 2020, **11**:3112.

3. Husnik F, Tashyreva D, Boscaro V, George EE, Lukeš J, Keeling PJ: **Bacterial and archaeal symbioses with protists**. *Curr Biol* 2021, **31**:R862-R877.

4. Koskinen K, Pausan MR, Perras AK, Beck M, Bang C, Mora M, Schilhabel A, Schmitz R, Moissl-Eichinger C: **First insights into the diverse human archaeome: specific detection of archaea in the gastrointestinal tract, lung, and nose and on skin**. *mBio* 2017, **8**:e00824-00817.

5. Parks DH, Chuvochina M, Rinke C, Mussig AJ, Chaumeil P-A, Hugenholtz P: **GTDB: an ongoing census of bacterial and archaeal diversity through a phylogenetically consistent, rank normalized and complete genome-based taxonomy**. *Nucleic Acids Res* 2022:D785-D794.

6. Tahon G, Geesink P, Ettema TJ: **Expanding archaeal diversity and phylogeny: past, present, and future**. *Annu Rev Microbiol* 2021, **75**:359-381.

7. Mahnert A, Blohs M, Pausan M-R, Moissl-Eichinger C: **The human archaeome: methodological pitfalls and knowledge gaps**. *Emerg Top Life Sci* 2018, **2**:469-482.

8. Borrel G, Brugère J-F, Gribaldo S, Schmitz RA, Moissl-Eichinger C: **The host-associated archaeome**. *Nat Rev Microbiol* 2020, **18**:622-636.

9. •• Chibani CM, Mahnert A, Borrel G, Almeida A, Werner A, Brugère J-F, Gribaldo S, Finn RD, Schmitz RA, Moissl-Eichinger C: **A catalogue of 1,167 genomes from the human gut archaeome**. *Nat Microbiol* 2022, **7**:48-16761
This study suggests the split of Methanobrevibacter smithii clased into two distinct clades, one of which is represented by *Candidatus* M. intestini.

10. • Djemai K, Drancourt M, Tidjani Alou M: **Bacteria and methanogens in the human microbiome: a review of syntrophic interactions**. *Microb Ecol* 2021:1-19
This study presents a broad analysis of archaeal taxonomy and describes new host-associated archaea including *Methanothermobacter*.

11. Sereme Y, Mezouar S, Grine G, Mege JL, Drancourt M, Corbeau P, Vitte J: **Methanogenic Archaea: emerging partners in the field of allergic diseases**. *Clin Rev Allergy Immunol* 2019, **57**:456-466.

12. Sogodogo E, Drancourt M, Grine G: **Methanogens as emerging pathogens in anaerobic abscesses**. *Eur J Clin Microbiol Infect Dis* 2019, **38**:811-818.

13. Bang C, Schmitz RA: **Archaea: forgotten players in the microbiome**. *Emerg Top Life Sci* 2018, **2**:459-468.

14. Moissl-Eichinger C, Pausan M, Taffner J, Berg G, Bang C, Schmitz RA: **Archaea are interactive components of complex microbiomes**. *Trends Microbiol* 2018, **26**:70-85.

15. Nkamga VD, Henrissat B, Drancourt M: **Archaea: essential inhabitants of the human digestive microbiota**. *Hum Microbiome J* 2017, **3**:1-8.

16. Bang C, Schmitz RA: **Archaea associated with human surfaces: not to be underestimated**. *FEMS Microbiol Rev* 2015, **39**:631-648.

17. Lurie-Weinberger MN, Gophna U: **Archaea in and on the human body: health implications and future directions**. *PLoS Pathog* 2015, **11**:e1004833.

18. Horz H-P: **Archaeal lineages within the human microbiome: absent, rare or elusive?** *Life* 2015, **5**:1333-1345.

19. Mauri M, Elli T, Caviglia G, Uboldi G, Azzi M: **RAWGraphs: a visualisation platform to create open outputs**. *Proceedings of the 12th Biannual Conference on Italian SIGCHI Chapter* 2017:1-5.

20. Nottingham P, Hungate R: **Isolation of methanogenic bacteria from feces of man**. *J Bacteriol* 1968, **96**:2178-2179.

21. Miller TL: **Methanobrevibacter**. *Bergey's Manual of Systematics of Archaea and Bacteria*. 2015:1-14.

22. Samuel BS, Hansen EE, Manchester JK, Coutinho PM, Henrissat B, Fulton R, Latreille P, Kim K, Wilson RK, Gordon JI: **Genomic and metabolic adaptations of *Methanobrevibacter smithii* to the human gut**. *Proc Natl Acad Sci U S A* 2007, **104**:10643-10648.

23. Khelaifia S, Drancourt M: **Susceptibility of archaea to antimicrobial agents: applications to clinical microbiology**. *Clin Microbiol Infect* 2012, **18**:841-848.

24. Tyakht AV, Kostryukova ES, Popenko AS, Belenikin MS, Pavlenko AV, Larin AK, Karpova IY, Selezneva OV, Semashko TA, Ospanova EA: **Human gut microbiota community structures in urban and rural populations in Russia**. *Nat Commun* 2013, **4**:1-9.

25. •• Ruaud A, Esquivel-Elizondo S, de la Cuesta-Zuluaga J, Waters JL, Angenent LT, Youngblut ND, Ley RE: **Syntrophy via interspecies H_2 transfer between *Christensenella* and *Methanobrevibacter* underlies their global cooccurrence in the human gut**. *mBio* 2020, **11**:e03235-03219
This study together with Ref. [27] confirm the syntrophic interaction between *Methanobrevibacter* and *Christensenella* and that *Christensenella* might support the metabolism of *Methanobrevibacter*.

26. Traore SI, Khelaifia S, Armstrong N, Lagier J, Raoult D: **Isolation and culture of *Methanobrevibacter smithii* by co-culture with hydrogen-producing bacteria on agar plates**. *Clin Microbiol Infect* 2019, **25**:1561-1565.

27. •• Kumpitsch C, Fischmeister FPS, Mahnert A, Lackner S, Wilding M, Sturm C, Springer A, Madl T, Holasek S, Högenauer C: **Reduced B12 uptake and increased gastrointestinal formate are associated with archaeome-mediated breath methane emission in humans**. *Microbiome* 2021, **9**:1-18
This study reports the increased efficiency of fibre break-down when archaea are present in the human GI tract.

28. Gaci N, Borrel G, Tottey W, O'Toole PW, Brugère J-F: **Archaea and the human gut: new beginning of an old story**. *World J Gastroenterol* 2014, **20**:16062.

29. Rinke C, Chuvochina M, Mussig AJ, Chaumeil P-A, Davín AA, Waite DW, Whitman WB, Parks DH, Hugenholtz P: **A standardized archaeal taxonomy for the Genome Taxonomy Database**. *Nat Microbiol* 2021, **6**:946-959.

30. • Sereme Y, Guindo CO, Filleron A, Corbeau P, Tran TA, Drancourt M, Vitte J, Grine G: **Meconial *Methanobrevibacter smithii* suggests intrauterine methanogen colonization in preterm neonates**. *Curr Res Microb Sci* 2021, **2**:100034
This study places *Methanobrevibacter smithii* as the early colonizer of the human GIT.

31. Grine G, Boualam M, Drancourt M: ***Methanobrevibacter smithii*, a methanogen consistently colonising the newborn stomach**. *Eur J Clin Microbiol Infect Dis* 2017, **36**:2449-2455.

32. • Roswall J, Olsson LM, Kovatcheva-Datchary P, Nilsson S, Tremaroli V, Simon M-C, Kiilerich P, Akrami R, Krämer M, Uhlén M: **Developmental trajectory of the healthy human gut microbiota during the first 5 years of life**. *Cell Host Microbe* 2021, **29**:765-776.e63
This study places *Methanobrevibacter* together with Christensenellaceae as the late 432 inhabitants of the human GIT.

33. Hirai K, Maeda H, Omori K, Yamamoto T, Kokeguchi S, Takashiba S: **Serum antibody response to group II chaperonin from *Methanobrevibacter oralis* and human chaperonin CCT**. *Pathog Dis* 2013, **68**:12-19.

34. Horz H, Robertz N, Vianna M, Henne K, Conrads G: **Relationship between methanogenic archaea and subgingival microbial complexes in human periodontitis**. *Anaerobe* 2015, **35**:10-12.

35. Vianna M, Holtgraewe S, Seyfarth I, Conrads G, Horz H: **Quantitative analysis of three hydrogenotrophic microbial groups, methanogenic archaea, sulfate-reducing bacteria, and acetogenic bacteria, within plaque biofilms associated with human periodontal disease**. *J Bacteriol* 2008, **190**:3779-3785.

36. Huynh HT, Pignoly M, Drancourt M, Aboudharam G: **A new methanogen "*Methanobrevibacter massiliense*" isolated in a case of severe periodontitis**. *BMC Res Notes* 2017, **10**:1-4.

37. Hassani Y, Brégeon F, Aboudharam G, Drancourt M, Grine G: **Detection of *Methanobrevobacter smithii* and *Methanobrevibacter oralis* in lower respiratory tract microbiota**. *Microorganisms* 2020, **8**:1866.

38. Probst AJ, Auerbach AK, Moissl-Eichinger C: **Archaea on human skin**. *PLoS One* 2013, **8**:e65388.

39. Bang C, Weidenbach K, Gutsmann T, Heine H, Schmitz RA: **The intestinal archaea *Methanosphaera stadtmanae* and *Methanobrevibacter smithii* activate human dendritic cells**. *PLoS One* 2014, **9**:e99411.

40. Adamiak N, Krawczyk KT, Locht C, Kowalewicz-Kulbat M: **Archaeosomes and gas vesicles as tools for vaccine development**. *Front Immunol* 2021:3738.

41. Jangi S, Gandhi R, Cox LM, Li N, Von Glehn F, Yan R, Patel B, Mazzola MA, Liu S, Glanz BL: **Alterations of the human gut microbiome in multiple sclerosis**. *Nat Commun* 2016, **7**:1-11.

42. Tremlett H, Fadrosh DW, Faruqi AA, Hart J, Roalstad S, Graves J, Lynch S, Waubant E, Aaen G, Belman A: **Gut microbiota composition and relapse risk in pediatric MS: a pilot study**. *J Neurol Sci* 2016, **363**:153-157.

43. Djemai K, Gouriet F, Michel J, Radulesco T, Drancourt M, Grine G: ***Methanobrevibacter smithii* tonsillar phlegmon: a case report**. *New Microbes New Infect* 2021, **42**:100891.

44. Vlasova A, Isakov V, Pilipenko V, Sheveleva S, Markova YM, Polyanina A, Maev I: ***Methanobrevibacter smithii* in irritable**

bowel syndrome: a clinical and molecular study. *Ter Arkhiv* 2019, **91**:47-51.

45. Grine G, Drouet H, Fenollar F, Bretelle F, Raoult D, Drancourt M: **Detection of *Methanobrevibacter smithii* in vaginal samples collected from women diagnosed with bacterial vaginosis**. *Eur J Clin Microbiol Infect Dis* 2019, **38**:1643-1649.

46. Drancourt M, Djemai K, Gouriet F, Grine G, Loukil A, Bedotto M, Levasseur A, Lepidi H, Bou-Khalil J, Khelaifia S: ***Methanobrevibacter smithii* archaemia in febrile patients with bacteremia, including those with endocarditis**. *Clin Infect Dis* 2021, **73**:e2571-e2579.

47. Grine G, Lotte R, Chirio D, Chevalier A, Raoult D, Drancourt M, Ruimy R: **Co-culture of *Methanobrevibacter smithii* with enterobacteria during urinary infection**. *EBioMedicine* 2019, **43**:333-337.

48. Camara A, Konate S, Alou MT, Kodio A, Togo AH, Cortaredona S, Henrissat B, Thera MA, Doumbo OK, Raoult D: **Clinical evidence of the role of *Methanobrevibacter smithii* in severe acute malnutrition**. *Sci Rep* 2021, **11**:1-11.

49. Sogodogo E, Doumbo O, Aboudharam G, Kouriba B, Diawara O, Koita H, Togora S, Drancourt M: **First characterization of methanogens in oral cavity in Malian patients with oral cavity pathologies**. *BMC Oral Health* 2019, **19**:1-6.

50. Coker OO, Wu WKK, Wong SH, Sung JJ, Yu J: **Altered gut archaea composition and interaction with bacteria are associated with colorectal cancer**. *Gastroenterology* 2020, **159**:1459-1470.e5.

51. Djemai K, Gouriet F, Sielezneff I, Mege D, Drancourt M, Grine G: **Detection of methanogens in peri-appendicular abscesses: report of four cases**. *Anaerobe* 2021, **72**:102470.

52. Djemai K, Gouriet F, Argenson J-N, Seng P, Stein A, Drancourt M: **First detection of methanogens in orthopedic prosthesis infection: a four-case founding series**. *Prosthesis* 2022, **4**:38-47.

53. Ponziani FR, Picca A, Marzetti E, Calvani R, Conta G, Del Chierico F, Capuani G, Faccia M, Fianchi F, Funaro B: **Characterization of the gut-liver-muscle axis in cirrhotic patients with sarcopenia**. *Liver Int* 2021, **41**:1320-1334.

54. Takakura W, Oh SJ, Singer-Englar T, Mirocha J, Leite G, Fridman A, Pimentel M, Mathur R, Pichetshote N, Rezaie A: **Comparing the rates of methane production in patients with and without appendectomy: results from a large-scale cohort**. *Sci Rep* 2020, **10**:1-7.

55. Romano S, Savva GM, Bedarf JR, Charles IG, Hildebrand F, Narbad A: **Meta-analysis of the Parkinson's disease gut microbiome suggests alterations linked to intestinal inflammation**. *NPJ Parkinson Dis* 2021, **7**:1-13.

56. Sogodogo E, Fellag M, Loukil A, Nkamga VD, Michel J, Dessi P, Fournier P-E, Drancourt M: **Nine cases of methanogenic archaea in refractory sinusitis, an emerging clinical entity**. *Front Public Health* 2019, **7**:38.

57. Miller TL, Wolin MJ: ***Methanosphaera stadtmaniae* gen. nov., sp. nov.: a species that forms methane by reducing methanol with hydrogen**. *Arch Microbiol* 1985, **141**:116-122.

58. Fricke WF, Seedorf H, Henne A, Krüer M, Liesegang H, Hedderich R, Gottschalk G, Thauer RK: **The genome sequence of *Methanosphaera stadtmanae* reveals why this human intestinal archaeon is restricted to methanol and H_2 for methane formation and ATP synthesis**. *J Bacteriol* 2006, **188**:642-658.

59. Hoedt EC, Parks DH, Volmer JG, Rosewarne CP, Denman SE, McSweeney CS, Muir JG, Gibson PR, Cuív PÓ, Hugenholtz P: **Culture-and metagenomics-enabled analyses of the *Methanosphaera* genus reveals their monophyletic origin and differentiation according to genome size**. *ISME J* 2018, **12**:2942-2953.

60. Lurie-Weinberger MN, Peeri M, Tuller T, Gophna U: **Extensive inter-domain lateral gene transfer in the evolution of the human commensal *Methanosphaera stadtmanae***. *Front Genet* 2012, **3**:182.

61. Blais Lecours P, Marsolais D, Cormier Y, Berberi M, Haché C, Bourdages R, Duchaine C: **Increased prevalence of *Methanosphaera stadtmanae* in inflammatory bowel diseases**. *PLoS One* 2014, **9**:e87734.

62. Barnett DJ, Mommers M, Penders J, Arts IC, Thijs C: **Intestinal archaea inversely associated with childhood asthma**. *J Allergy Clin Immunol* 2019, **143**:2305.

63. Vierbuchen T, Bang C, Rosigkeit H, Schmitz RA, Heine H: **The human-associated archaeon *Methanosphaera stadtmanae* is recognized through its RNA and induces TLR8-dependent NLRP3 inflammasome activation**. *Front Immunol* 2017, **8**:1535.

64. • Cozannet M, Borrel G, Roussel E, Moalic Y, Allioux M, Sanvoisin A, Toffin L, Alain K: **New insights into the ecology and physiology of Methanomassiliicoccales from terrestrial and aquatic environments**. *Microorganisms* 2021, **9**:30

This study showed the co-occurrence of Methanomassiliicoccales and dihydrogen-generating and acetate-generating bacterial cells which are mostly found in the GIT.

65. Paul K, Nonoh JO, Mikulski L, Brune A: **"Methanoplasmatales," Thermoplasmatales-related archaea in termite guts and other environments, are the seventh order of methanogens**. *Appl Environ Microbiol* 2012, **78**:8245-8253.

66. Borrel G, McCann A, Deane J, Neto MC, Lynch DB, Brugère J-F, O'Toole PW: **Genomics and metagenomics of trimethylamine-utilizing Archaea in the human gut microbiome**. *ISME J* 2017, **11**:2059-2074.

67. De La Cuesta-Zuluaga J, Spector TD, Youngblut ND, Ley RE: **Genomic insights into adaptations of trimethylamine-utilizing methanogens to diverse habitats, including the human gut**. *mSystems* 2021, **6**:e00939-00920.

68. Borrel G, Harris HM, Tottey W, Mihajlovski A, Parisot N, Peyretaillade E, Peyret P, Gribaldo S, O'Toole PW, Brugère J-F: **Genome sequence of "*Candidatus* Methanomethylophilus alvus" Mx1201, a methanogenic archaeon from the human gut belonging to a seventh order of methanogens**. *Am Soc Microbiol* 2012:6944-6945.

69. Borrel G, Harris HM, Parisot N, Gaci N, Tottey W, Mihajlovski A, Deane J, Gribaldo S, Bardot O, Peyretaillade E: **Genome sequence of "*Candidatus* Methanomassiliicoccus intestinalis" Issoire-Mx1, a third Thermoplasmatales-related methanogenic archaeon from human feces**. *Genome Announc* 2013, **1**:e00453-00413.

70. Horz H-P, Seyfarth I, Conrads G: ***mcrA* and *16S rRNA* gene analysis suggests a novel lineage of Archaea phylogenetically affiliated with Thermoplasmatales in human subgingival plaque**. *Anaerobe* 2012, **18**:373-377.

71. Mihajlovski A, Doré J, Levenez F, Alric M, Brugère JF: **Molecular evaluation of the human gut methanogenic archaeal microbiota reveals an age-associated increase of the diversity**. *Environ Microbiol Rep* 2010, **2**:272-280.

72. Dridi B, Henry M, Richet H, Raoult D, Drancourt M: **Age-related prevalence of *Methanomassiliicoccus luminyensis* in the human gut microbiome**. *APMIS* 2012, **120**:773-777.

73. Borrel G, O'Toole PW, Harris HM, Peyret P, Brugere J-F, Gribaldo S: **Phylogenomic data support a seventh order of methylotrophic methanogens and provide insights into the evolution of methanogenesis**. *Genome Biol Evol* 2013, **5**:1769-1780.

74. • Kröninger L, Steiniger F, Berger S, Kraus S, Welte CU, Deppenmeier U: **Energy conservation in the gut microbe *Methanomassiliicoccus luminyensis* is based on membrane-bound ferredoxin oxidation coupled to heterodisulfide reduction**. *FEBS J* 2019, **286**:3831-3843

This study indicated that the enzymes responsible for ion translocation in Methanomassiliicoccales are distinct from those of other methanogens.

75. Borrel G, Parisot N, Harris HM, Peyretaillade E, Gaci N, Tottey W, Bardot O, Raymann K, Gribaldo S, Peyret P: **Comparative genomics highlights the unique biology of Methanomassiliicoccales, a Thermoplasmatales-related seventh order of methanogenic archaea that encodes pyrrolysine**. *BMC Genom* 2014, **15**:1-24.

76. Tang WW, Wang Z, Kennedy DJ, Wu Y, Buffa JA, Agatisa-Boyle B, Li XS, Levison BS, Hazen SL: **Gut microbiota-dependent trimethylamine N-oxide (TMAO) pathway contributes to both development of renal insufficiency and mortality risk in chronic kidney disease**. *Circ Res* 2015, **116**:448-455.

77. Le Bras A: **Targeting the gut to protect the heart**. *Nat Rev Cardiol* 2018, **15**:581.

78. Brugère J-F, Borrel G, Gaci N, Tottey W, O'toole PW, Malpuech-Brugère C: **Archaebiotics: proposed therapeutic use of archaea to prevent trimethylaminuria and cardiovascular disease**. *Gut Microbes* 2014, **5**:5-10.

79. Bang C, Vierbuchen T, Gutsmann T, Heine H, Schmitz RA: **Immunogenic properties of the human gut-associated archaeon *Methanomassiliicoccus luminyensis* and its susceptibility to antimicrobial peptides**. *PLoS One* 2017, **12**: e0185919.

80. Tourna M, Freitag TE, Nicol GW, Prosser JI: **Growth, activity and temperature responses of ammonia-oxidizing archaea and bacteria in soil microcosms**. *Environ Microbiol* 2008, **10**:1357-1364.

81. Adam PS, Borrel G, Brochier-Armanet C, Gribaldo S: **The growing tree of Archaea: new perspectives on their diversity, evolution and ecology**. *ISME J* 2017, **11**:2407-2425.

82. Beam JP, Jay ZJ, Kozubal MA, Inskeep WP: **Niche specialization of novel Thaumarchaeota to oxic and hypoxic acidic geothermal springs of Yellowstone National Park**. *ISME J* 2014, **8**:938-951.

83. Moissl-Eichinger C, Probst AJ, Birarda G, Auerbach A, Koskinen K, Wolf P, Holman H-YN: **Human age and skin physiology shape diversity and abundance of Archaea on skin**. *Sci Rep* 2017, **7**:1-10.

84. Caporaso JG, Lauber CL, Costello EK, Berg-Lyons D, Gonzalez A, Stombaugh J, Knights D, Gajer P, Ravel J, Fierer N: **Moving pictures of the human microbiome**. *Genome Biol* 2011, **12**:1-8.

85. Dame-Teixeira N, de Cena JA, Côrtes DA, Belmok A, dos Anjos Borges LG, Marconatto L, Giongo A, Kyaw CM: **Presence of Archaea in dental caries biofilms**. *Arch Oral Biol* 2020, **110**:104606.

86. Oxley AP, Lanfranconi MP, Würdemann D, Ott S, Schreiber S, McGenity TJ, Timmis KN, Nogales B: **Halophilic archaea in the human intestinal mucosa**. *Envirol Microbiol* 2010, **12**:2398-2410.

87. Nam Y-D, Chang H-W, Kim K-H, Roh SW, Kim M-S, Jung M-J, Lee S-W, Kim J-Y, Yoon J-H, Bae J-W: **Bacterial, archaeal, and eukaryal diversity in the intestines of Korean people**. *J Microbiol* 2008, **46**:491-501.

88. Kim JY, Whon TW, Lim MY, Kim YB, Kim N, Kwon M-S, Kim J, Lee SH, Choi H-J, Nam I-H: **The human gut archaeome: identification of diverse haloarchaea in Korean subjects**. *Microbiome* 2020, **8**:1-17.

BMC Microbiology

RESEARCH

Open Access

Age-related dynamics of predominant methanogenic archaea in the human gut microbiome

Rokhsareh Mohammadzadeh[1], Alexander Mahnert[1], Tejus Shinde[1], Christina Kumpitsch[1], Viktoria Weinberger[1], Helena Schmidt[2] and Christine Moissl-Eichinger[1,3*]

Abstract

Background The reciprocal relationship between aging and alterations in the gut microbiota is a subject of ongoing research. While the role of bacteria in the gut microbiome is well-documented, specific changes in the composition of methanogens during extreme aging and the impact of high methane production in general on health remain unclear. This study was designed to explore the association of predominant methanogenic archaea within the human gut and aging.

Methods Shotgun metagenomic data from the stool samples of young adults ($n=127$, Age: 19–59 y), older adults ($n=86$, Age: 60–99 y), and centenarians ($n=34$, age: 100–109 years) were analyzed.

Results Our findings reveal a compelling link between age and the prevalence of high methanogen phenotype, while overall archaeal diversity diminishes. Surprisingly, the archaeal composition of methanogens in the microbiome of centenarians appears more akin to that of younger adults, showing an increase in *Methanobrevibacter smithii*, rather than *Candidatus* Methanobrevibacter intestini. Remarkably, *Ca.* M. intestini emerged as a central player in the stability of the archaea-bacteria network in adults, paving the way for *M. smithii* in older adults and centenarians. Notably, centenarians exhibit a highly complex and stable network of these two methanogens with other bacteria. The mutual exclusion between *Lachnospiraceae* and these methanogens throughout all age groups suggests that these archaeal communities may compensate for the age-related drop in *Lachnospiraceae* by co-occurring with *Oscillospiraceae*.

Conclusions This study underscores the dynamics of archaeal microbiome in human physiology and aging. It highlights age-related shifts in methanogen composition, emphasizing the significance of both *M. smithii* and *Ca.* M. intestini and their partnership with butyrate-producing bacteria for potential enhanced health.

Keywords Aging, Gut microbiota, methanogenic archaea, Butyrate-producing bacteria, Metagenome

*Correspondence:
Christine Moissl-Eichinger
christine.moissl-eichinger@medunigraz.at
[1]Diagnostic and Research Institute of Hygiene, Microbiology and Environmental Medicine, Medical University of Graz, Neue Stiftingtalstraße 6, Graz 8010, Austria
[2]Division of Molecular Biology and Biochemistry, Medical University of Graz, Graz, Austria
[3]BioTechMed, Graz 8010, Austria

© The Author(s) 2025. **Open Access** This article is licensed under a Creative Commons Attribution 4.0 International License, which permits use, sharing, adaptation, distribution and reproduction in any medium or format, as long as you give appropriate credit to the original author(s) and the source, provide a link to the Creative Commons licence, and indicate if changes were made. The images or other third party material in this article are included in the article's Creative Commons licence, unless indicated otherwise in a credit line to the material. If material is not included in the article's Creative Commons licence and your intended use is not permitted by statutory regulation or exceeds the permitted use, you will need to obtain permission directly from the copyright holder. To view a copy of this licence, visit http://creativecommons.org/licenses/by/4.0/.

Background

Aging is a complex process that affects the physiological, metabolic, and immune functions of humans often leading to chronic inflammation and metabolic issues [1]. It is uncertain whether the observed changes in the microbiota are a cause or consequence of aging. According to previous studies, elderly and centenarians tend to have distinct gut microbiome profiles as the latter are able to rearrange the microbiota that contribute to host health and physiology. This includes mitigating the depletion of *Ruminococcaceae*, *Lachnospiraceae*, and *Bacteroidaceae* through the promotion of potential health-enhancing subdominant species like *Akkermansia*, *Bifidobacterium*, and *Christensenellaceae* [2–5]. It is however challenging to determine whether these microbial differences contribute to extreme aging or result from a healthier lifestyle [6]. Animal studies suggest that age-related microbial imbalances can impact lifespan, with some animals benefiting from supplementation with a microbiome of younger ones [7] and others experiencing intestinal problems and premature mortality due to aging-associated microbiome changes [8]. Despite uncertainties regarding whether gut dysbiosis is a cause or consequence of aging and the subsequent inflammatory disorders, maintaining gut microbiota homeostasis is believed to be crucial for healthy aging and potentially supportive of human longevity [9, 10].

Since short chain fatty acids (SCFAs) produced by the microbiota are absorbed into the host bloodstream through the intestinal epithelium, it is plausible that microbiota-derived metabolites could have a substantial impact on human longevity [11]. The decline in metabolic health observed in old age may partly result from altered levels of intestinal SCFAs, and in particular, butyrate, leading to the disruption of gut barrier integrity, increased vulnerability to infections, and affecting conditions like insulin sensitivity and energy expenditure [12]. The study by Biagi et al., which is one of the few studies on the microbiome of centenarians residing in Western Europe, revealed the changes in gut microbial composition of these subjects, characterized by a decrease in core abundant taxa like *Bacteroides*, *Roseburia*, and *Faecalibacterium* species, along with an increase in rare taxa. Interestingly, they also observed a change in the population of butyrate-producing bacteria among centenarians. This suggests the possibility that, to achieve longevity, a complex and pervasive remodeling, which includes alterations of gut microbiota, should occur, favoring the balance between inflammatory and anti-inflammatory processes [13].

The human microbiome is not solely composed of bacteria; methanogenic archaea also play a significant but often overlooked role [14]. However, our understanding of age-related changes in gut-associated methanogens is limited. It is known that *Methanobrevibacter smithii*, as the predominant archaeal species within the human gut, gradually becomes the dominant archaeal colonizer in early life, with reported higher relative abundances in centenarians [13]. Moreover, Methanomassiliicoccales have been frequently observed in elderlies as compared to younger adults (prevalence of 40% vs. 10%) [15], and similarly, a significant age-related upward trajectory was observed for *Methanomassiliicoccus luminyensis* and *Candidatus* Methanomassiliicoccus intestinalis [16]. Yet, the specific alterations in the composition of methanogens and their co-occurrence between bacterial members of the human gut during extreme aging remains unknown. It is noteworthy that a considerable proportion of the human population, approximately 20% of Western adults, falls into the category of high methane emitters, which have been characterized by a 1000-fold increase in *M. smithii* relative abundance in their gut microbiome. While an association between high methane emissions and complexity within the gastrointestinal microbiome of younger populations has been reported [17], the precise distribution of subjects with high methanogen phenotype and their microbiome across various age groups remains an aspect yet to be elucidated.

Furthermore, recently, the existence of two distinct species within *Methanobrevibacter smithii* has been suggested [18]. Indeed, a recent study of archaeal metagenome-assembled genomes (MAGs) underscores the pronounced dissimilarities between *M. smithii_A* and *M. smithii* genomes within the Genome Taxonomy Database (GTDB), to the extent that these distinctions fulfill the threshold criteria for species differentiation, as stipulated by the average nucleotide identity (ANI) metric (> 95%). Consequently, *M. smithii_A* has been designated as '*Candidatus* Methanobrevibacter intestini' [18]. It remains an open question whether the distribution of *Ca.* M. intestini within the human population varies with age and whether there is a contribution of this archaeal species to methane production, analogous to its counterpart.

In the scope of this study, we sought to discern the diversity and distribution patterns of methanogenic archaea across different age groups of adults. Our study also encompasses a comprehensive examination of the prevalence for a high methanogen phenotype, within varying age groups. In addition, we embark on an exploration of the potential implications and associations of the presence of high methanogen phenotype in the context of extreme longevity. This research provides invaluable insights into the intricacies of archaeal dynamics within the human microbiome, and their age-related patterns.

Materials and methods

Study population

To include different age groups, our study incorporated three cohorts. As a young adult cohort, we used fecal samples from 91 subjects enrolled in Graz, Austria, which were initially collected for a study by Kumpitsch et al. (Cohort A) [17]. To encompass the older adults, a total of 94 participants aged 46–86 (68 ± 9.5) years (female: 51.6%) (Cohort B) were recruited at the Medical University of Graz, and finally, to include centenarians (Cohort C) in our study, we chose the metagenomes available in the Sequence Read Archive (SRA) repository under BioProject number PRJNA553191 from the study of Rampelli et al. [19], due to the close proximity of the subjects (Emilia Romagna region, Italy) to those enrolled for the first two cohorts.

Sample collection and DNA extraction

Following collection, stool samples were promptly placed in a stool collection tube and immediately placed on ice. Subsequently, the samples were divided into separate Eppendorf tubes, suspended in a solution of approximately 0.1 gram of fecal material and 0.9% (w/v) DNA-free phosphate-buffered saline, and stored at -20 °C for subsequent analyses.

Genomic DNA extraction was carried out on 250 µl of fecal samples using the DNeasy PowerSoil Kit (QIAGEN, USA) according to the manufacturer's protocol with a slight modification as previously described [17]. DNA was eluted in 80 µl elution buffer and the concentration was measured using the Qubit dsDNA HS Assay Kit (Thermo Fisher Scientific, USA).

Metagenomic sequencing

Extracted DNA from fecal samples, was sent for sequencing to Macrogen (Seoul, South Korea). Libraries were generated via Nextera XT DNA Library construction kit and sequenced on NovaSeq 6000 Illumina platform with a read length of 151. Raw reads were obtained in fastq format with a mean read count of 27,623,362 for each sample.

Taxonomic classification

Reads were quality checked and human reads were removed as previously described [19]. In summary, quality of all reads was assessed with fastqc (v0.11.8) [20], and subsequently filtered with trimmomatic (v0.38) [21] (a minimal length of 50 bp and a Phred quality score of 20 in a sliding window of 5 bp was applied). To filter out the human-mapped reads after quality filtering against the human chromosome GRCh38, bowtie2 (v2.3.5) and samtools (v1.9) were employed [22]. Subsequently, bedtools (v2.29.0) was used to extract the fastq files from the bam files [23]. We then used Kraken2 v.2.1.2 [24] to profile these final quality filtered reads with the Unified Human Gastrointestinal Genome (UHGG v.2.0.1) database of genomes, which consists of more than 289.000 archaeal and bacterial genomes. In order to increase the specificity and to compensate for the chance of returning the incorrect lowest common ancestor (LCA) of all genomes, a confidence threshold of 0.3 was chosen for Kraken2 v.2.1.2. To determine the relative abundance of bacterial and archaeal species, the Kraken2 output was subjected to analysis using Bracken v.2.7 [25]. with default settings. The report files were then merged to obtain an abundance table of microbial species which was used for further analysis.

Removal of the batch effect

Differences in experimental designs and sequencing protocols have the potential to impact the distribution of microbiome data [26]. Due to the inclusion of diverse age demographics within three distinct cohorts A, B, and C, and our aim to combine these cohorts for the comprehensive exploration of the microbiome in various age groups, we opted to mitigate the influence of unwanted batch variations arising from distinct study designs and sequencing protocols employed. For this purpose, to generate a batch-corrected table of microbiome read counts for further analyses, we utilized the ConQuR tool [27]. This tool effectively addresses read distribution through quantile regression and handles the presence or absence of microbes using conditional quantile regression. We used Cohort B as the reference batch since it removed batch effects the most (the least PERMANOVA R2) and used it across all taxa to keep the overall composition of microbiome and used the presence of high methanogen phenotype (defined based on *Methanobrevibacter* relative abundance as described previously [17]), age classification, and sex as variables.

Statistical analyses and visualization

Relative and differential abundance of archaea and bacteria were plotted in R (R-Core-Team, 2022) using the ggplot2 package (v3.3.3). Differentially abundant taxa were defined by q2-ALDex2 [28, 29] in QIIME2 [30]. To display those taxa in boxplots in R (packages: ggplot2 [31], dplyr [32], reshape [33]) the data of relative abundance were first CLR (centered log-ratio) transformed in R [34]. For statistical analyses, IBM SPSS Amos v26 was used. The normal distribution of parameters was checked using the Shapiro-Wilk test for the selection of the suitable statistical test. Throughout the manuscript, uncorrected significance values are reported as p-values and Benjamini-Hochberg corrected p-values are termed as q-values.

Co-occurrence analysis

The sparse nature of metagenomic data, which can be attributed to various factors, including sample variations and sequencing depth, presents a challenge when inferring co-occurrence patterns. These variables can introduce challenges in statistical analysis, potentially leading to false-positive results and misleading correlations. To address this issue, we applied a prevalence filter that excluded microbial species present in less than 20% of samples in each age group. We chose this prevalence threshold based on the number of reads for *Ca*. M. intestini to avoid losing this particular species of interest. This approach alleviated the impact of matrix sparsity on our results.

To infer species-level associations of *M. smithii* and *Ca.* M. intestini with other bacteria within the abundance matrix of each age group separately, we employed SparCC [35] within the SCNIC tool (Sparse Co-occurrence Network Investigation for Compositional data) [36]. This method for inferring microbial associations incorporates the compositionality of microbiome data and considers the possibility of indirect correlations. Co-occurrence events with correlation of >|0.4| were visualized in Cytoscape v.3.10.0 where nodes represent taxa and edges represent positive and negative co-occurrences according to the SparCC R values. Betweenness and closeness centrality of nodes within the networks were also analyzed in Cytoscape.

Gene catalog construction and analysis

Protein-coding genes were initially identified using Prodigal v.2.6.3 through the ATLAS workflow [37]. Elimination of duplicate genes was achieved through linclust with minid = 0.9 and coverag = 0.9 parameters [38]. The quantification of gene abundance per sample was performed using the combine_gene_coverages function within the ATLAS workflow, aligning high-quality filtered reads to the gene catalog via the BBmap suite v.39.01-1 [39]. Taxonomic and functional annotations were assigned based on the EggNOG database 5.0, employing eggnog-mapper (v.2.0.1) [40]. Subsequently, KEGG annotations were extracted from the output [41–43]. Read counts were implemented from the quality control workflow in ATLAS. The resultant outputs from ATLAS were analyzed in RStudio, following the procedures outlined in (https://github.com/metagenomce-atlas/Tutorial/blobs/master/R/Analyze_genecatalog.Rmd).

To ensure comparability of mapped read fractions for each sample, genes with annotations were acquired and normalized using the median of ratios method through DESeq2 [44]. Prefiltering was applied to retain only rows with a count of at least 10 for a minimum number of samples, which was determined based on the number of subjects with high methanogen phenotype. Furthermore, a differential expression analysis was conducted between subjects exhibiting a high methanogen phenotype and other subjects, employing the DESeq2 package in R Studio.

Gene correlation with taxonomic information

The normalized abundance of genes was then correlated with the CLR transformed abundance of species from the shotgun sequencing data in R. This analysis was performed separately for each age group after the application of ConQuR on the count data. Only the genes of interest coding for enzymes responsible for butyrate and propionate formation were correlated with the taxonomic data using Spearman rank correlations [45]. The analysis was plotted in a heatmap using ggplot2.

Results

Study overview

We studied three distinct cohorts; cohort A, consisting of young adults recruited in Graz, Austria ($n = 91$, ages 19–37 years), cohort B consisting mostly of older adults also recruited in Graz, Austria ($n = 94$, ages 46–86 years) and cohort C with subjects enrolled in the Emilia Romagna (Italy) by Rampelli et al. [19] ($n = 62$, ages 22–109 years) which was geographically very close to the other cohorts and mostly included centenarians (Supplementary Fig. 1).

Overall, the study cohorts included a total of 247 subjects, of three age groups; 127 subjects aged 19–59 y (young adults, "YAs"), 86 subjects aged 60–99 y (older adults, "OAs"), and 34 subjects aged 100–109 (centenarians, "CENT").

The analysis of age distribution among the three study groups (Cohort A, B, and C) revealed statistically significant differences, as expected. One-way analysis of variance (ANOVA) was conducted to compare the mean ages of participants in each cohort. The results indicated a significant variation in age across the cohorts ($F = 391.323$, $p < 0.001$), confirming the representation of different age groups by each cohort. On the other hand, a similar distribution of males and females existed within the investigated cohorts as shown by the chi-square test of independence ($\chi^2 = 5.871$, $df = 2$, $p = 0.053$).

It is important to note that the three cohorts under study may exhibit variations in numerous potential covariates that have remained unrecorded. Moreover, as differences in sample processing could result in bias in data analysis, we implemented a batch effect correction procedure based on the available metadata (see below).

Removal of batch effect allows for comparison across datasets

The abundance profiling of the combined datasets based on UHGG showed a total of 4,253 distinct species, which

were identified across 247 different samples. In order to remove the batch effects between studies and eradicate the high data variability, we employed the ConQuR. tool. Additionally, since all covariates (e.g., dietary information) could not be obtained for each subject in the study of Rampelli et al. [19], ConQur could to some extent account for these cofounders.

It was evident that ConQuR significantly diminished the study-related variation observed in the raw count data, as indicated by the Bray-Curtis and Aitchison distance analyses (Supplementary Fig. 2). PERMANOVA test showed no differences in the Bray-curtis and Aitchison distances before (Bray-curtis $p = 0.001$, Aitchison $p = 0.001$) and after (Bray-curtis $p = 0.001$, Aitchison $p = 0.001$) applying ConQur. However, when looking at the raw count scale, ConQur made significant adjustments to both the average values (centroids) and the spread of the data (size of the ellipses). Specifically, this tool aligned the averages of the three datasets to the same point, as depicted by the ellipses connecting the 95th percentile of points for each set in the bivariate plot (Supplementary Fig. 2).

Moreover, based on the PERMANOVA analysis on the count data, the initial $R^2 = 0.10026030$ (before applying ConQuR), reduced to $R^2 = 0.01868353$ (after applying ConQuR), which was lower than the effect of age ($R^2 = 0.03042544$, after ConQuR vs. $R^2 = 0.05358378$, before ConQuR) and effect of the presence of high methanogen phenotype ($R^2 = 0.02614169$; after ConQuR vs. $R^2 = 0.03092168$; before ConQuR).

Aging is mirrored in the overall microbiome profile

After applying ConQuR for the 247 samples analyzed, the average number of raw reads for metagenomic analyses per subject from each age group ranged from 7,741,637, 6,993,479.8, and 10,103,384 for YAs, OAs, and CENT, respectively, with archaeal reads constituting 0.4972%, 0.4001%, and 0.9476% of all reads corresponding to each age classification in the mentioned order, indicating almost the highest distribution of archaeal read counts in CENT (Mann-Whitney U-test; YAs: OAs $p = 0.07$, YAs: CENT $p = 0.219$, OAs: CENT $p = 0.463$) (Supplementary Fig. 3A).

For alpha diversity analysis of the overall microbiome, we calculated the Shannon, richness, and evenness indices. The Shannon index of CENT was significantly lower than that of YAs (Wilcoxon test, $p = 0.002$) and OAs (Wilcoxon test, $p = 0.005$) (Fig. 1A). The same trend was observed for the evenness index as it was significantly lower in CENT compared to YAs (Wilcoxon test, $p = 0.003$) and OAs (Wilcoxon test, $p = 0.002$) (Supplementary Fig. 3B). The richness index decreased with age (Supplementary Fig. 3B); however, this was not significant (Supplementary Fig. 3B). These results suggest a lack of statistical divergence in the alpha diversity of the microbiota community between YAs and OAs; however, alpha diversity of CENT was significantly lower as compared with the other two age groups. This significant drop in the Shannon diversity measure of CENT was in line with observations made in previous studies [12, 46].

To characterize gut microbial patterns associated with aging, we also performed a β-diversity analysis using principal coordinates analysis (PCoA) and Non-Metric Multidimensional Scaling (NMDS). A major overlap was observed in the PCoA and NMDS plots, however, PERMANOVA under 999 permutations showed a significant difference ($p < 0.001$; stress (NMDS): 0.2577) between the beta-diversity of the three age groups (Fig. 1B, Supplementary Fig. 3C), as observed previously [6].

With respect to the bacteriome, we could observe that at phylum level, Firmicutes, Proteobacteria, Actinobacteriota, and Bacteroidota were the dominant bacterial taxa in each age group, which was in accordance with previous reports with different cohorts (Fig. 1C) [47]. However, both Firmicute_A and Bacteroidota exhibited significantly lower levels in CENT when contrasted with YAs and OAs (Firmicute_A $p < 0.01$, $q < 0.01$; Bacteroidota $p < 0.001$, $q < 0.001$; Wilcoxon test).

The composition of methanogens in centenarians is similar to that of young adults

The potential impact of archaea, as the understudied members of the human microbiome, on aging was investigated in more detail. Aging affected the alpha diversity of methanogenic archaea as exhibited by the statistically significant decrease in the Shannon index ($p < 0.001$) across the studied age groups (Fig. 1D). This results is in contrast with previous reports based on 16S rRNA gene amplicon sequencing [15].

We observed distinct age-related shifts in the archaeome profile. Focusing first on the class Methanobacteria, there was a non-significant decline trend of increasing relative abundance with age [16, 48]. Within this class, the family *Methanobacteriaceae* showed a slight, non-significant decline in relative abundance in OAs compared to YAs and CENT (Fig. 1E, Supplementary Material 1). At the species level (same family), *Methanobrevibacter* spp. exhibited notable age-related differences: *Methanobrevibacter smithii* was less abundant in OAs compared to both YAs and CENT, while *Candidatus* Methanobrevibacter intestini, a newly identified species [18], increased in OAs relative to YAs before declining in CENT (Fig. 1E, Supplementary Material 1).

Shifting focus to the class Thermoplasmata, a statistically significant increase in relative abundance was observed in OAs compared to both YAs and CENT (Fig. 1E, Supplementary Material 1). This increase was

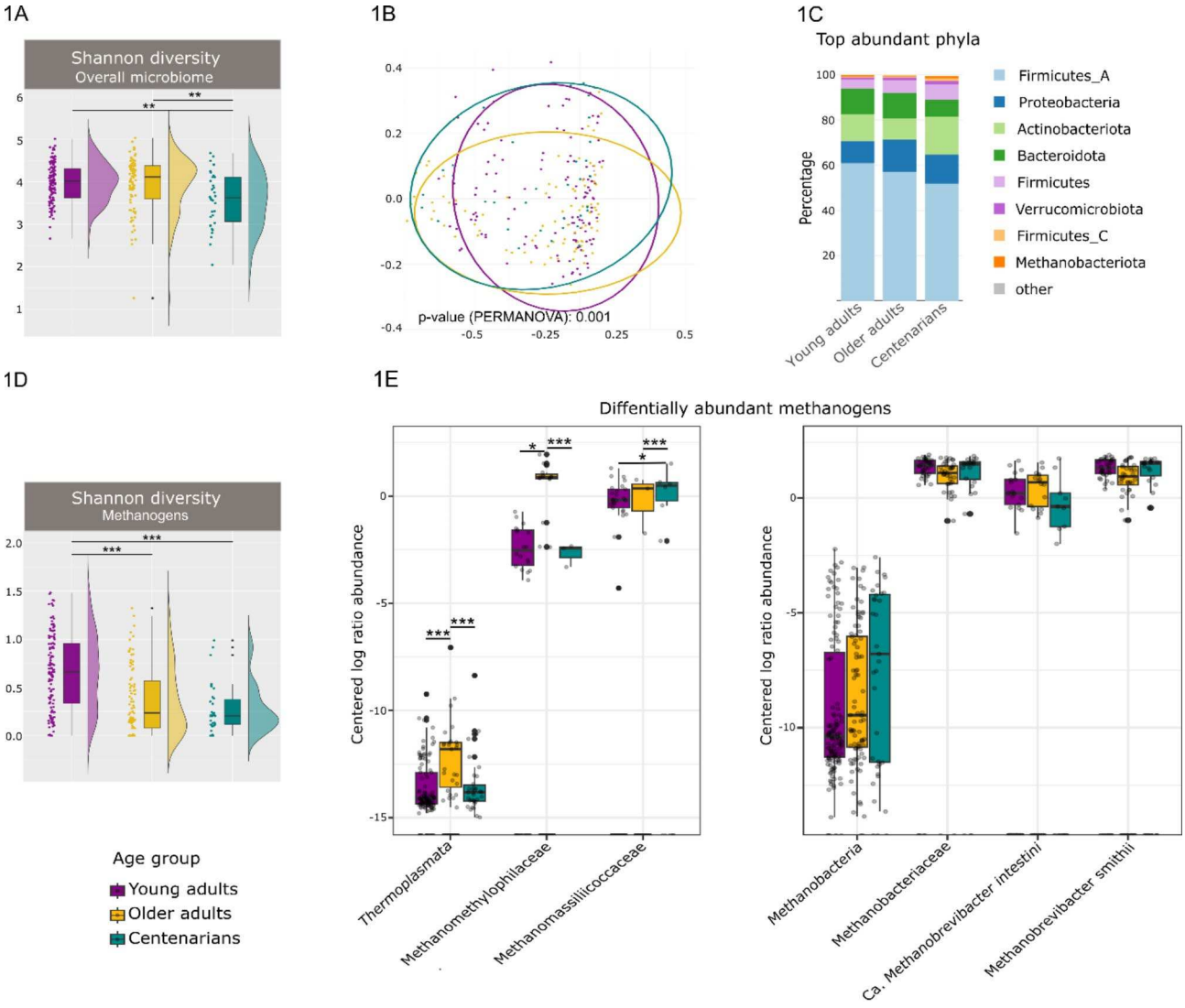

Fig. 1 Comparative analysis of fecal microbiome diversity and methanogens in different age groups. (**A**) Comparison of Shannon diversity between three age groups of YAs, OAs, and CENT. (**B**) Beta diversity of fecal microbiomes between YAs, OAs, and CENT. (**C**) Stacked bar plot of relative abundances of the top microbial phyla is displayed by age groups (**D**) Shannon diversity of methanogens in different age groups of YAs, OAs, and CENT. (**E**) Box plot of CLR-transformed abundances of the methanogenic archaea in each age group (Methanobacteria: YAs: OAs $q = 0.162$, YAs: CENT $q = 0.489$; OAs: CENT $q > 0.5$; *Methanobacteriaceae*: YAs: OAs, $q = 0.062$; YAs: CENT $q > 0.5$; OAs: CENT, $q > 0.5$; *Methanobrevibacter smithii*: YAs: OAs $q > 0.5$, YAs: CENT $q > 0.5$; OAs: CENT; *Candidatus* Methanobrevibacter intestini: YAs: OAs $q = 0.263$; YAs: CENT $q = 0.0905$, OAs: CENT $q > 0.5$; Thermoplasmata: YAs: OAs, $q < 0.001$, YAs: CENT $q = 0.00102$ OAs: CENT $q = 0.00102$; *Methanomethylophylaceae*: YAs: OAs $q < 0.001$, YAs: CENT $q > 0.5$; OAs: CENT $q < 0.001$; *Methanomassiliicocaceae*: YAs: OAs $q > 0.5$; YAs: CENT $q = 0.019$; OAs: CENT $q = 0.0013$). Line in boxes is a median of index scores, boxes represent interquartile range, whiskers represent lowest and highest values, and dots represent each sample. Statistical significance in 1 A and 1D is indicated by $^{**}p < 0.001$ $^{**}p < 0.01$ and $^{*}p < 0.05$. Statistical significance levels of ALDEx2 test in 2E after adjustment for multiple comparison are indicated with $^{***}q < 0.001$, $^{**}q < 0.01$, $^{*}q < 0.05$

primarily driven by two families: *Methanomethylophylaceae* and *Methanomassiliicocaceae*. *Methanomethylophylaceae* were significantly more abundant in OAs compared to YAs and CENT, while *Methanomassiliicocaceae* showed a more complex pattern. Although OAs had higher levels of *Methanomassiliicocaceae* than YAs, the difference was not significant. However, CENT exhibited significantly elevated levels compared to both YAs and OAs (Fig. 1E, Supplementary Material 1), consistent with previous studies.

In summary, while both OAs and CENT showed decreased methanogen diversity, the methanogenic archaea composition in CENT more closely mirrors that of YAs than OAs. This similarity is most evident at the family and species levels, particularly in the relative abundance of *Methanomethylophylaceae* and *Methanobacteriaceae* (at family level), and *M. smithii* (at species level), where patterns in CENT align more closely with those of YAs.

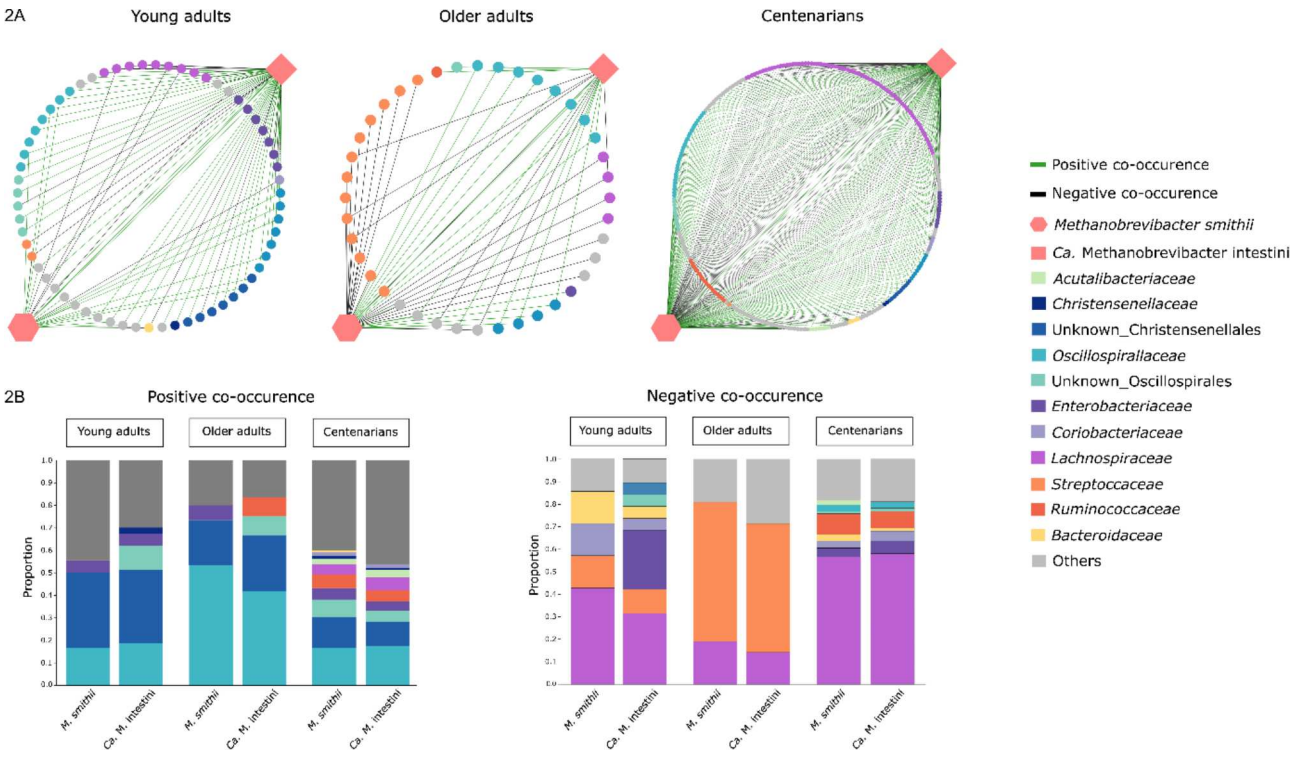

Fig. 2 SparCC co-occurrence networks of *M. smithii* and *Ca.* M. intestini in all samples irrespective of the presence of high methanogen phenotype (**A**). Each node represents a single microbial species, and each edge a single association between a pair of microbial species. Positive and negative SparCC co-occurrences are indicated in green and black, respectively. These co-occurrences are elaborated in (**B**)

Table 1 Parameters of *M. smithii* and *Ca.* M. intestini networks with the gut microbial community of the studied subjects

Archaeal species	Network parameter	Network inference for all studied subjects			Network inference for subjects with high methanogen phenotype		
		YAs	OAs	CENT	YAs	OAs	CENT
M. smithii	Node degree (+/-) *	25 (18+, 7-)	37 (15+, 21-)	231 (132+, 98-)	82 (46 - /36 +)	117 (62+/55-)	169 (47-, 122+)
	Betweenness centrality	0.246	0.832	0.659	0.507	0.902	0.790
	Closeness centrality	0.627	0.911	0.871	0.442	0.678	0.734
Ca. M. intestini	Node degree (+/-) *	56 (37+, 19-)	19 (12+, 7-)	190 (121+, 69-)	156 (90 -/66+)	48 (27+/21-)	120 (60 +/60 -)
	Betweenness centrality	0.876	0.251	0.424	0.864	0.416	0.593
	Closeness centrality	0.901	0.661	0.770	0.626	0.421	0.649

* Positive (co-presence) /negative (mutually excluded) association

The two predominant *Methanobrevibacter* species co-exist and demonstrate co-occurrence with health-associated bacterial species

Microbial networks, which are constructed based on correlations in species abundances, offer insights into co-occurrences among microbes within a community. In order to gain a better understanding of the microbes with potential co-occurrence with *M. smithii* and *Ca.* M. intestini in the gut across different age groups, we utilized abundance data of taxa from each group to generate three distinct networks (Fig. 2A). Of note, while these networks reveal niche-sharing patterns, they do not necessarily indicate direct physical or biochemical interactions between microbes [49].

Our analysis of the networks revealed, that *M. smithii* and *Ca.* M. intestini had the highest degree of interconnectivity in CENT (Table 1), suggesting that these methanogens play a more central role in the gut microbiome of this age group. In contrast, OAs exhibited the lowest interconnectivity, pointing to a less complex network structure for these methanogens.

Centrality metrics, including betweenness and closeness centrality, as well as node degree, revealed a shift in the key drivers of these networks across age groups (Table 1). In YAs, *Ca.* M. intestini emerged as the

keystone species, driving microbial networks, whereas in OAs and CENT, *M. smithii* took on this role (Table 1).

A detailed examination of microbial species in these networks highlights the consistent co-occurrence of *M. smithii* and *Ca.* M. intestini across all three age groups (Fig. 2A), which is unexpected given their similar resource requirements. The persistence of both species suggests that competition does not entirely exclude one from the niche, indicating a more complex dynamic between these two species.

Additionally, certain microbial taxa showed consistent associations with these methanogens. Members of the orders Oscillospirales and Christensenellales (specifically families *Oscillospiraceae* and *Christensenellaceae*) frequently co-occurred with both *M. smithii* and *Ca.* M. intestini in all age groups (Fig. 2A and B). This aligns with previous findings of positive associations between *Oscillospira* spp. and *Christensenellaceae* with *M. smithii* [17, 50].

However, the family *Lachnospiraceae* exhibited mixed associations. While species within this family, like *Roseburia hominis*, *Blautia hansenii*, and *Blautia massiliensis* positively co-occurred with *M. smithii* and *Ca.* M. intestini in CENT, a larger proportion of *Lachnospiraceae* members were associated with negative co-occurrences (mutual exclusion) across all age groups (Fig. 2B).

Age-specific patterns were also observed for other abundant bacterial taxa. For instance, *Streptococcus* emerged as a key taxon showing mutual exclusion with both *M. smithii* and *Ca.* M. intestini predominantly in OAs (Fig. 2B). This may reflect a shift toward "oralization" of the gut microbiome, possibly influenced by the use of proton pump inhibitors [51].

Furthermore, while some opportunistic pathogens within the family *Enterobacteriaceae* exhibited positive co-occurrences with *M. smithii* and *Ca.* M. intestini, mutual exclusion with pathogens like *Klebsiella*, *Salmonella*, and *Proteus* was mostly observed in YAs and CENT, suggesting a more protective role of these methanogens against harmful bacteria in YAs and CENT.

High methanogen phenotype is twice as common in centenarians

Since the focus of our study was on the human archaeome and its association with aging, a phenotypic grouping of individuals according to their archaeal profile was necessary. A bimodal pattern has been demonstrated for the prevalence of *Methanobrevibacter* in the human gut, indicating that it is either highly prevalent or almost absent [52]. However, some subjects might still show a certain relative abundance of *Methanobrevibacter*, while not being categorized as high methanogen phenotype. To investigate how methanogens are linked with the overall microbiome composition, subjects were stratified into high and low methanogen phenotype based on the relative abundance of *Methanobrevibacter* according to our previous observations [17]. Interestingly, the prevalence of the subjects with high methanogen phenotype within distinct age groups was as follows: 25.2% (32/127; 95% CI: 19.6–31.6%) among YAs, 41.86% (36/86; 95% CI: 32.6–51.1%) among OAs, and 58.82% (20/34; 95% CI: 41.3–73.1%) among CENT (Supplementary Fig. 4A). This observation suggests an elevated prevalence of subjects with high methanogen phenotype with respect to aging. According to the results of Pearson's chi-square test the prevalence percentages of subjects with high methanogen phenotype appear to be significantly different among different age groups (chi-square = 13.762, df = 2, $p = 0.001027$), and the presence of high methanogen phenotype and age group variables are significantly associated (chi-square = 15.458, df = 2, $p < 0.001$) (Supplementary Fig. 4B). In fact, based on these results, it was evident that the highest association between the presence or the frequency of high methanogen phenotype was in centenarians, while the reduced frequency of high methanogen phenotype was positively associated with YAs.

The presence of high methanogen phenotype affects microbiome characteristics across age groups

A significantly higher Shannon diversity was observed in subjects with high methanogen phenotype compared to those without in YAs and OAs (Fig. 3A) (Shannon index = 4.247 ± 0.353, $p < 0.001$ for YAs; Shannon index = 4.171 ± 0.265, $p = 0.025$ for OAs) (consistent with previous results [17]). There was also a consistent and statistically significant elevation in microbial richness attributed to the high methanogen phenotype, across all three age groups ($p < 0.001$; t-test), indicating a higher diversity of microbial signatures in the presence of high methanogen phenotype. The evenness measure, however, exhibited significant elevation with respect to the high methanogen phenotype only among YAs ($p = 0.002$; t-test) (Supplementary Fig. 5A).

The microbial community composition revealed statistically significant differentiation between clusters of subjects characterized by the presence of the high methanogen phenotype and those lacking it (within the age groups of YAs $p = 0.001$, OAs $p = 0.004$, and CENT $p = 0.034$) (Fig. 3B).

It is important to note that the variability within the microbial communities of subjects with high methanogen phenotype was notably higher in both YAs and OAs compared to CENT (YAs $p < 0.001$, OAs $p = 0.005$, CENT $p = 0.028$; PERMANOVA). The finding that subjects with high methanogen phenotype in CENT do not exhibit a strongly significant difference in their microbiome compared to those subjects within YAs and OAs might suggest that the gut microbiota of these subjects within the

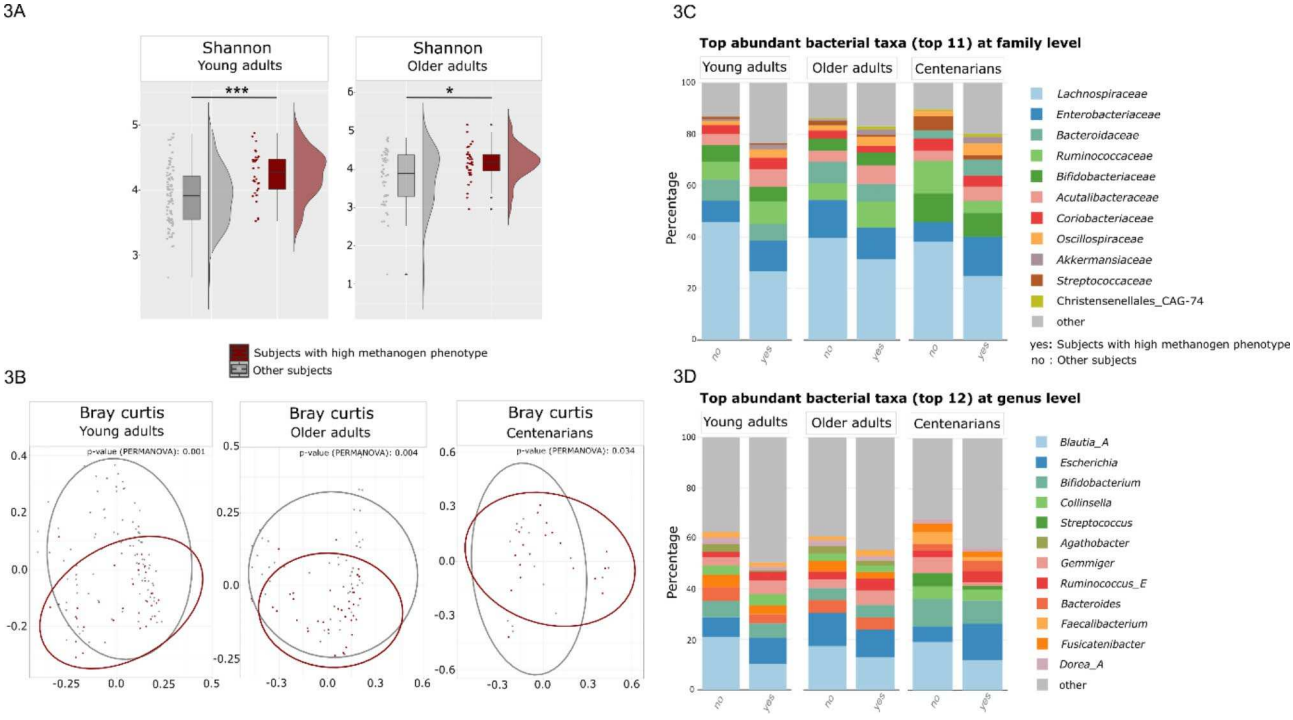

Fig. 3 Differences in alpha and beta diversity, and top abundant taxa based on the metagenomics shotgun sequencing between subjects with high methanogen phenotype and other subjects in different age groups. (**A**) An examination of Shannon diversity index revealed significant differences in alpha diversity based on high methanogen phenotype in both YAs and OAs (***$p < 0.001$, *$p < 0.05$). However, all subjects either with or without high methanogen phenotype within CENT showed similar trends regarding Shannon index. (**B**) The microbiome of subjects with the high methanogen phenotype clustered significantly differently in the PCoA plots, regardless of age classification. However, this significance was notably higher only in YAs and OAs. (**C**) Bar chart of the most abundant bacterial taxa at family level and (**D**) genus level compared regarding the presence of high methanogen phenotype with respect to each age classification of YAs and OAs, as well as CENT

CENT might possess less unique microbiota as compared with those without high methanogen phenotype in this age group.

The results centered around the presence of the high methanogen phenotype revealed consistent variations in the relative abundance of some specific taxa, regardless of their categorization within a specific age group. Specifically, the family *Lachnospiraceae* and within this family, at genus level, *Agathobacter*, *Blautia*, *Dorea* (known butyrate-producing taxa) [53–55] were reduced in relative abundance in subjects with high methanogen phenotype across all age groups (Fig. 3B and C, Supplementary Fig. 5A, B, Supplementary Material 1). Additionally, diminished relative abundance of the family *Streptococcaceae* and the genus *Streptococcus* was documented in these subjects across all age groups (Fig. 3C, Supplementary Fig. 6A, B), while *Acutalibacteriaceae*, Christensenellales_CAG-74, and *Oscillospiraceae* showed high relative abundances within the high methanogen phenotype subjects regardless of their age (Fig. 3C, Supplementary Fig. 6A, B, Supplementary Material 1).

The microbial composition of those with a high methanogen phenotype was particularly similar in YAs and OAs. In contrast, CENT exhibited slightly varied microbial composition for the high methanogen phenotype, highlighting a distinct microbial ecosystem within this age group. Particularly, a noteworthy observation was made within CENT, where *Gemmiger* and *Faecalibacterium* as well as *Ruminococcaceae* demonstrated a marked reduction in subjects with the high methanogen phenotype (Fig. 3C and D, Supplementary Fig. 6A, B, Supplementary Material 1). On the other hand, *Ruminococcaceae* showed increased relative abundance in subjects with high methanogen phenotype in YAs and OAs. Interestingly, although not statistically significant, *Ruminococcus_E* was highly abundant in subjects with high methanogen phenotype within all three age groups (Fig. 3D, Supplementary Fig. 6B, Supplementary Material 1), which was consistent with previous reports [17]. *Ruminococcus* demonstrates a significant correlation with dietary fibers, owing to its efficient breakdown of microcrystalline cellulose. Previous studies conducted by researchers have indeed elucidated a link between cellulose degradation and the subsequent emission of methane [56].

Co-occurring bacterial consortium of predominant *Methanobrevibacter* spp. Is complex and dynamic in subjects with high methanogen phenotype across all age groups

When examining the microbial networks of *M. smithii* and *Ca.* M. intestini in individuals exhibiting a high methanogen phenotype, it became apparent that the stability of the microbial networks for these two archaeal species remained consistent in these subjects, irrespective of age categorization. Each network displayed comparable complexity. Interestingly, the network complexity and co-occurring microbes were mostly similar in subjects with high methanogen phenotype within YAs and CENT. The microbiome composition and co-occurring taxa are often linked to health status. In aging, OAs commonly experience inflammaging, a chronic low-grade inflammation where the microbiome plays a pivotal role [57]. Centenarians may exhibit a unique microbial profile associated with superior health and longevity, reflecting a more similar composition of co-occurring taxa.

The betweenness and closeness centrality metrics for *M. smithii* and *Ca.* M. intestini exhibited comparable patterns to those seen in all subjects, irrespective of the presence of high methanogen phenotype (Table 1). Among YAs with high methanogen phenotype, *Ca.* M. intestini played a central role in the microbial network, whereas in OAs and CENT with high methanogen phenotype, *M. smithii* emerged as the primary driver of the microbial network (Table 1).

Taking a closer look at *M. smithii* and *Ca.* M. intestini edges within networks, mutual exclusion of these archaeal species with members of *Ruminococcaceae*, *Bacteroidaceae*, and *Streptococcaceae*/*Streptococcus*, and co-presence with Oscillospirales/*Oscillospiraceae* as well as Christensenellales were observed (Supplementary Fig. 7), which was similar to the trends observed before, irrespective of the presence or absence of high methanogen phenotype.

Of note, while most members of *Lachnospiraceae*, including *Acetatifactor* (YAs, CENT), *Agathobacter* (all age groups), *Blautia* (all age groups), *Dorea* (all age groups), *Eubacterium* (YAs, CENT), *Fusicatenibacter* (all age groups), *Lachnospira* (YAs, CENT), and *Roseburia* (YAs, CENT), showed co-presence with *M. smithii* and *Ca.* M. intestini, some of the genera within this family including *Eisenbergiella* (all age groups) and *Mediterranibacter* (all age groups), showed mutual exclusion with these archaeal species. This could be attributed to potential different ecological roles or metabolic functions of these bacteria leading to competition or niche differentiation as well as difference in their adaptation to specific environmental conditions.

High methanogen phenotype is associated with the upregulation of genes involved in butyrate and propionate production

The decrease in *Lachnospiraceae*, known butyrate producers, has been consistently documented in CENT in several studies, irrespective of the geographical region [13, 58, 59]. This prompts the hypothesis that individuals having detectable *M. smithii* and *Ca.* M. intestini in their gut microbiome may better cope with decline during aging, as evidenced by the consistent co-occurrence of these archaeal species with *Oscillospiraceae*, another known butyrate-producing component of the gut microbiota. Notably, an increased relative abundance of *Oscillospiraceae* was observed in subjects exhibiting a high methanogen phenotype (Fig. 2, Supplementary Figs. 6, 7).

Diverse and abundant genes related to butyrate metabolism are present in the metagenomic datasets. Specifically, pathways such as the butyryl-CoA: acetate-CoA pathway and the butyrate kinase pathway contribute to the formation of butyrate. Genes encoding enzymes directly involved in butyrate production were analyzed and individuals with a high methanogen phenotype exhibited varying levels of these genes (Fig. 4A).

In YAs, the majority of genes involved in both pathways, were significantly elevated in individuals exhibiting a high methanogen phenotype compared to other subjects (Fig. 4A). In OAs and CENT, only the genes associated with pyruvate ferredoxin oxidoreductase (K00169, K00170) were significantly elevated ($q < 0.05$) within the butyryl-CoA: acetate-CoA pathway, though most other genes in this pathway also showed an increased level (Supplementary Material 1). Intriguingly, in subjects with high methanogen phenotype within these age groups, butyrate kinase (K00929), the terminal enzyme in the butyrate kinase pathway responsible for synthesizing butyrate, exhibited statistically elevated levels ($q < 0.01$) and the gene coding for phosphate butyryltransferase (K00634) displayed an increasing trend (though not reaching statistically significance), hinting at the potential significance of the butyrate kinase pathway in the elevated butyrate levels in these individuals (Fig. 4A).

Both butyrate kinase and acetate-CoA transferase are key enzymes in butyrate production, and butyrate kinase levels were significantly higher in all age groups in individuals with a high methanogen phenotype (Supplementary Material 1). A closer examination revealed a positive correlation between butyrate production genes via the butyrate kinase pathway and *Oscillospiraceae*, while a negative correlation was observed with *Lachnospiraceae* (Fig. 4B, Supplementary Fig. 8). This observation supports our hypothesis that individuals with a high methanogen phenotype, may compensate for the reduction in butyrate levels by harboring elevated levels of *Oscillospiraceae*, particularly through the butyrate kinase pathway.

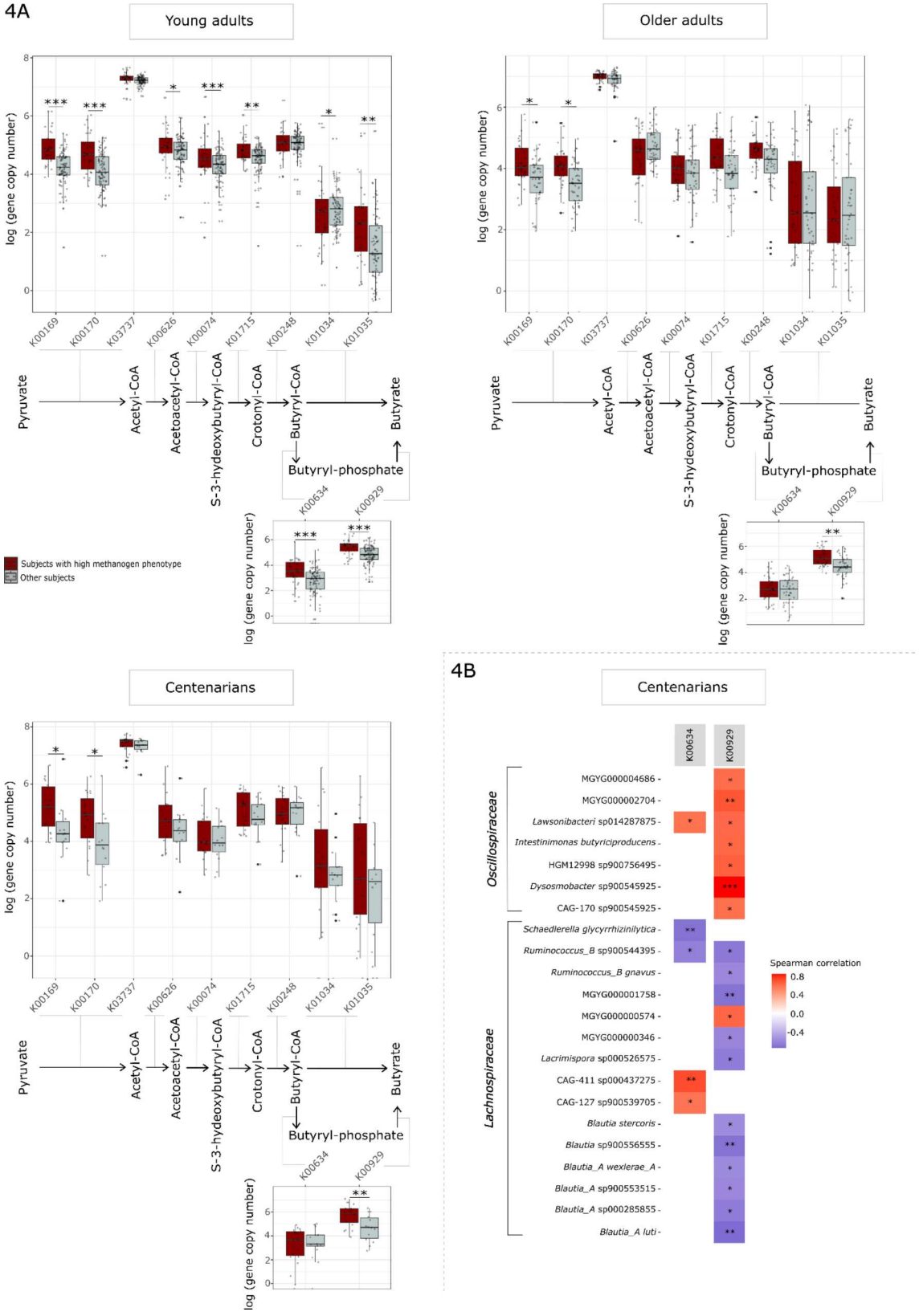

Fig. 4 (See legend on next page.)

(See figure on previous page.)

Fig. 4 (**A**) Boxplot of gene copy numbers (metagenomic abundance) involved in butyrate production. K00169, K0017, K03737: Pyruvate ferredoxin oxidoreductase [EC: 1.2.7.1]; K00626: Acetyl-CoA acetyltransferase [EC: 2.3.1.9]; K00074: 3-hydroxylbutyryl-CoA dehydrogenase [EC: 1.1.1.157]; K01715: Enoyl-CoA hydratase [EC: 4.2.1.17]; K00248: butyryl-CoA dehydrogenase [EC: 1.3.8.1]; K01034, K01035: Acetate-CoA transferase [EC: 2.8.3.8]; K00634: phosphate butyryltransferase [EC: 2.3.1.19]; K00929: butyrate kinase [EC: 2.7.2.7]. Significance levels are indicated as ***q < 0.001, **q < 0.01, *q < 0.05, for differentially abundance testing by DESeq2. (**B**) Correlation of butyrate kinase pathway genes in centenarians with bacterial taxa. ***q < 0.001, **q < 0.01, *q < 0.05

Discussion

Aging-associated changes in the gut microbiome have been tackled in several studies [60], however, despite the vital importance of the gut archaeome, there is a significant gap in our understanding regarding how age, and especially longevity, affects the distribution of archaea within the gut and vice versa. Specifically, the role of methanogenic archaea with a profound impact on the structure and functionality of the entire gastrointestinal microbiome remains poorly elucidated. Moreover, since *Methanobrevibacter smithii*, as the predominant archaeal species within the human gut, has been recently divided into two clades, namely *M. smithii* and *Candidatus* Methanobrevibacter intestini, highly resolved investigation of gut archaeome helps to deepen our understanding of the association of these two archaeal species with aging and their role in the emergence of high methanogen phenotype.

Our study revealed that, with aging, the gut archaeome richness and/or diversity decreased, which was in contrast to the previous reports based on 16S rRNA gene sequencing [15]. We then delved more into the differences of the archaeal profile of different age groups. The increased relative abundance of *M. smithii* with advancement of age, and the possible increased relative abundance of this methanogen prior to longevity has been previously reported [6].

Similarly, our study suggests a trend where the relative abundance of Methanobacteria generally shows increased abundance in older age groups. However, we observed that OAs in our study showed a higher relative abundance of *Ca*. M. intestini compared to YAs and CENT, rather than *M. smithii*. It is important to note that these observations are based on cross-sectional data. Hence, observed differences could be also influenced by varying health statuses among the studied age groups.

Thermoplasmata is another commonly found archaeal taxon in the human gut that tends to be more abundant in OAs. This has led to the hypothesis that since these archaea have environmental origins, age could play a role in promoting their survival in certain individuals [16]. Our observations also indicated the high relative abundance of these archaea in OAs compared with YAs, however, interestingly, the relative abundance of Thermoplasmata in CENT showed reduction as compared with OAs and was observed to be rather comparable to YAs. There is evidence suggesting that Thermoplasmata could potentially contain genes responsible for producing certain metabolites such as methylglyoxal, indole, and acetaldehyde with the potential of disrupting DNA or signaling pathways [61, 62]. Although further molecular experiments and longitudinal studies are required to fortify the involvement of these archaea in disease progression, there might be a potential link between the presence of Thermoplasmata and disease, which could explain why they appear to be less abundant in individuals with a longer lifespan. Interestingly, according to the literature, within this archaeal order, certain species may counteract trimethylamine (TMA, involved in the progression of atherosclerosis), while some species lack this capability. On the other hand, the high relative abundance of *Ca*. Methanomassilicocales intestinalis in frail individuals raises questions about its role and it is not clear whether its high relative abundance is favored due to factors like altered gut transit or independently contributing to inflammation. Further research is needed to assess the immune potential of dominant Methanomassiliicoccales, especially those using TMA, and determine if their role is primarily positive through TMA removal or more nuanced [48].

According to the archaeal abundance, subjects could be stratified into low and high methanogen phenotypes. Our study revealed that the prevalence of subjects with high methanogen phenotype increases with age. Interestingly, not only *M. smithii*, but also *Ca.* M. intestini was found to contribute to the emergence of high methanogen phenotype, with a more evident contribution of *Ca.* M. intestini in OAs, which can be argued by the increased relative abundance of this archaeal species in this age group. The exact cause of the link between the higher prevalence of high methanogen phenotype in older age remains somewhat elusive, however, the slower digestive transit times often observed in aging individuals, as well as their differences in dietary habits and contact with livestock could contribute to the overrepresentation of archaea [63, 64]. Moreover, the centenarians lifelong adherence to traditional dietary patterns, such as the Mediterranean diet [65] likely plays a significant role in shaping their gut microbiome and the overrepresentation of methanogens like *Methanobrevibacter* and the subsequent higher prevalence of high methanogen phenotypes. One key factor is the high intake of dietary fiber from plant-based foods, which supports the breakdown of complex carbohydrates into C1 metabolites. These metabolites serve as substrates for *Methanobrevibacter*, fueling methanogenesis and resulting in higher methane emissions in the

gut [17]. However, a notable limitation of our study is the lack of precise nutritional data for each sample. This constraint prevented a more detailed analysis of the specific dietary contributions to high methanogen prevalence in each age group and gut archaeome composition. Additionally, the association between *Methanobrevibacter* and a lean phenotype [66, 67] may also help explain its higher abundance in centenarians, since Italian centenarians remained physically active throughout their lives, maintaining lean body types [65].

Subjects with high methanogen phenotype showed different microbiome signatures and higher microbial diversity, especially evident in YAs and OAs rather than CENT. Interestingly, a significantly higher alpha diversity has been frequently linked to improved stability and resistance to disruptions [68]. This increased diversity of microbial species in subjects with high methanogen phenotype has been previously linked to the ability of methanogens to reduce the hydrogen partial pressure and thus facilitating the microbial fermentation, which is otherwise restricted by the hydrogen accumulation and inhibition of NAD coenzyme regeneration [69]. In CENT with high methanogen phenotype, only the richness index was significantly higher and not the evenness. In general, despite occasional contradictions [70], lower gut microbial alpha diversity has been shown in CENT compared to that of YAs and OAs [12, 71]. A variety of confounding factors can influence the controversial reports regarding microbiota alpha diversity with respect to aging. These factors include host and/or lifestyle factors as well as geography or the number of included subjects in cohorts. Moreover, although the CENT cohort represents a healthy population, the process of aging, particularly in its later stages, is associated with a natural decline in gastrointestinal function and the host immune response. This decline may contribute to the onset of chronic low-grade inflammation and metabolic disorders [72–74]. Therefore, a reduction in alpha diversity measures of high methanogen phenotype in CENT compared to those within YAs and OAs is not surprising.

When examining the relationship between the bacterial taxa associated with *M. smithii* or *Ca.* M. intestini in different age groups, we observed that in CENT, these species had more complex networks with other bacterial taxa compared to YAs and OAs, which was more akin to those seen in individuals with a high methanogen phenotype, who showed a dynamic archaea-bacteria network. Upon closer examination of these networks, we found that *M. smithii* or *Ca.* M. intestini consistently co-occurred regardless of the age group, which was in contrast to previous findings based on Sanger sequencing [75]. Additionally, the family *Christensenellaceae* was consistently associated with these archaeal species across all age groups. The co-occurrence of *Christensenella* with *M. smithii* or *Ca.* M. intestini was consistent with previous research that demonstrated a mutually beneficial relationship between *Christensenella* and *Methanobrevibacter* through interspecies hydrogen transfer [76]. *Methanobrevibacter* spp. play a crucial role in efficiently digesting complex polysaccharides by optimizing hydrogen levels for bacterial polysaccharide digestion and consuming the end products of bacterial fermentation. In our analysis of bacteria-archaea networks, we identified *Oscillospiraceae* known for butyrate production [77, 78] and subsequent anti-inflammatory properties to co-occur with both *M. smithii* and *Ca.* M. intestini. This suggests a mutualistic or syntrophic relationship between these gut bacteria and archaea. Conversely, we observed a significant negative association between these archaeal species and members of the *Lachnospiraceae* family, which are also known butyrate producers in the gut [79]. The mutual exclusion between *Lachnospiraceae* and methanogens is not surprising, given that *Lachnospiraceae* functions as acetogens, utilizing hydrogen and carbon dioxide in the gut to produce acetate. In contrast, although some methanogens, such as *Methanosarcina*, can use acetate as the sole energy source, the predominant gut methanogens employ hydrogen and carbon dioxide for methanogenesis. Consequently, these microorganisms engage in a competitive relationship for substrates [80, 81].

Interestingly, the cumulative presence of *Lachnospiraceae*, recognized as butyrate-producing bacteria, decreases with age [13]. Our findings reveal that individuals with a high methanogen phenotype in the OAs and CENT age group exhibit elevated levels of genes (metagenome) associated with the butyrate production pathway, particularly the butyrate kinase pathway. Our correlation analysis highlights a positive association between the gene responsible for butyrate kinase, a pivotal enzyme in the butyrate production pathway, and members of *Oscillospiraceae*. This underscores the significance of these microbial taxa in butyrate production, a known health-promoting factor, among individuals with a high methanogen phenotype. Hence, it can be inferred that these individuals may compensate for the decline in *Lachnospiraceae* not only through the co-occurrence of *M. smithii* and Ca. *M. intestini* with *Oscillospiraceae* but also through an increased abundance of the latter in their microbiota. Consequently, it is plausible to suggest that, as individuals age, the reduction in *Lachnospiraceae* (potentially due to dietary factors) could be more manageable for those with high methanogen phenotype, as indicated by comparable butyrate levels to the microbiome of subjects lacking this phenotype. Therefore, having high methanogen phenotype could be potentially associated with the maintenance of optimal butyrate levels in the gut.

Another interesting observation was the consistent negative co-occurrence of *M. smithii* or *Ca.* M. intestini with *Streptoccocus*, especially in OAs. It is noteworthy to mention that increased levels of metabolic makers of dysregulation has been associated with increased abundance of *Streptococcus* and therefore it is mostly linked with unhealthy aging [82], suggesting that the presence of these methanogens might be associated with healthy aging rather than the progression of disease. However, more longitudinal studies are required to confirm this hypothesis.

Conclusion

This study again supports the relevance of the archaeal microbiome component on human physiology and aging. Our research highlights the dynamic age-related associations in methanogen composition, and particularly the higher prevalence of the high methanogen phenotype in centenarians. Our study emphasizes the significance of *Ca.* M. intestini, evident in its surge in older adults, its co-occurrence with *M. smithii*, and its substantial role in subjects with high methanogen phenotype. This is the first insight into the critical role of this new archaeal representative for the human host. Moreover, our findings underscore the importance of methanogens partnering with specific butyrate-producing bacteria using the butyrate kinase pathway, enhancing the health status of individuals with high methanogen phenotype.

Abbreviations

M. smithii	*Methanobrevibacter smithii*
Ca. M. intestini	*Candidatus* Methanobrevibacter instestini
YAs	Young adults
OAs	Older adults
CENT	Centenarians

Supplementary Information

The online version contains supplementary material available at https://doi.org/10.1186/s12866-025-03921-9.

Supplementary Material 1

Supplementary Material 2: Fig. 1. Conceptual outline of study cohorts. Three different study populations were used. For Cohort A, stool samples collected for a study by Kumpitsch et al. [17] were used. Cohorts A and B were collected from the same location but at different time points and from different subjects. Samples from Cohorts A and B were processed the same way and a similar method for library preparation was employed. Subjects within Cohort C were enrolled in a study with a close location to cohorts A and B by Rampelli et al. [19], and the deposited sequences were used for further evaluations. In order to mitigate the study effect and remove the bias based on the methods employed in sequencing, ConQuR was used for correcting the read counts. Fig. 2. Principal Coordinate Analysis (PCoA) plots were generated to visualize the clustering of study cohorts based on Bray-Curtis and Aitchison dissimilarity computed using raw count data. Each data point on the plot corresponds to a sample, while each ellipse represents a batch (study cohorts A, B, or C), with the centroid denoting the mean. The size of the ellipse reflects the dispersion of data points within each batch, and the angle of the ellipse indicates higher-order characteristics specific to the batch. Furthermore, the ellipse connects the 95th percentile of data points, providing a visual representation of the batch's overall distribution. Fig. 3. Alpha and beta diversity indices of overall microbiome in different age groups (A) Evenness and richness indices tended to decrease with aging. T-test was used for statistical analysis of the richness index due to the normal distribution of the values while evenness values were not normally distributed. (B) NMDS analysis shows a shift of the clusters based on aging. Statistical significance is indicated by $^{**}p < 0.001$ $^{**}p < 0.01$ and $^{*}p < 0.05$. C). Fig. 4. Age-dependent prevalence of high methanogen phenotype. (A) The prevalence of high methanogen phenotype increases with age. (B) Association plot visualizing that high frequency of high methanogen phenotype is associated with the CENT age group rather than other age groups. Area of the box is proportional to the difference in observed and expected frequencies of the presence of high methanogen phenotype. The baseline (dotted line) indicates independence of high methanogen phenotype to aging. The boxes rising above the baseline indicate that the observed frequency of a cell is greater than the expected one (if the data were random), and vice versa. Cells representing negative residuals are drawn below the baseline and vice versa. The width of each of the bar elements in the mosaic reflects the relative magnitude of its value. Fig. 5. An examination of the richness index revealed significant differences based on the presence of high methanogen phenotype irrespective of the age classification, with those with high methanogen phenotype showing significantly higher richness. However, the evenness index was only significantly higher in the presence of high methanogen phenotype in YAs. $^{***}p < 0.001$, $^{**}p < 0.01$. Fig. 6. Box plot of CLR-transformed abundances of the top bacterial taxa per age group based on the presence of high methanogen phenotype. (A) Top bacterial taxa at family level per age group. (B) Top bacterial taxa at genus level. Significance levels are indicated as ***q < 0.001, **q < 0.01, *q< 0.05, for differentially abundance testing by ALDEx. Fig. 7. SparCC co-occurrence networks of ***M. smithii*** and ***Ca.*** M. intestini in samples with high methanogen phenotype in different age groups of YAs, OAs, and CENT (2 A). Positive and negative SparCC co-occurrences are indicated in green and black, respectively. The details of these co-occurrences are shown in more detail in (2B). Fig. 8. Correlation of butyrate kinase pathway genes in young adults with bacterial taxa. ***q < 0.001, **q < 0.01, *q < 0.05.

Acknowledgements

We express our gratitude for the computational resources provided by the MedBioNode at the Medical University of Graz, funded through the Austrian Federal Ministry of Education, Science, and Research, specifically under the Hochschulraum-Strukturmittel 2016 grant as part of BioTechMed Graz. Additionally, we appreciate the support extended by the ZMF team at the Core Facility Computational Bioanalytics, located at the Medical University of Graz. RM was supported by the local PhD program MolMed.

Author contributions

RM did the DNA extraction and data analysis, produced most of the figures and wrote the manuscript. AM supported data analysis and study outline. TS supported data analysis. VW contributed to figure preparations. CK and HS performed sampling. CME designed the study, supervised all activities, and wrote the manuscript. AM, TS, CK, and VW contributed to the writing of the manuscript.

Funding

This research was funded in whole or in part by the Austrian Science Fund (FWF) [grants P 32697, P 30796, COE 7, given to CME]. For open access purposes, the author has applied a CC BY public copyright license to any author-accepted manuscript version arising from this submission.

Data availability

Raw nucleotide data generated and used in the study (Cohorts A and B) can be found in the Sequence Read Archive under the project accession PRJEB72212. All scripts, bracken output, and all the relevant metadata for the cohorts are provided in (https://github.com/Roxy-mzh/Archaea_And_Aging).

Declarations

Ethics approval and consent to participate

The study was evaluated and approved according to the Declaration of Helsinki by the local ethics committee of the Medical University of Graz with

the approval number of 26–573 ex 13/14. Before participation, all participants signed informed consent.

Consent for publication
Not applicable.

Competing interests
The authors declare no competing interests.

Received: 6 May 2024 / Accepted: 20 March 2025
Published online: 04 April 2025

References

1. Baechle JJ, Chen N, Makhijani P, Winer S, Furman D, Winer DA. Chronic inflammation and the hallmarks of aging. Mol Metab. 2023;74:101755.
2. Nagpal R, Mainali R, Ahmadi S, Wang S, Singh R, Kavanagh K, et al. Gut microbiome and aging: physiological and mechanistic insights. Nutr Healthy Aging. 2018;4(4):267–85.
3. Ghosh TS, Shanahan F, O'Toole PW. The gut microbiome as a modulator of healthy ageing. Nat Rev Gastroenterol Hepatol. 2022;19(9):565–84.
4. Cătoi AF, Corina A, Katsiki N, Vodnar DC, Andreicuț AD, Stoian AP, et al. Gut microbiota and aging-a focus on centenarians. Biochimica et biophysica acta (BBA) -. Mol Basis Disease. 2020;1866(7):165765.
5. Santoro A, Ostan R, Candela M, Biagi E, Brigidi P, Capri M, et al. Gut microbiota changes in the extreme decades of human life: a focus on centenarians. Cell Mol Life Sci. 2018;75(1):129–48.
6. Li C, Luan Z, Zhao Y, Chen J, Yang Y, Wang C, et al. Deep insights into the gut microbial community of extreme longevity in South Chinese centenarians by ultra-deep metagenomics and large-scale culturomics. Npj Biofilms Microbiomes. 2022;8(1):28.
7. Bárcena C, Valdés-Mas R, Mayoral P, Garabaya C, Durand S, Rodríguez F, et al. Healthspan and lifespan extension by fecal microbiota transplantation into progeroid mice. Nat Med. 2019;25(8):1234–42.
8. Fransen F, van Beek AA, Borghuis T, Aidy SE, Hugenholtz F, van der Gaast-de Jongh C, et al. Aged gut microbiota contributes to systemical inflammaging after transfer to Germ-Free mice. Front Immunol. 2017;8:1385.
9. Santacroce L, Man A, Charitos IA, Haxhirexha K, Topi S. Current knowledge about the connection between health status and gut microbiota from birth to elderly. A narrative review. Front Biosci (Landmark Ed). 2021;26(6):135–48.
10. Bosco N, Noti M. The aging gut microbiome and its impact on host immunity. Genes Immun. 2021;22(5–6):289–303.
11. Cong J, Zhou P, Zhang R. Intestinal microbiota-derived short chain fatty acids in host health and disease. Nutrients. 2022;14(9).
12. Biagi E, Nylund L, Candela M, Ostan R, Bucci L, Pini E, et al. Through ageing, and beyond: gut microbiota and inflammatory status in seniors and centenarians. PLoS ONE. 2010;5(5):e10667.
13. Biagi E, Franceschi C, Rampelli S, Severgnini M, Ostan R, Turroni S, et al. Gut microbiota and extreme longevity. Curr Biol. 2016;26(11):1480–5.
14. Mohammadzadeh R, Mahnert A, Duller S, Moissl-Eichinger C. Archaeal key-residents within the human microbiome: characteristics, interactions and involvement in health and disease. Curr Opin Microbiol. 2022;67:102146.
15. Mihajlovski A, Dore J, Levenez F, Alric M, Brugere JF. Molecular evaluation of the human gut methanogenic archaeal microbiota reveals an age-associated increase of the diversity. Environ Microbiol Rep. 2010;2(2):272–80.
16. Dridi B, Henry M, Richet H, Raoult D, Drancourt M. Age-related prevalence of *Methanomassiliicoccus luminyensis* in the human gut Microbiome. Apmis. 2012;120(10):773–7.
17. Kumpitsch C, Fischmeister FPS, Mahnert A, Lackner S, Wilding M, Sturm C, et al. Reduced B12 uptake and increased gastrointestinal formate are associated with archaeome-mediated breath methane emission in humans. Microbiome. 2021;9(1):193.
18. Chibani CM, Mahnert A, Borrel G, Almeida A, Werner A, Brugere JF, et al. A catalogue of 1,167 genomes from the human gut archaeome. Nat Microbiol. 2022;7(1):48–61.
19. Rampelli S, Soverini M, D'Amico F, Barone M, Tavella T, Monti D et al. Shotgun metagenomics of gut microbiota in humans with up to extreme longevity and the increasing role of xenobiotic degradation. mSystems. 2020;5(2).
20. Price MN, Dehal PS, Arkin AP. FastTree 2–approximately maximum-likelihood trees for large alignments. PLoS ONE. 2010;5(3):e9490.
21. Bolger AM, Lohse M, Usadel B. Trimmomatic: a flexible trimmer for illumina sequence data. Bioinformatics. 2014;30(15):2114–20.
22. Langmead B, Salzberg SL. Fast gapped-read alignment with bowtie 2. Nat Methods. 2012;9(4):357–9.
23. Quinlan AR, Hall IM. BEDTools: a flexible suite of utilities for comparing genomic features. Bioinformatics. 2010;26(6):841–2.
24. Wood DE, Salzberg SL. Kraken: ultrafast metagenomic sequence classification using exact alignments. Genome Biol. 2014;15(3):R46.
25. Lu J, Breitwieser FP, Thielen P, Salzberg SL. Bracken: estimating species abundance in metagenomics data. PeerJ Comput Sci. 2017;3:e104.
26. Kim D, Hofstaedter CE, Zhao C, Mattei L, Tanes C, Clarke E, et al. Optimizing methods and dodging pitfalls in Microbiome research. Microbiome. 2017;5(1):52.
27. Ling W, Lu J, Zhao N, Lulla A, Plantinga AM, Fu W, et al. Batch effects removal for Microbiome data via conditional quantile regression. Nat Commun. 2022;13(1):5418.
28. Fernandes AD, Macklaim JM, Linn TG, Reid G, Gloor GB. ANOVA-like differential expression (ALDEx) analysis for mixed population RNA-Seq. PLoS ONE. 2013;8(7):e67019.
29. Fernandes AD, Reid JNS, Macklaim JM, McMurrough TA, Edgell DR, Gloor GB. Unifying the analysis of high-throughput sequencing datasets: characterizing RNA-seq, 16S rRNA gene sequencing and selective growth experiments by compositional data analysis. Microbiome. 2014;2(1):15.
30. Bolyen E, Rideout JR, Dillon MR, Bokulich NA, Abnet CC, Al-Ghalith GA, et al. Reproducible, interactive, scalable and extensible microbiome data science using QIIME 2. Nat Biotechnol. 2019;37(8):852–7.
31. Wickham H, Sievert C. SpringerLink. ggplot2: elegant graphics for data analysis. Use R! 2nd 2016. ed. Cham: Springer Springer International Publishing: Imprint: Springer; 2016.
32. Wickham H, François R, Henry L, Müller K, Vaughan D. dplyr: A Grammar of Data Manipulation. R package version 1.1.4. 2023. https://github.com/tidyverse/dplyr.
33. Wickham H. Reshaping data with the reshape package. J Stat Softw. 2007;21(12):1–20.
34. R Core Team. R: A Language and Environment for Statistical Computing. R Foundation for Statistical Computing, Vienna, Austria. 2021. https://www.R-project.org/
35. Friedman J, Alm EJ. Inferring correlation networks from genomic survey data. PLoS Comput Biol. 2012;8(9):e1002687.
36. Shaffer M, Thurimella K, Sterrett JD, Lozupone CA. SCNIC: sparse correlation network investigation for compositional data. Mol Ecol Resour. 2023;23(1):312–25.
37. Kieser S, Brown J, Zdobnov EM, Trajkovski M, McCue LA. ATLAS: a snakemake workflow for assembly, annotation, and genomic Binning of metagenome sequence data. BMC Bioinformatics. 2020;21(1):257.
38. Steinegger M, Soding J. Clustering huge protein sequence sets in linear time. Nat Commun. 2018;9(1):2542.
39. Bushnell B. BBMap. 2015. https://sourceforge.net/projects/bbmap/.
40. Cantalapiedra CP, Hernandez-Plaza A, Letunic I, Bork P, Huerta-Cepas J. eggNOG-mapper v2: functional annotation, orthology assignments, and domain prediction at the metagenomic scale. Mol Biol Evol. 2021;38(12):5825–9.
41. Kanehisa M, Goto S. KEGG: Kyoto encyclopedia of genes and genomes. Nucleic Acids Res. 2000;28(1):27–30.
42. Kanehisa M, Furumichi M, Sato Y, Kawashima M, Ishiguro-Watanabe M. KEGG for taxonomy-based analysis of pathways and genomes. Nucleic Acids Res. 2023;51(D1):D587–92.
43. Kanehisa M. Toward Understanding the origin and evolution of cellular organisms. Protein Sci. 2019;28(11):1947–51.
44. Love MI, Huber W, Anders S. Moderated Estimation of fold change and dispersion for RNA-seq data with DESeq2. Genome Biol. 2014;15(12):550.
45. JH Z. Spearman rank correlation. Encyclopedia Biostatistics. 2005;7.
46. Greenhalgh K, Meyer KM, Aagaard KM, Wilmes P. The human gut microbiome in health: establishment and resilience of microbiota over a lifetime. Environ Microbiol. 2016;18(7):2103–16.
47. Wu L, Zeng T, Zinellu A, Rubino S, Kelvin DJ, Carru C. A Cross-Sectional study of compositional and functional profiles of gut microbiota in Sardinian centenarians. mSystems. 2019;4(4).
48. Borrel G, McCann A, Deane J, Neto MC, Lynch DB, Brugere JF, et al. Genomics and metagenomics of trimethylamine-utilizing archaea in the human gut Microbiome. ISME J. 2017;11(9):2059–74.
49. Carr A, Diener C, Baliga NS, Gibbons SM. Use and abuse of correlation analyses in microbial ecology. ISME J. 2019;13(11):2647–55.

50. Hansen EE, Lozupone CA, Rey FE, Wu M, Guruge JL, Narra A, et al. Pan-genome of the dominant human gut-associated archaeon, *Methanobrevibactersmithii*, studied in twins. Proc Natl Acad Sci U S A. 2011;108(Suppl 1):4599–606.
51. Naito Y, Kashiwagi K, Takagi T, Andoh A, Inoue R. Intestinal dysbiosis secondary to proton- pump inhibitor use. Digestion. 2018;97(2):195–204.
52. Lahti L, Salojarvi J, Salonen A, Scheffer M, de Vos WM. Tipping elements in the human intestinal ecosystem. Nat Commun. 2014;5:4344.
53. Yang C, Deng Q, Xu J, Wang X, Hu C, Tang H, et al. Sinapic acid and resveratrol alleviate oxidative stress with modulation of gut microbiota in high-fat diet-fed rats. Food Res Int. 2019;116:1202–11.
54. Zheng S, Piao C, Liu Y, Liu X, Liu T, Zhang X, et al. Glycan biosynthesis ability of gut microbiota increased in primary hypertension patients taking antihypertension medications and potentially promoted by macrophage-adenosine monophosphate-activated protein kinase. Front Microbiol. 2021;12:719599.
55. Siptroth J, Moskalenko O, Krumbiegel C, Ackermann J, Koch I, Pospisil H. Variation of butyrate production in the gut microbiome in type 2 diabetes patients. Int Microbiol. 2023;26(3):601–10.
56. Chassard C, Delmas E, Robert C, Bernalier-Donadille A. The cellulose-degrading microbial community of the human gut varies according to the presence or absence of methanogens. FEMS Microbiol Ecol. 2010;74(1):205–13.
57. Franceschi C, Garagnani P, Parini P, Giuliani C, Santoro A. Inflammaging: a new immune-metabolic viewpoint for age-related diseases. Nat Rev Endocrinol. 2018;14(10):576–90.
58. Ren M, Li H, Fu Z, Li Q. Succession analysis of gut microbiota structure of participants from long-lived families in Hechi, Guangxi, China. Microorganisms. 2021;9(12).
59. Wei ZY, Rao JH, Tang MT, Zhao GA, Li QC, Wu LM, et al. Characterization of changes and driver microbes in gut microbiota during healthy aging using A captive monkey model. Genomics Proteom Bioinf. 2022;20(2):350–65.
60. Kim M, Benayoun BA. The microbiome: an emerging key player in aging and longevity. Translational Med Aging. 2020;4:103–16.
61. Nokin MJ, Durieux F, Bellier J, Peulen O, Uchida K, Spiegel DA, et al. Hormetic potential of methylglyoxal, a side-product of glycolysis, in switching tumours from growth to death. Sci Rep. 2017;7(1):11722.
62. Louis P, Hold GL, Flint HJ. The gut microbiota, bacterial metabolites and colorectal cancer. Nat Rev Microbiol. 2014;12(10):661–72.
63. Levitt MD, Furne JK, Kuskowski M, Ruddy J. Stability of human methanogenic flora over 35 years and a review of insights obtained from breath methane measurements. Clin Gastroenterol Hepatol. 2006;4(2):123–9.
64. Remond D, Shahar DR, Gille D, Pinto P, Kachal J, Peyron MA, et al. Understanding the gastrointestinal tract of the elderly to develop dietary solutions that prevent malnutrition. Oncotarget. 2015;6(16):13858–98.
65. Franceschi C, Ostan R, Santoro A. Nutrition and inflammation: are centenarians similar to individuals on calorie-restricted diets? Annu Rev Nutr. 2018;38:329–56.
66. Goodrich JK, Waters JL, Poole AC, Sutter JL, Koren O, Blekhman R, et al. Human genetics shape the gut Microbiome. Cell. 2014;159(4):789–99.
67. Le Chatelier E, Nielsen T, Qin J, Prifti E, Hildebrand F, Falony G, et al. Richness of human gut microbiome correlates with metabolic markers. Nature. 2013;500(7464):541–6.
68. Lloyd-Price J, Abu-Ali G, Huttenhower C. The healthy human microbiome. Genome Med. 2016;8(1):51.
69. Villanueva-Millan MJ, Leite G, Wang J, Morales W, Parodi G, Pimentel ML, et al. Methanogens and hydrogen sulfide producing bacteria guide distinct gut microbe profiles and irritable bowel syndrome subtypes. Am J Gastroenterol. 2022;117(12):2055–66.
70. Kong F, Hua Y, Zeng B, Ning R, Li Y, Zhao J. Gut microbiota signatures of longevity. Curr Biol. 2016;26(18):R832–3.
71. Odamaki T, Kato K, Sugahara H, Hashikura N, Takahashi S, Xiao JZ, et al. Age-related changes in gut microbiota composition from newborn to centenarian: a cross-sectional study. BMC Microbiol. 2016;16:90.
72. Badal VD, Vaccariello ED, Murray ER, Yu KE, Knight R, Jeste DV et al. The gut microbiome, aging, and longevity: A systematic review. Nutrients. 2020;12(12).
73. Clemente JC, Manasson J, Scher JU. The role of the gut microbiome in systemic inflammatory disease. BMJ. 2018;360:j5145.
74. Palmas V, Pisanu S, Madau V, Casula E, Deledda A, Cusano R et al. Gut microbiota markers and dietary habits associated with extreme longevity in healthy Sardinian centenarians. Nutrients. 2022;14(12).
75. Low A, Lee JKY, Gounot JS, Ravikrishnan A, Ding Y, Saw WY, et al. Mutual exclusion of methanobrevibacter species in the human gut microbiota facilitates directed cultivation of a *Candidatus* Methanobrevibacter intestini representative. Microbiol Spectr. 2022;10(4):e0084922.
76. Ruaud A, Esquivel-Elizondo S, de la Cuesta-Zuluaga J, Waters JL, Angenent LT, Youngblut ND et al. Syntrophy via interspecies H(2) transfer between *Christensenella* and *Methanobrevibacter* underlies their global cooccurrence in the human gut. mBio. 2020;11(1).
77. Gophna U, Konikoff T, Nielsen HB. Oscillospira and related bacteria - From metagenomic species to metabolic features. Environ Microbiol. 2017;19(3):835–41.
78. Dai Z, Wang X, Liu Y, Liu J, Xiao S, Yang C et al. Effects of dietary microcapsule sustained-release sodium butyrate on the growth performance, immunity, and gut microbiota of yellow broilers. Anim (Basel). 2023;13(23).
79. Vacca M, Celano G, Calabrese FM, Portincasa P, Gobbetti M, De Angelis M. The controversial role of human gut lachnospiraceae. Microorganisms. 2020;8(4).
80. Li Z, Wang X, Alberdi A, Deng J, Zhong Z, Si H, et al. Comparative microbiome analysis reveals the ecological relationships between rumen methanogens, acetogens, and their hosts. Front Microbiol. 2020;11:1311.
81. Karekar S, Stefanini R, Ahring B. Homo-acetogens: their metabolism and competitive relationship with hydrogenotrophic methanogens. Microorganisms. 2022;10(2).
82. DeJong EN, Surette MG, Bowdish DME. The gut microbiota and unhealthy aging: disentangling cause from consequence. Cell Host Microbe. 2020;28(2):180–9.

Publisher's note

Springer Nature remains neutral with regard to jurisdictional claims in published maps and institutional affiliations.

nature communications

Article

https://doi.org/10.1038/s41467-026-69711-7

Cross-domain metabolic interactions link *Methanobrevibacter smithii* to colorectal cancer microbial ecosystems

Received: 9 July 2025

Accepted: 4 February 2026

Published online: 20 February 2026

Check for updates

Rokhsareh Mohammadzadeh[1], Alexander Mahnert[1], Tamara Zurabishvili[1], Lisa Wink[1], Christina Kumpitsch[1], Hansjoerg Habisch[2], Jannik Sprengel[3,4], Klara Filek[1], Polona Mertelj[1], Dominique Pernitsch[5], Kerstin Hingerl[5], Marija Durdevic[6,7], Gregor Gorkiewicz[6,8], Christian Diener[1], Alexander Loy[9], Dagmar Kolb[5], Christoph Trautwein[3,4,10,11,12], Tobias Madl[2,8] & Christine Moissl-Eichinger[1,8]

The human gut is colonized by trillions of microbes that influence the health of their human host. Whereas many bacterial species have now been linked to a variety of different diseases, the involvement of Archaea, an evolutionarily distinct group of microbes, in human disease remains elusive. By analyzing 19 independent clinical studies, we demonstrate that associations between Archaea and human diseases are widespread yet highly heterogeneous, with a pronounced and consistent enrichment of *Methanobrevibacter smithii* in colorectal cancer (CRC) patients. Metabolic modelling and in vitro co-culture identified distinct mutualistic interactions of *M. smithii* with CRC-causing bacteria such as *Fusobacterium nucleatum*, including metabolic enhancement. Metabolomics further reveal archaeal-derived compounds with tumor-modulating properties. Together, our results provide mechanistic insights into how the human gut archaeome may participate in CRC-associated microbial networks through metabolic cooperation with bacteria.

Alterations in the gastrointestinal microbiome have been implicated in a wide range of diseases, including inflammatory bowel diseases (IBD), metabolic disorders like obesity and type 2 diabetes (T2D), cardiovascular conditions, and neurodegenerative or neuropsychiatric diseases, including Parkinson's disease (PD), Alzheimer's disease (AD), schizophrenia (SCZ), and multiple sclerosis (MS)[1–8]. Establishing mechanistic links between specific microbes and disease phenotypes remains a major challenge due to the inherent complexity and interdependence of microbial ecosystems. Microbiomes are shaped by intricate networks of cross-feeding, competition and host interactions across domains of life, including a complex interplay of bacteria, fungi, viruses, and archaea.

Archaea, in particular methane-forming representatives, can constitute up to 4% of the gut microbiome[9], but remain severely under-

[1]Diagnostic and Research Institute of Hygiene, Microbiology and Environmental Medicine, Medical University of Graz, Graz, Austria. [2]Medicinal Chemistry, Otto Loewi Research Center, Medical University of Graz, Graz, Austria. [3]Core Facility Metabolomics, Medical Faculty University of Tübingen, Tübingen, Germany. [4]M3 Research Center for Malignome, Metabolome & Microbiome, Medical Faculty University of Tübingen, Tübingen, Germany. [5]Core Facility Ultrastructure Analysis, Medical University of Graz, Graz, Austria. [6]Institute of Pathology, Medical University of Graz, Graz, Austria. [7]Core Facility Computational Bioanalytics, Center for Medical Research, Medical University of Graz, Graz, Austria. [8]BioTechMed, Graz, Austria. [9]Division of Microbial Ecology, Centre for Microbiology and Environmental Systems Science, University of Vienna, Vienna, Austria. [10]Department of Preclinical Imaging and Radiopharmacy, Werner Siemens Imaging Center, University Hospital Tübingen, Tübingen, Germany. [11]Cluster of Excellence CMFI (EXC 2124) "Controlling Microbes to Fight Infections", Eberhard Karls University of Tübingen, Tübingen, Germany. [12]Cluster of Excellence iFIT (EXC 2180) "Image Guided and Functionally Instructed Tumor Therapies", University of Tübingen, Tübingen, Germany. e-mail: christine.moissl-eichinger@medunigraz.at

researched. The most abundant genus is *Methanobrevibacter*, whose representatives are generally considered commensal and have not been linked to pathogenicity in humans or other hosts[10]. Yet, their metabolic activity, primarily the consumption of bacterial fermentation products (H_2, CO_2) to produce methane, positions them as key microbial interactors[11]. *Methanobrevibacter* abundance has been associated with beneficial outcomes, including higher short-chain fatty acid levels, reduced body mass index (BMI), and increased longevity[9,12–14]. Archaeal depletion has been observed in several disorders, such as IBD[15], obesity[16], and irritable bowel syndrome with diarrhea (IBS-D)[17,18]. Conversely, elevated *Methanobrevibacter* levels have also been linked to constipation-dominant IBS (IBS-C)[19], intestinal methanogen overgrowth (a small intestinal bacterial overgrowth subtype)[20,21], and in some reports, colorectal cancer (CRC)[22]. These associations suggest that methanogens may modulate host physiology both directly, through metabolite production, and indirectly, by shaping bacterial activity through otherwise inhibiting H_2 removal.

Despite their potential significance, archaea are largely neglected in most microbiome studies due to methodological limitations. Standard 16S rRNA gene-targeted primers lack archaeal coverage, reference genome databases remain incomplete, cultivation is tricky, and many computational pipelines are not optimized to detect archaeal signatures[23,24]. Most existing data on archaea come from using low-resolution methods, such as breath methane testing or 16S rRNA gene profiling, which cannot resolve species-level taxa or infer metabolic functions. As a result, key hypotheses remain untested: that distinct diseases may induce characteristic shifts in gut archaeome (the archaeal community residing in the human gut); that methanogens may be selectively enriched or depleted depending on the disease context; that certain archaeal taxa could serve as reliable, disease-specific biomarkers across diverse cohorts; and that archaeal metabolites, whether unique to this domain or produced via syntrophic interactions, may exert biologically relevant effects on host physiology and disease processes.

To address these knowledge gaps, we performed a multi-level study, starting with the first comprehensive meta-analysis of the human gut archaeome across multiple diseases, leveraging high-quality shotgun metagenomes from around 3000 fecal samples derived from 19 studies spanning 12 countries. This dataset covered a spectrum of conditions: CRC, T2D, CD, UC, MS, AD, SCZ, and PD. Using a unified analytical framework, we systematically quantified archaeal prevalence, identified disease-specific patterns, and assessed the significance of these associations across cohorts while adjusting for major confounders, including age, sex, and BMI, when possible. Observed correlations with CRC were further addressed by genome-scale metabolic modeling and archaeal-bacterial co-culture experiments, involving CRC-associated pathogens, such as *Fusobacterium nucleatum*. Functional interactions were resolved by metabolomics, revealing that *M. smithii* engages in complex exchanges that have the potential to shape the tumor microenvironment.

Our findings position *M. smithii* as a potentially active metabolic and ecological contributor within CRC-associated microbial networks. By redefining its role from a passive H_2 scavenger to a dynamic modulator of microbial interactions and host-relevant metabolites, this study highlights the importance of integrating archaeal functions into microbiome-disease frameworks.

Results

Systematic reprocessing of human gut metagenomes enables standardized archaeal profiling across diverse studies

We systematically collected, reprocessed, and reanalyzed raw microbiome datasets, selecting only those studies that provided publicly accessible metagenome sequencing data (in FASTQ or FASTA format) derived from stool samples, accompanied by disease metadata (i.e., case versus control classifications) for at least 20 subjects per category. Out of an initial pool of 627 studies, 573 were excluded after abstract screening, resulting in 54 eligible studies. Subsequent refinements led to the exclusion of an additional 35 studies due to missing metadata, inconsistencies between sample identifiers in metadata and sequencing files, unavailable data or full texts, or the use of 16S rRNA amplicon sequencing instead of metagenomic shotgun sequencing, the latter being essential for our meta-analysis due to its superior species-level resolution for archaea. Ultimately, 19 studies were retained for meta-analysis (Fig. 1a and Supplementary Fig. 1).

The dataset initially comprised one fecal metagenome sample each for 3243 subjects. For the study by Zhou et al.[25], only individuals who had not received any medication for MS treatment were included in the analysis to minimize confounding effects[26]. Additionally, for datasets where antibiotic use was explicitly reported in the metadata (e.g., Franzosa et al. study[27] and Wallen et al. study[28]), we excluded those samples to avoid potential microbiome alterations due to antibiotic exposure. To minimize confounding effects of sex, age, and BMI, factors known to influence both the archaeome and microbiome[28–31], we matched case-control samples separately within each study whenever possible. In the studies conducted by Yu et al. and Jo et al.[32,33], case-control sample matching based on these covariates was not feasible due to incomplete metadata. However, both studies reported no significant differences in sex, age, or BMI between case and control groups. In contrast, case-control samples in datasets from Feng et al., Boktor et al., and Bedarf et al.[34–36] had already been pre-matched for sex, age, and BMI. In Franzosa et al. study[27], case-control matching was performed solely by age, as BMI and sex information were not available. For all remaining 13 studies, we applied case-control matching based on sex, age (±5 years), and BMI (±3 units), resulting in a final dataset of 2214 samples (without combining the datasets) (Supplementary Data 1 and Fig. 1b).

A detailed summary of the included studies, covering study design, geographic origin, sample sizes, processing methods, and sequencing protocols, is provided in Supplementary Data 1. While the studies utilized different DNA extraction kits, sequencing platforms, and sample accession numbers, each study maintained methodological consistency within its own framework. To ensure consistency, metagenomic data from all included studies were uniformly processed following a standardized protocol, and each study underwent independent analysis to avoid the batch effect (Fig. 1c). To gain additional insight into diseases represented by multiple cohorts, datasets were also analyzed in pooled form. Post-correction PERMANOVA (Bray–Curtis dissimilarity) analyses confirmed a substantial reduction in inter-study variance across all disease cohorts after batch correction: from $R^2 = 0.154$ to $R^2 = 0.080$ ($p < 0.001$) for CRC, from $R^2 = 0.055$ to $R^2 = 0.011$ ($p = 0.001$) for pre-AD, and from $R^2 = 0.144$ to $R^2 = 0.087$ ($p = 0.001$) for PD datasets. Due to the lack of consistent covariate information across studies, case-control matching based on the aforementioned metadata was not feasible in the combined dataset.

Alpha and beta diversity of the gut archaeome is cohort- and disease-dependent

To investigate differences in archaeal composition between disease (case) and control groups, we performed a comprehensive re-analysis of multiple independent datasets. This approach enabled the identification of both shared and disease-specific archaeal taxa across different conditions.

To investigate the relationship between gut metagenome archaeal composition and disease, we assessed the beta diversity of the samples using Bray–Curtis distance to quantify microbial community dissimilarities, and principal coordinate analysis (PCoA) was employed to visualize clustering patterns based on species abundances derived from metagenomic shotgun sequencing. Associations between archaeome beta diversity and disease states were identified in CRC and pre-AD. Among CRC studies, 4 out of 9 (conducted by Feng et al.[34]

https://doi.org/10.1038/s41467-026-69711-7

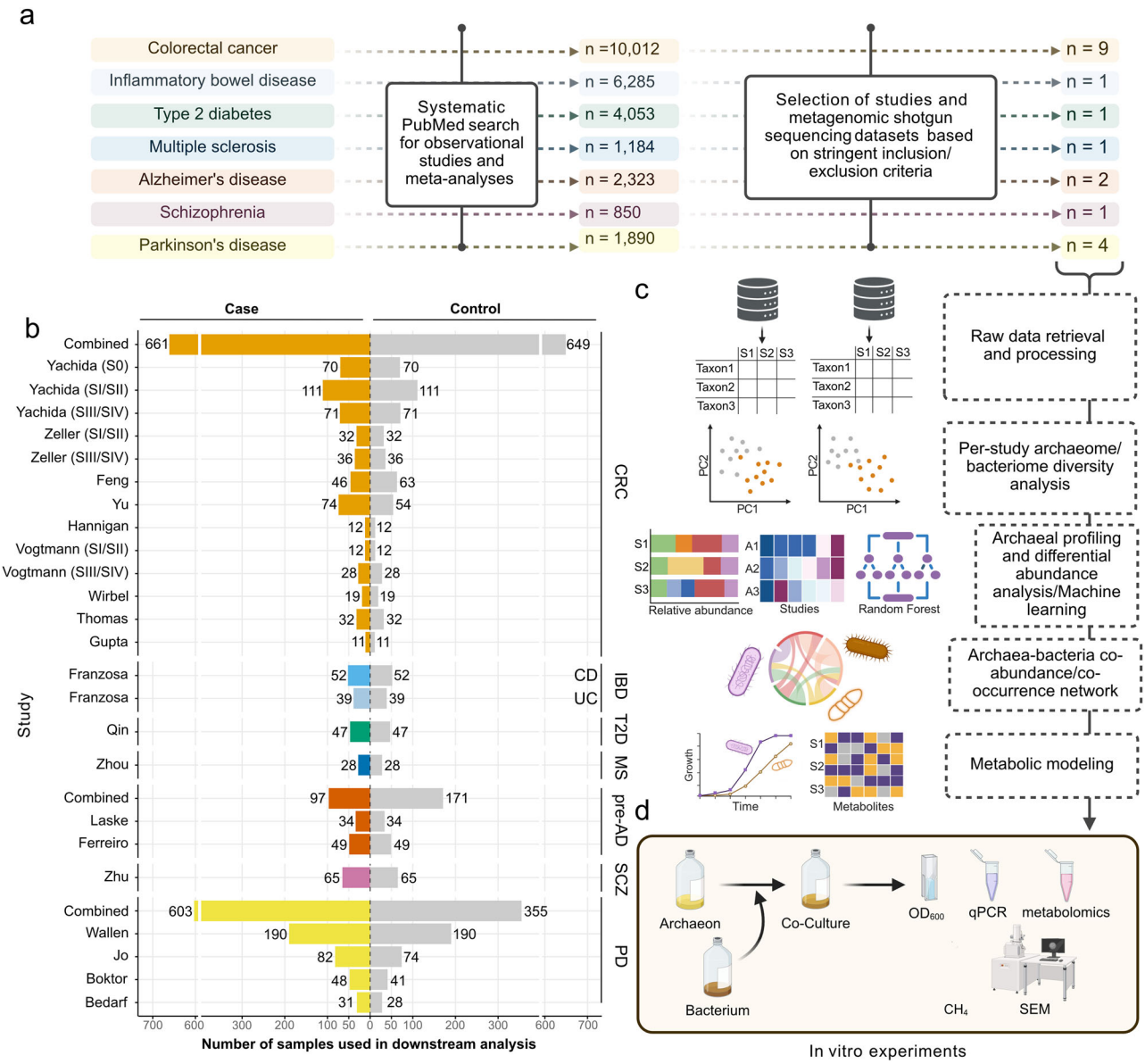

Fig. 1 | Schematic overview of the study. a Metagenomic sequencing datasets were selected using stringent inclusion and exclusion criteria. **b** Nine studies were retained for downstream analysis, and samples were adjusted for confounders, such as sex, age, and BMI, when possible. For diseases represented by more than one dataset (CRC, pre-AD, and PD), each dataset was first analyzed individually, and subsequently, the datasets were combined to enable integrative analyses. **c** Raw reads were retrieved, quality-controlled, and filtered to remove human sequences, followed by taxonomic classification using Kraken2 and Bracken. For pooled datasets, MMUPHin was performed for batch-effect removal. Archaeal profiles were then extracted, and differential abundance testing was performed. Machine learning was additionally performed for the pooled CRC dataset in order to assess the diagnostic potential of archaeal compositional differences in CRC. Co-abundance correlations between *Methanobrevibacter smithii* and CRC-associated bacterial taxa were assessed, and their co-occurrence and presence–absence patterns were further examined to evaluate potential ecological associations. Metabolic modeling was used to explore metabolite exchange between *Methanobrevibacter smithii* and CRC-associated bacteria. **d** In vitro experiments were conducted to understand the dynamics between *M. smithii* and CRC-associated bacteria. CRC colorectal cancer, CD Crohn's disease, UC ulcerative colitis, T2D type 2 diabetes, MS multiple sclerosis, pre-AD pre-Alzheimer's disease, SCZ schizophrenia, PD Parkinson's disease. Figure **a**, **c**, **d** were created in BioRender (Neumann, C. (2026) https://BioRender.com/r338i6l). **b** Visualization was performed using the ggplot2 package, and axis breaks were introduced using ggbreak[113,114].

(R^2 = 0.029, p = 1E-03), Yu et al.[33] (R^2 = 0.036, p = 4E-03), Thomas et al.[37] (R^2 = 0.064, p = 1.4E-02), and Gupta et al.[38] (R^2 = 0.368, p = 9E-03)) showed significant divergence. For pre-AD, both studies analyzed (Laske et al.[39], R^2 = 0.037, p = 4E-02; Ferreiro et al.[40], R^2 = 0.040, p = 1E-02) demonstrated archaeal compositional differences (Supplementary Fig. 2). No detectable archaeal community variations were found when comparing cases to controls for CD, UC, T2D, SCZ, or PD (Supplementary Fig. 2).

Interestingly, in CRC studies where archaeal beta diversity exhibited significant case-control differences, bacterial beta diversity followed a similar trend (Supplementary Figs. 2 and 3), suggesting a potential relationship between archaeal and bacterial communities in CRC within the gut, while this trend was not observed in pre-AD. Moreover, in other datasets, including two CRC studies (Zeller et al.[41]; both stages I/II and III/IV; and Wirbel et al.[42]), IBD (both UC and CD), three PD studies (Wallen et al.[28], Jo et al.[32], and Boktor et al.[35]), and the SCZ study, bacterial beta diversity showed distinct clustering between cases and controls, whereas archaeal beta diversity remained unchanged.

Overall, these findings suggest that archaeal beta diversity differences in disease states are not consistently observed across studies.

This variability may stem from the lower relative abundance of archaea, which limits statistical power, or from the possibility that archaea are less responsive to disease-related microbiome shifts compared to bacteria in these datasets. Furthermore, differences in cohort composition, geographic and environmental factors, patient individuality, dietary habits, different DNA extraction protocols, as well as variances in sequencing methodologies may have contributed to the inconsistencies observed across studies, potentially influencing archaeal beta diversity outcomes[24].

Analysis of alpha diversity using the Shannon index revealed significant reductions in archaeal diversity in only one of the nine CRC studies, namely the Wirbel et al. study[42], where cases had lower diversity compared to controls ($p = 3.1E-2$), while in another study (Gupta et al.[38]), CRC patients showed higher Shannon diversity compared to the control ($p = 3.3E-2$). In contrast, UC cases (Franzosa et al. study[27]) exhibited significantly reduced archaeal diversity compared to controls ($p = 4.5E-2$), suggesting a potential link UC and alterations in the archaeal community (Supplementary Fig. 4).

Notably, in studies where significant archaeal Shannon index reductions were observed, bacterial Shannon index differences followed a parallel trend, with cases showing reduced diversity compared to controls (Supplementary Figs. 4 and 5). However, this consistent relationship was not observed across all studies of the same disease, nor in diseases for which only a single dataset was available. These findings again indicate the study-dependent shifts in archaeal diversity.

Predominant gut-associated archaea show an increasing trend in certain diseases, such as CRC

Next, we investigated if specific archaeal species are more prevalent in disease compared to the control. We first analyzed the combined dataset to identify overall trends, and then examined each study separately (to account for study-specific confounders), to assess the composition of the archaeome, and compared the presence and relative abundance of archaeal species in healthy and diseased individuals.

In total, our analysis identified eight validly described archaeal species, five taxa assigned to provisional species within known genera (e.g., Methanobrevibacter_A_sp900769095), and additional genomes with low taxonomic resolution (here referred to as unclassified), defined by the unified human gastrointestinal genome (UHGG) reference catalog.

The gut archaeome was consistently dominated by various species of the genus *Methanobrevibacter*, particularly Methanobrevibacter_A_smithii (UHGG representative of *M. smithii*), Methanobrevibacter_A_smithii_A (UHGG representative of *M. intestini*), and Methanobrevibacter_A_sp900766745. These species were universally detected across all studies, regardless of the participants' disease status. Additional *Methanobrevibacter* species, including Methanobrevibacter_A_woesei, Methanobrevibacter_A_sp900769095, and Methanobrevibacter_A_oralis, were observed at lower abundances but were consistently detected (Fig. 2a). These observations suggest that members of the genus *Methanobrevibacter* are stable and persistent colonizers of the human gut, irrespective of host disease conditions.

Aside from *Methanobrevibacter*, substantial contributions to the gut archaeome included species from the genus *Methanosphaera*. Methanosphaera_sp900322125 was detected in nearly all studies and patient groups (Fig. 2a).

Further diversity within the gut archaeome was represented by species from the genera *Methanomassiliicoccus*, *Methanomethylophilus*, and *Methanobacterium*. Notably, Methanomassiliicoccus_luminyensis was exclusively identified in PD patients, appearing in three out of four PD-related studies (Wallen et al.[28], Boktor et al.[35], and Bedarf et al.[36] studies) (Fig. 2a).

To explore disease-specific variations, we first evaluated the combined dataset to identify general disease-associated patterns, when possible, and then compared cases and controls within individual studies to account for study-specific effects. Differential abundance analysis (CLR + Wilcoxon, BH-FDR) of archaeal species were conducted in the context of the whole microbiome to account for their compositional relationships with the broader bacterial community. Among the five most prevalent archaeal species, Methanobrevibacter_A_smithii demonstrated significant (CLR + Wilcoxon, p-adjusted <0.05) differences across multiple studies (Supplementary Data 2 and 3).

A potential association of *Methanobrevibacter* was observed for neurological disorders. Methanobrevibacter_A_smithii exhibited significant enrichment in SCZ patients (p-adjusted = 2.10E-02). Indeed, the association of higher abundances of *Methanobrevibacter* with cognitive impairment and SCZ has been reported in patients in one study[43], whereas in healthy individuals, high methanogen phenotypes showed improved cognitive function in another study[3]. This archaeal species showed a markedly higher abundance in the combined PD datasets (p-adjusted = 3.64E-08). However, after subject matching, this association was no longer statistically significant within the individual datasets, although three out of four studies (Wallen et al.[28] Jo et al.[32] and Boktor et al.[35]) still exhibited an increased abundance of this species. Increased transcriptional activity of *M. smithii* has also been previously linked to alterations in microbial metabolism in the gut of PD patients[44]. The other prevalent member of the *Methanobrevibacter* genus, Methanobrevibacter_A_smithii_A (*M. intestini*), similarly displayed significant enrichment in PD patients in the combined analysis (p-adjusted = 9.55E-08). As with the previous species, the significance was lost after matching cases and controls in the individual studies, yet a consistent, though nonsignificant, enrichment trend was observed across all four cohorts. Similar patterns were observed for Methanomassiliicoccus_luminyensis and Methanomassiliicoccus_A intestinalis, which were significantly enriched in PD patients in the pooled dataset (p-adjusted = 4.94E-02 and p-adjusted = 5.69E-04, respectively), but lost statistical significance in the case-control matched, study-specific analyses.

An opposite trend was observed in CD, where several archaeal species were significantly reduced under disease conditions. This depletion included Methanobrevibacter_A_smithii (p-adjusted = 2.90E-03), Methanobrevibacter_A_smithii_A (*M. intestini*) (p-adjusted = 1.10E-03), Methanobrevibacter_A_oralis (p-adjusted = 2.47E-02) and Methanobrevibacter_A_sp900769095 (p-adjusted = 2.47E-02), while Methanobrevibacter_A_sp900766745 (p-adjusted = 1.72E-02) was shown to be higher compared to healthy controls (Fig. 2b and Supplementary Fig. 6).

In the pooled CRC dataset, Methanobrevibacter_A_smithii showed a significant enrichment in CRC patients compared to controls (p-adjusted = 9.78E-05). Consistently, in the individual studies, this trend remained evident (except for Thomas's study[37]), reaching statistical significance in two cohorts (Feng et al.[34], p-adjusted = 1.56E-03; Gupta et al.[38], p-adjusted = 4.85E-03) (Fig. 2b). In the cohorts where CRC staging could be assessed after case-control matching (Yachida et al.[45], Zeller et al.[41], and Vogtmann et al.[46]), we observed a stage-dependent trend in the abundance of Methanobrevibacter_A_smithii. While in the Yachida et al. cohort[45], *M. smithii* was already enriched in stage 0 lesions, this archaeon tended to be depleted in early-stage CRC (stages I–II), but showed enrichment in advanced stages (III–IV). Similar correlations between CRC progression and *Methanobrevibacter* abundance in the gut has also been reported before[47,48].

Methanobrevibacter_A_smithii_A (*M. intestini*) similarly displayed significant enrichment in CRC patient groups in studies by Feng et al.[34] (p-adjusted = 2.61E-03) and Gupta et al.[38] (p-adjusted = 4.93E-03). Methanobrevibacter_A_sp900766745 was also enriched in CRC patients in Feng et al. study[34] (p-adjusted = 3.89E-02) (Fig. 2b).

https://doi.org/10.1038/s41467-026-69711-7

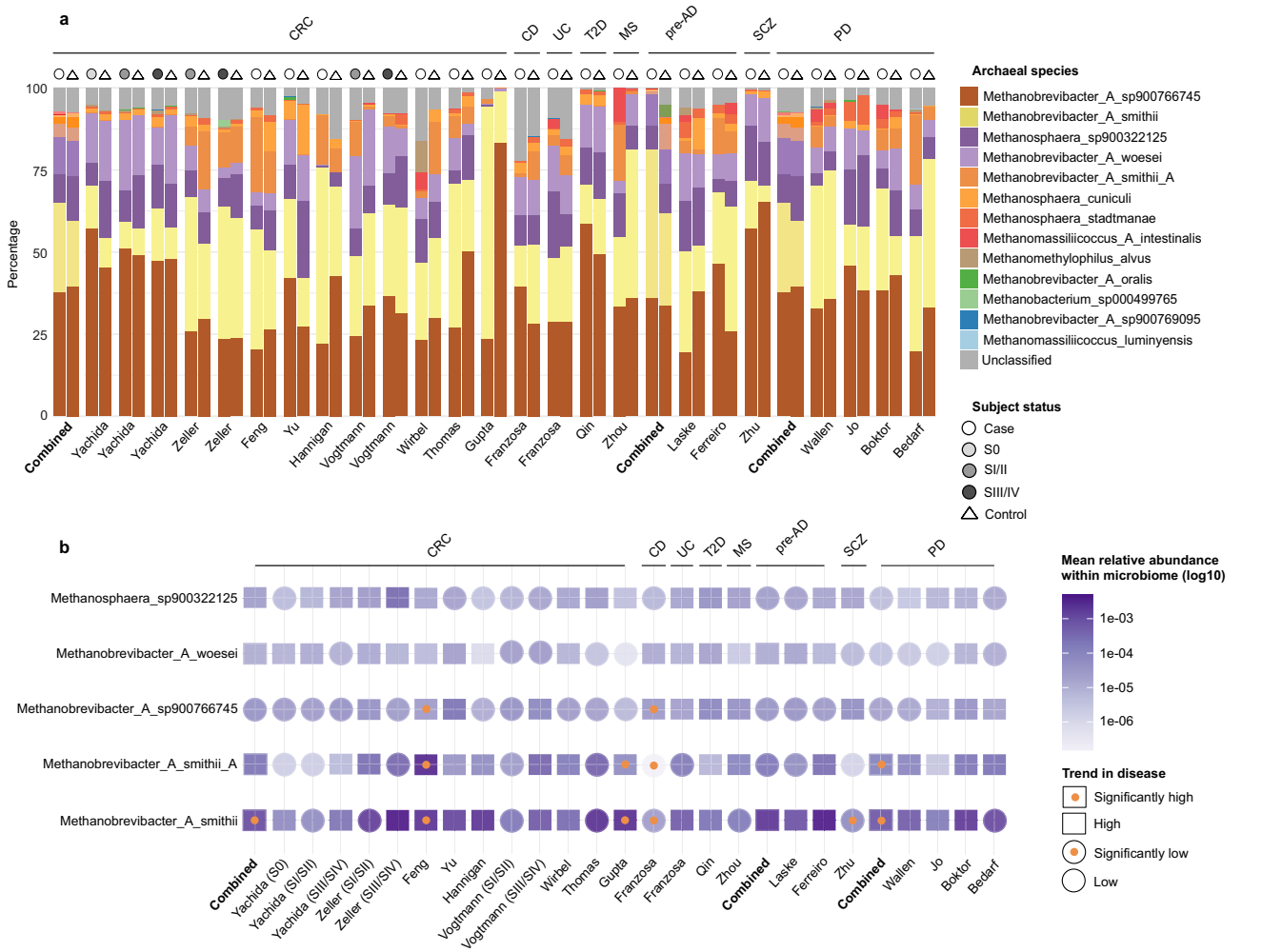

Fig. 2 | Archaeal community profiles and differential abundance analysis across disease cohorts. a Stacked bar plots showing the relative abundances of archaeal species across shotgun metagenomic datasets, stratified by disease and study. Within each study, samples are grouped according to disease status (cases vs. controls). For the Yachida et al.[45], Zeller et al.[41], and Vogtmann et al.[46] cohorts, where sufficient information and sample sizes were available, subjects were further stratified by colorectal cancer (CRC) stage. **b** Five abundant archaeal species are represented, each with a symbol indicating the direction of abundance change between disease and control groups: squares denote higher abundance in disease, and circles denote lower abundance in disease. An orange dot inside the symbol indicates a statistically significant difference (FDR-adjusted <0.05), while empty symbols represent nonsignificant trends. Archaeal species are represented by their corresponding UHGG (unified human gastrointestinal genome) identifiers. Differential abundance was assessed using CLR-transformed (centered log-ratio) data and two-sided Wilcoxon rank-sum test with FDR (false discovery rate) correction. CRC colorectal cancer, S0 stage 0, SI/SII stage I/II, SIII/SIV stage III/IV, CD Crohn's disease, UC ulcerative colitis, T2D type 2 diabetes, MS multiple sclerosis, pre-AD pre-Alzheimer's disease, SCZ schizophrenia, PD Parkinson's disease. Source data are provided as a Source data file.

Considering that not all studies might have used an archaea-suitable methodology[24], these associations are a strong indicator for a potential association of *Methanobrevibacter* species with CRC. Similar positive associations of *Methanobrevibacter* signatures with CRC have been previously reported in 16S rRNA gene-based studies[49], and a recent meta-analysis of shotgun metagenomic data[22].

Metabolic cross-feeding between *M. smithii* and CRC-associated bacteria suggests functional integration

A consistent, significant, and positive association between elevated *M. smithii* abundance and CRC was demonstrated across three independent studies (studies by Feng et al.[34], Yu et al.[33], and Gupta et al.[38]), and was also confirmed by a recent CRC meta-analysis[22] and our study (Fig. 2b). To evaluate whether observed differences in *M. smithii* abundance were detectable within a multivariate microbiome classification framework, we applied a random forest (RF) classification model trained on microbial relative abundances of the pooled dataset. Across all folds, the model achieved a mean receiver operating characteristic (ROC) area under the curve (AUC) of 0.74 ± 0.03, indicating a stable discriminative performance between CRC and control microbiomes (Supplementary Fig. 7a). The learning curve showed convergence between training and validation AUC values, confirming generalization without overfitting.

Notably, the archaeon Methanobrevibacter_A_smithii ranked among the top discriminatory features, indicating that archaeal abundances substantially contributed to the signal captured by the model (Supplementary Fig. 7b). SHAP analysis further characterized model behavior, indicating that Methanobrevibacter_A_smithii contributed to the random forest's classification of CRC and control samples (Supplementary Fig. 7c). This observation is consistent with a recent meta-analysis, in which *M. smithii* was also identified among the top features in a CRC diagnostic model[22]. The consistent identification of *M. smithii* as both significantly enriched in CRC (Fig. 2b) and as a high-impact classifier feature (Supplementary Fig. 7b, c) suggests that this archaeon contributes to the model's discrimination between CRC and control samples.

Given that methanogenic archaea rely on metabolic by-products of bacterial fermentation, we aimed to explore the ecological and functional interactions between *M. smithii* and bacterial species previously associated with CRC.

We curated a set of twelve bacterial taxa identified as CRC microbial biomarkers based on a literature review (Supplementary Data 4). Taxa are referred to by their original names in UHGG v.2.0.1 datasets, with updated nomenclature (GTDB r226) provided in parentheses where applicable. The selected taxa include Prevotella_copri_A (updated to Segatella_copri), Mediterraneibacter_torques, Prevotella_intermedia, Peptostreptococcus_stomatis, Porphyromonas_asaccharolytica, Parvimonas_micra, Gemella_morbillorum, Clostridium_Q_symbiosum (updated to Otoolea_symbiosa), Akkermansia_muciniphila, Escherichia_coli_D (updated to Escherichia_coli), Bacteroides_fragilis, and Fusobacterium_nucleatum.

We validated the presence and enrichment of these bacterial biomarkers in our compiled CRC dataset through differential abundance analysis. In the combined dataset, 9 of the bacterial CRC biomarkers showed significant differential abundance, whereas Prevotella_A_copri, Mediterraneibacter_torques, and Porphyromonas_asaccharolytica were not significantly enriched (Supplementary Fig. 8). Across individual studies, after we controlled for confounding factors, such as age, sex, and BMI, 10 bacterial CRC biomarker species exhibited significant differential abundance across at least two independent studies (CLR-transformed data with the Wilcoxon rank-sum test, p-adjusted <0.05), whereas Prevotella_A_copri and Akkermansia_muciniphila each demonstrated differential abundance in only one study (Supplementary Fig. 8). Notably, all taxa, except Mediterraneibacter_torques, appeared at least once in our selected CRC datasets, and our differential abundance findings aligned mostly with the original articles, with some small differences, which could be due differences in case-control sample matching (Supplementary Fig. 8 and Supplementary Data 5).

Correlation analysis between these CRC-associated bacterial taxa and Methanobrevibacter_A_smithii revealed predominantly positive abundance-based associations across both the combined and individual datasets, with all taxa showing positive correlations with this archaeon except for Otoolea_symbiosa, which exhibited mostly negative correlations (Supplementary Fig. 9 and Supplementary Data 6). In addition, co-occurrence analysis based on presence–absence patterns showed that Methanobrevibacter_A_smithii exhibited mainly positive co-occurrence with CRC-associated bacterial taxa, with both the frequency and magnitude of these associations being higher in CRC than in controls. Although the differences in co-occurrence strength between groups were not statistically significant, the overall trend indicates a more pronounced archaeal–bacterial co-association under disease conditions (Supplementary Fig. 10), which was in accordance with previous studies where co-occurrence of *M. smithii* and these bacterial taxa were shown[22].

The *M. smithii* genome encodes an extensive array of transporters (see transporter file in gapseq output of *M. smithii* in Data availability), including those for amino acids (e.g., aspartate, arginine, glutamate, glutamine, or histidine), but also organic acids (e.g., succinate), indicating that the archaeal-bacterial metabolite exchange might go well beyond H_2 and CO_2 transfer. Experimental cultivation of *M. smithii* ALI (mono-culture in rich MS medium, Supplementary Data 7) confirmed the uptake of several amino acids (leucine, valine, isoleucine, alanine, arginine, glutamic acid, methionine, asparagine, lysine, cystine, glycine, threonine, tyrosine, histidine, phenylalanine, and tryptophane) and other compounds (butyrate, propionate, lactic acid, and acetic acid etc.) from its environment (Supplementary Fig. 11 and Supplementary Data 7).

To functionally explore archaeal-bacterial cross-feeding potential, we performed in silico co-culture metabolic modeling using PyCoMo[50]. The models included all 12 bacterial CRC biomarkers (one in each simulated co-culture), and, as a control, the non-CRC-associated *Christensenella minuta*, given its known syntrophic interaction with *M. smithii*[14].

A key finding was the universal predicted export of succinate by all bacterial partners ($n = 13$, 100%), and the predicted import of this compound by *M. smithii* (Fig. 3). This widespread pattern suggests that succinate-mediated cross-feeding could be a conserved feature of archaeal-bacterial interactions. Succinate is a common fermentation by-product during carbohydrate fermentation, primarily from fumarate respiration, serving for electron disposal[51,52]. *M. smithii*, encoding succinate-specific transporters, succinate dehydrogenase (Sdh) and succinyl-CoA synthetase (Suc), is thus well equipped to utilize this metabolite, potentially for redox balancing or as an anaplerotic substrate in its incomplete reductive TCA cycle[53,54].

The relevance of succinate extends beyond microbial metabolism. Succinate, produced by bacteria, such as *Fusobacterium nucleatum*, has been shown to serve as a critical metabolic signaling molecule implicated in promoting CRC metastasis by activating the transcription factor STAT3, which induces epithelial-to-mesenchymal transition and enhances tumor invasiveness and metastatic potential[55].

Additionally, succinate suppresses the cGAS-interferon-β signaling pathway, reducing CD8 + T cell infiltration in tumors and consequently contributing to impaired anti-tumor immunity[56,57]. This positions succinate cross-feeding as a mechanistic link between microbiome metabolism and host oncogenic processes[58].

Beyond succinate, *M. smithii* models consistently exported riboflavin in all pairwise interactions. Riboflavin is an essential precursor for the synthesis of flavin coenzymes, flavin adenine dinucleotide (FAD) and flavin mononucleotide, which play a central role in oxidation-reduction reactions, redox metabolism[59] and consequently, *M. smithii* may be beneficial to its bacterial partners. Additional predicted export-import dynamics were observed for metabolites, such as amino acids (L-asparagine, L-glutamine), taurine, ornithine, various carbohydrates, methanol, and acetaldehyde (Fig. 3).

Notably, in interactions with CRC-associated bacteria, *M. smithii* models exhibited uptake of amino acids, including L-asparagine*, L-glutamine*, L-leucine*, L-threonine*, L-valine*, L-lysine*, L-serine*, L-arginine*, L-aspartate, L-glutamate (Fig. 3). Most of these amino acids (indicated by *) have previously been linked to CRC[55,56,60–67]. These amino acids contribute to CRC progression by supporting structural protein synthesis, providing alternative energy sources, and activating oncogenic pathways, such as mTORC1 (mechanistic target of rapamycin complex 1). Their elevated levels in tumor tissues reflect increased uptake and metabolic reprogramming by cancer cells and have been shown to be further shaped by gut microbial interactions. The uptake of these amino acids by *M. smithii* suggests a potential co-feeding pattern that may not only support microbial interactions but could also influence host metabolic or signaling pathways. Notably, while amino acid and organic acid uptake is not unique to *M. smithii*, our goal was not to establish metabolic specificity but rather to delineate potential routes of archaeal–bacterial metabolite exchange.

Co-culture with *M. smithii* promotes bacterial growth and metabolite production linked to CRC biomarkers

To investigate the interactions between *M. smithii* and CRC-associated bacteria, we performed a series of controlled co-cultivation experiments under strictly anoxic conditions (Fig. 1d and Supplementary Fig. 12). We selected *F. nucleatum*, enterotoxigenic *Bacteroides fragilis*, and *Escherichia coli* (*E.coli*) and their well-documented roles in CRC pathogenesis. These bacteria are known to contribute to tumor development through specific virulence factors, including colibactin, cytolethal distending toxin (CDT), cycle-inhibiting factor (CIF), and cytotoxic necrotizing factor (CNF) in *E. coli*; the adhesin FadA in *F. nucleatum*; and the enterotoxin Bft in *B. fragilis*[68]. Notably, the *E. coli* strain, previously referred to as strain D, was isolated in our previous

https://doi.org/10.1038/s41467-026-69711-7

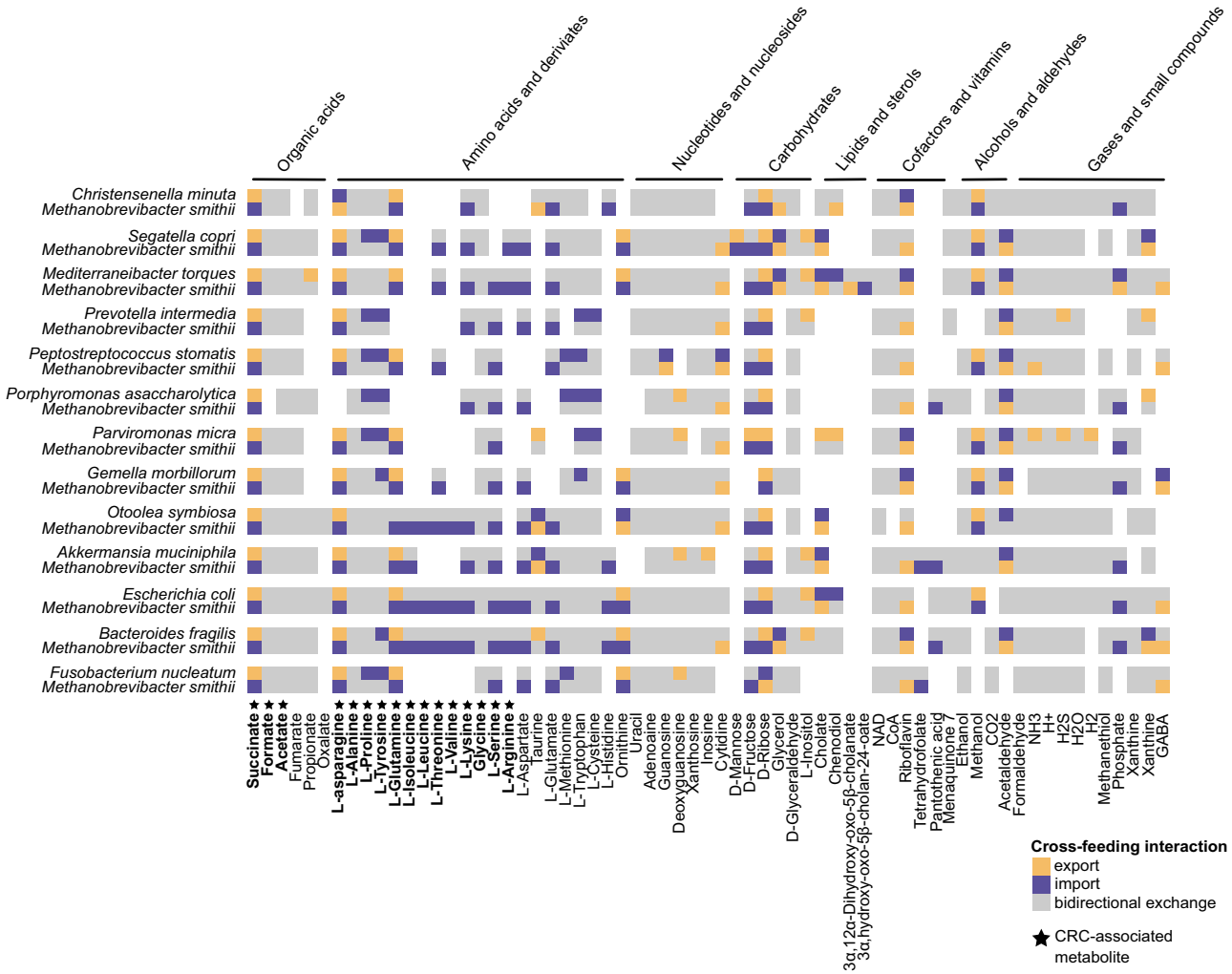

Fig. 3 | Integration of metabolic modeling analysis in colorectal cancer (CRC) datasets. Community-scale metabolic models show predicted cross-feeding interactions between *Methanobrevibacter smithii* and CRC-associated bacterial biomarkers in gut medium, generated using PyCoMo. Metabolite exchanges were calculated independently of growth rates for each archaeon–bacterium pair. Colors indicate metabolite export or production (yellow), import or consumption (purple), or both (gray). Only metabolites involved in cross-feeding interactions are shown. Metabolites highlighted in bold have been previously linked to CRC in the literature. Source data are provided as a Source data file.

study from a methane-producing patient, where it was found to co-occur with *M. smithii*[69]. As archaeal representative, we chose the human gut strain *M. smithii* ALI (the type strain of *M. smithii* was isolated from an anaerobic digester).

SEM analysis revealed close proximity between *M. smithii* ALI and bacterial partners in all co-culture conditions, without showing any specific morphological alterations relative to mono-cultures. All co-cultures appeared densely populated and contained numerous archaeal and bacterial cells undergoing division (Fig. 4a). Consistent with SEM observations, fluorescence microscopy revealed the presence of *M. smithii* strain ALI cells in co-cultures exhibiting the characteristic shape of this archaeal strain and F_{420}-based autofluorescence in both the mono- and co-culture conditions, indicating active growth.

Co-culture dynamics were highly specific. *M. smithii* ALI exhibited increased growth ($p = 4.1E-02$) (evidenced by elevated *mcrA* gene copy numbers) only in the presence of *B. fragilis* compared to mono-culture conditions. *F. nucleatum* ($p = 3.07E-06$) and *E. coli* ($p = 4.61E-06$) displayed significantly enhanced 16S rRNA gene copy numbers at time point 1 compared to mono-cultures, indicating archaeon-mediated stimulation of bacterial growth speed (Supplementary Fig. 13 and Supplementary Data 8). However, methane production by *M. smithii* ALI was not significantly different between mono-cultures and none of the co-cultures (Supplementary Fig. 14). Notably, none of the co-cultures resulted in a statistically significant mutual growth benefit, suggesting asymmetrical or unidirectional metabolic support (Supplementary Fig. 13).

Metabolic profiling further elucidated the biochemical landscape of the archaeal-bacterial interactions. In agreement with in silico modeling, all co-cultures produced higher amounts of succinate compared to their mono-cultures, confirming this metabolite as a conserved cross-feeding intermediate (Figs. 3, 4b, and Supplementary Fig. 15). While metabolic alteration in *B. fragilis* and *E. coli* co-cultures with *M. smithii* ALI were relatively modest beyond succinate, the *F. nucleatum*-*M. smithii* pairing exhibited a distinct and expansive metabolic signature.

Specifically, co-cultivation with *F. nucleatum* led to a significant accumulation of succinic acid*, acetic acid, lactic acid, propionic acid, butyric acid, and a range of amino acids, including alanine*, proline*, isoleucine*, leucine*, valine* and glycine*, arginine*, and phenylalanine*. Conversely, notable consumption of methionine, glucose, choline, glycerophosphocholine, and pyroglutamic acid was observed (Supplementary Data 9, 10, and 11). Several of these amino acids (marked with *) have previously been implicated in the metabolism of CRC[55,56,60–67], reinforcing their potential functional relevance.

https://doi.org/10.1038/s41467-026-69711-7

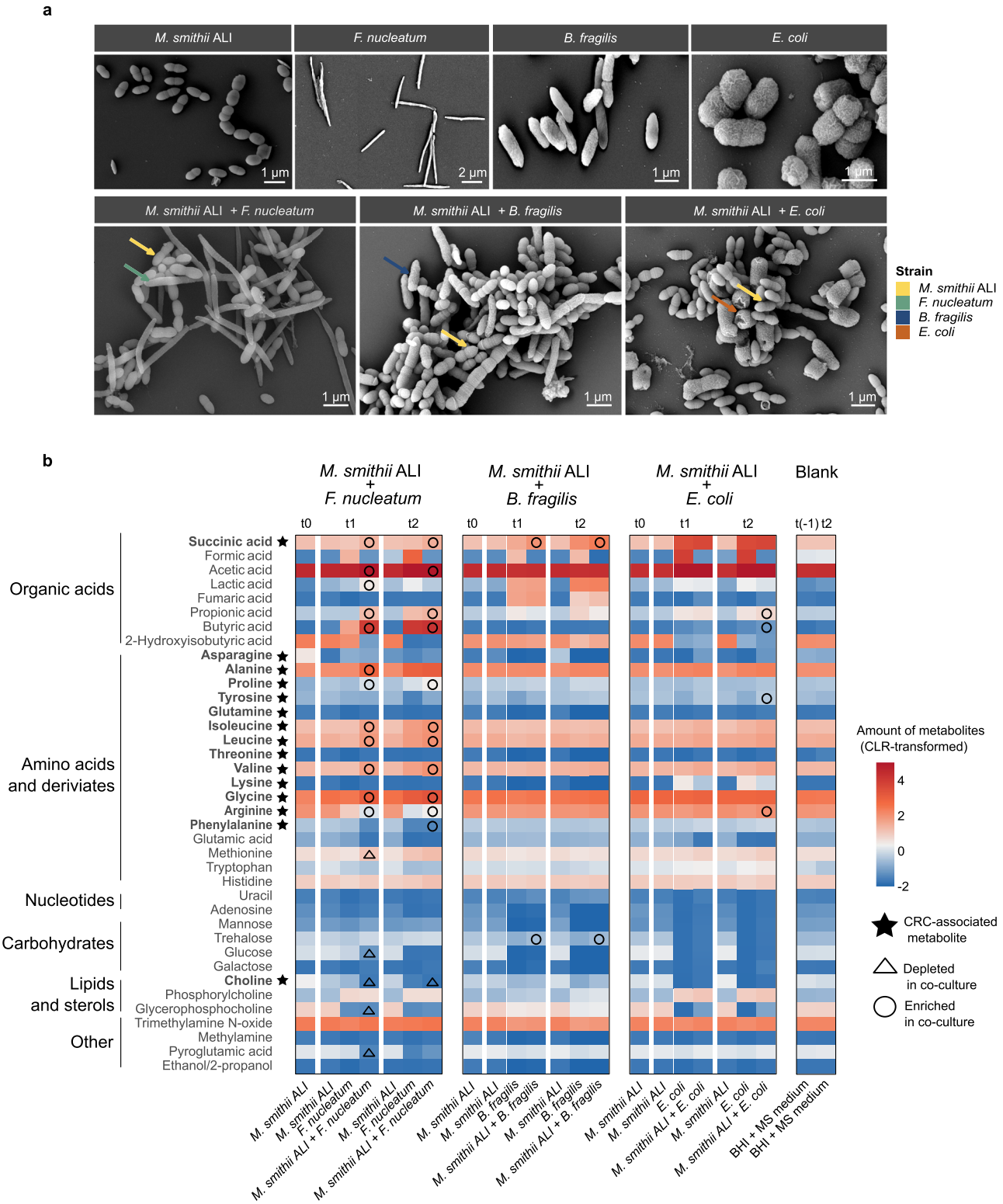

Although the co-culture results did not entirely recapitulate the in silico predictions (e.g., the predicted production of asparagine and glutamine could not be measured; Fig. 4b and Supplementary Fig. 15), both approaches converged on the identification of succinate and amino acids as key mediators of archaeal-bacterial metabolic exchange. These findings indicate *M. smithii* as an active participant in CRC-associated microbial networks, potentially shaping the tumor microenvironment through metabolite cross-feeding.

CRC-associated compounds are prominent in the *F. nucleatum*–*M. smithii* symbio-metabolome

To further investigate the metabolites present in co-culture, we subjected the supernatant from three replicates of *M. smithii* ALI and *F. nucleatum* co-culture at time point t1 (corresponding to the highest observed growth, as shown in Supplementary Fig. 13) to detailed mass spectrometry (MS) analysis. This analysis aimed to identify metabolites specifically enriched under co-culture conditions compared to the blank control medium (MS + BHI).

https://doi.org/10.1038/s41467-026-69711-7

Fig. 4 | Scanning electron microscopy and NMR metabolomic profiling of *Methanobrevibacter smithii* ALI in mono- and co-culture with colorectal cancer-associated bacterial strains. a Scanning electron microscopy (SEM) analysis of *M. smithii* ALI and the bacterial strains used in co-culture experiments, including the colorectal cancer-associated species *Fusobacterium nucleatum*, *Bacteroides fragilis*, and *Escherichia coli*. Imaging was performed for both monocultures and co-cultures with *M. smithii* ALI. The experiments were repeated two times independently with similar results. **b** The heatmap displays normalized area under the curve (AUC) values obtained from metabolomics analysis, representing the relative abundance of metabolites across conditions. For improved comparability and visualization, the amount of metabolites were centered, and log-ratio transformed. A metabolite was classified as enriched or depleted in co-culture only if its abundance was significantly higher or lower, respectively, compared to both *M. smithii* ALI and the corresponding bacterial mono-culture, as well as in relation to the blank medium. For each co-culture experiment, mono-cultures of *M. smithii* ALI and the respective bacterial strain were grown in parallel under identical conditions. Both monocultures and co-cultures were performed in five biological replicates, with blank medium included in three replicates. Metabolites previously associated with colorectal cancer are highlighted in bold and indicated with an asterisk. Time points are defined as follows: t(−1): initial of the experiment prior to inoculation; t0: 24 h post-inoculation of *M. smithii* ALI; t1: 24 h post-inoculation of the bacterial strain (48 h post *M. smithii* ALI inoculation), t2: 72 h post bacterial inoculation (96 h post *M. smithii* ALI inoculation). A blank medium control was included to account for background metabolite levels. Metabolite depletion (triangle) or enrichment (circle) in co-cultures was determined using two-sided Wilcoxon rank-sum test, adjusted-$p < 0.05$ (FDR). Source data are provided as a Source data file.

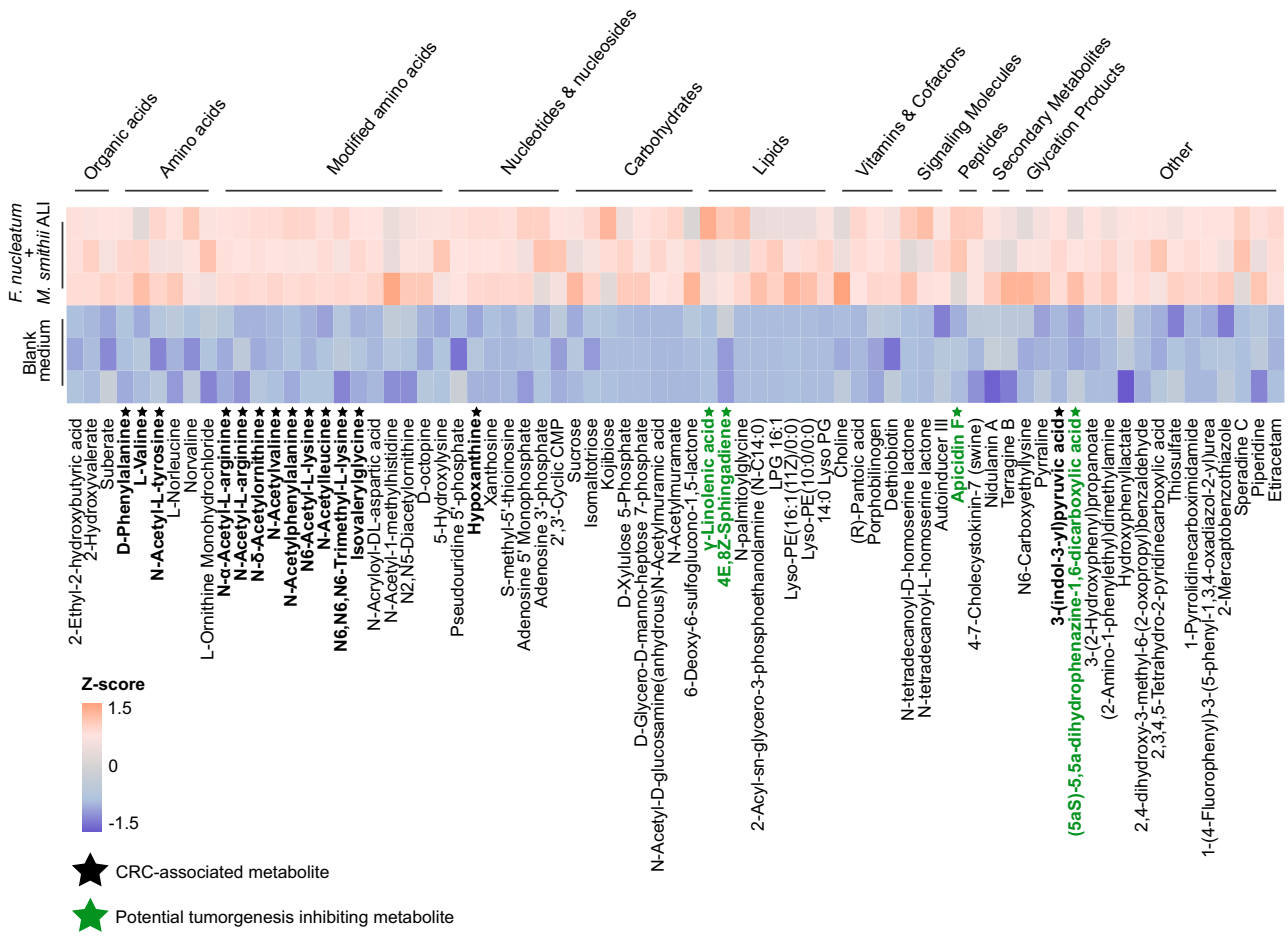

Fig. 5 | Mass spectrometry-based metabolomic profiling of the supernatant from *Methanobrevibacter smithii* ALI + *Fusobacterium nucleatum* co-culture (triplicates). Heatmap showing significantly increased metabolites (FC > 1.5, two-sided t-test, *p*-adjusted <0.05) detected by mass spectrometry in the co-culture of *F. nucleatum* and *M. smithii* ALI at t1 (24 h after addition of *F. nucleatum* to an established *M. smithii* ALI culture, coinciding with peak growth of both strains) compared to the blank medium (BHI + MS). Each cell represents the Z-score of the respective metabolite, calculated across all samples as the number of standard deviations from the mean. Metabolite concentrations were normalized using PQN and $\log_{10}$-transformed to adjust for cell count differences and dilution effects. Metabolites with reported CRC-related promoting effects are highlighted in black, while those with potential tumorigenesis-inhibiting effects are highlighted in green. Source data are provided as a Source data file.

The co-culture supernatant displayed a diverse range of metabolite classes, including organic acids, amino acids and their derivatives, nucleotides, carbohydrates, lipids, vitamins, signaling molecules, and peptides (Fig. 5 and Supplementary Data 12). Notably, several amino acids previously associated with CRC, such as phenylalanine and valine, as well as amino acid derivatives, including N-acetyl-tyrosine, N-acetyl-valine, N-acetyl-phenylalanine, N6-acetyl-L-lysine, N-acetylleucine, N6,N6,N6-trimethyl-L-lysine, and isovalerylglycine, were significantly enriched. These compounds are derivatives of CRC-associated parent amino acids, such as tyrosine, valine, phenylalanine, lysine, leucine, and glycine, which were previously highlighted in Figs. 3, 4b, and Supplementary Fig. 11. Their presence in the MS data is consistent with findings from NMR-based metabolomics (Fig. 4b). Additionally, we detected N-α-acetyl-L-arginine, N-acetyl-arginine, and N(δ)-acetylornithine, which are metabolites involved in the arginine biosynthesis and degradation pathways in the co-culture supernatant

(Fig. 5). Arginine serves as a precursor for nitric oxide (NO) and polyamines; while polyamines promote tumor growth[70], NO can exert either tumor-promoting or tumor-suppressive effects depending on its concentration[71].

Hypoxanthine, a key intermediate in purine metabolism, was also detected in the co-culture supernatant of *M. smithii* ALI + *F. nucleatum*. This metabolite is widely produced and utilized by both host and microbial cells. Previous studies have associated microbial hypoxanthine production, particularly by *Peptostreptococcus stomatis*, another CRC-associated bacterium (Supplementary Fig. 8 and Fig. 3), with altered gut motility and serotonin release, processes that may contribute to CRC progression[63,72–74].

Another interesting metabolite in the supernatant of the co-culture was 3(-indole-3-yl) pyruvic acid, also known as indole-3-pyruvic acid (I3P). I3P supplementation has been shown to rescue tumor cells under tryptophan starvation, identifying it as a critical oncometabolite and therapeutic target[75]. Microbial production of I3P could circumvent tryptophan restriction, suggesting tumor-microbiome metabolic cross-talk that may promote cancer progression, particularly in gut-associated cancers like CRC, where gut barrier dysfunction could be present[76,77].

Notably, several metabolites with known or potential antitumor activity were also identified in the co-culture supernatant (Fig. 5). Among these, γ-linolenic acid, previously derived from *Lactobacillus plantarum* MM89, has been shown to induce ferroptosis in tumor cells, suggesting a therapeutic mechanism for targeting CRC[78]. Another detected metabolite, 4E,8Z-sphingadiene, belongs to the sphingadiene class, has demonstrated pro-apoptotic effects in colon cancer cells and has been shown to suppress intestinal tumorigenesis in vivo, highlighting its potential in cancer prevention[79]. Intriguingly, both γ-linolenic acid and 4E,8Z-sphingadiene were also significantly enriched in *M. smithii* ALI mono-cultures (compared to *F. nucleatum* mono-cultures), implicating the archaeon (and not the bacterial partner) as a direct source of potentially bioactive, antitumor metabolites (Supplementary Fig. 16 and Supplementary Data 13).

Apicidin F, a structural analog of the histone deacetylase inhibitor apicidin, was also present, which has been previously isolated from the fungus *Fusarium fujikuroi*[80]. Its detection in the supernatant of co-culture suggests the potential ability of these two strains to also produce this compound (Supplementary Fig. 16). Notably, apicidin has shown anti-growth activity by inhibiting histone deacetylases in cancer cells[81]. Lastly, (5aS)-5,5a-dihydrophenazine−1,6-dicarboxylic acid, a derivative of phenazine−1,6-dicarboxylic acid, has been shown to be produced by strains, such as *Pseudomonas aeruginosa*, and has demonstrated strong anticancer activity against various cell lines, including CRC cells like HT29[82,83].

Discussion

Methanobrevibacter species dominate the human gut archaeome. Their activity metabolizes H_2 and CO_2 into methane, thereby relieving lumen gas pressure, and sustains redox conditions that favor bacterial fermentation[14,69,84]. Although viewed as commensal, shifts in *Methanobrevibacter* abundance have been linked to various metabolic and gastrointestinal disorders, suggesting a potential role in host health[30,85]. However, most existing studies rely on low-resolution methodologies, such as breath methane testing or 16S rRNA gene sequencing, which are limited to resolve archaeal taxonomy and to link archaeal species to physiological patterns[24].

To address these limitations, we performed a meta-analysis of 2959 shotgun-metagenomic datasets, drawn from 10 studies across 12 countries, and corrected for age, sex, and BMI, when possible, for study-individual analyses. The datasets included different disorders, including CRC, T2D, (IBD) (including Crohn's disease (CD) and ulcerative colitis (UC)), MS, AD, SCZ, and PD.

Our analysis uncovered disease-specific alterations in gut archaeal communities. For instance, patients with CD showed a significant reduction in *Methanobrevibacter* spp., with the notable exception of Methanobrevibacter_A_sp900766745, which was significantly enriched in these patients. While the underlying mechanisms remain unclear, the reduced stool transit time in patients with CD may interfere with the slower growth rate of human gastrointestinal archaea.

In contrast, SCZ patients exhibited a significant depletion of Methanobrevibacter_A_smithii, which confirms previously observed correlations of methanogen abundance and neurological function[3].

In PD, we initially observed significantly higher levels of methanogenic taxa, including *Methanobrevibacter* species, in the pooled dataset. However, once we applied strict matching for age, sex, and BMI, these associations did not remain significant within individual studies, although most cohorts continued to show a similar direction of change. This discrepancy compared to the findings of one of the included studies (Wallen et al.[28]), who reported significant increased abundance of in PD, highlights how sensitive archaeal signals can be to study design and metadata handling. It also reinforces that robust metadata and consistent analytical approaches are essential when interpreting archaeome dynamics in disease.

Moreover, in general, variability in pipelines, reference genome databases, and cohort metadata contributes to inconsistencies across studies. These challenges highlight the need for consistent profiling frameworks and more comprehensive metadata collection, including antibiotic use and medication history, which are often overlooked but likely influence archaeal dynamics. Dietary data were also not consistently reported across datasets, preventing us from accounting for potential differences in eating behaviors between case and control groups, for any of the included studies.

In CRC, methanogens showed a more consistent pattern. We observed overall significant enrichment of Methanobrevibacter_A_smithii in the pooled analysis, aligning with findings from a recent multicohort study[22]. Across individual cohorts, samples from CRC patients consistently demonstrated an increase in Methanobrevibacter_A_smithii and closely related taxa (e.g., Methanobrevibacter_A_smithii_A). While statistical significance varied between cohorts, the overall trend pointed toward the enrichment of methanogen in CRC. Notably, only one of the investigated studies (Gupta et al.[38]) explicitly reported increased *Methanobrevibacter* abundance in CRC, while others (e.g., Feng et al.[34]) broadly implicated archaeal overgrowth without specifying the taxonomy. In datasets with staging information, the abundance of Methanobrevibacter_A_smithii showed a nonlinear trend: elevated at stage 0, reduced in early cancer (stages I/II), and increased again in advanced disease (III/IV). This stage-associated trajectory aligns with a recent multicohort analysis of 3,741 stool metagenomes, which identified *M. smithii* among the top species enriched in metastatic CRC and previously noted methane-producer involvement in stage IV disease[45,48]. This pattern raises the question of whether methanogen expansion precedes tumor progression or reflects later shifts in the tumor-altered gut ecosystem. Notably, methanogens, including *M. smithii*, have also been associated with longevity[31], indicating that their increased abundance does not inherently imply pathogenicity. Strain-level heterogeneity among methanogens, as well as host-dependent or epigenetic interactions, may further shape their functional effects. Longitudinal and strain-resolved analyses will therefore be required.

Methane is the primary end-product of methanogen metabolism, and has been shown in animal models to slow intestinal transit[86]. Clinically, elevated baseline breath methane levels have been linked with constipation, which is a recognized risk factor for CRC[87,88]. These findings suggest a potential association between increased *M. smithii* abundance and CRC development. Notably, prior studies have reported enrichment of *M. smithii* in CRC patients even after considering gut

transit time[22], implying that factors beyond motility, including host–microbe interactions or microbial cross-talk, may play a role. However, methanogen abundance patterns remain susceptible to confounders, such as constipation, which is common in CRC and can influence archaeal composition. The lack of standardized metadata, particularly regarding transit time, in existing cohorts limits our ability to fully resolve these effects and interpret associations[88].

To investigate the potential functional contributions of *M. smithii*, we further explored its interactions with CRC-associated bacterial taxa. Methane production by *M. smithii* represents the final step of interspecies hydrogen transfer, a syntrophic process in which hydrogen (H_2) and carbon dioxide (CO_2) released by fermentative bacteria are consumed by methanogens to yield methane and water[54]. By removing H_2, *M. smithii* enhances bacterial fermentation efficiency and indirectly supports metabolic pathways of anaerobes that are frequently enriched in CRC microbiomes. This interspecies hydrogen transfer and metabolic coupling could facilitate the growth of CRC-associated bacteria, such as *F. nucleatum*, *P. stomatis*, and *P. micra*, which rely on efficient fermentative metabolism under strictly anaerobic conditions[89,90]. In this context, methane acts not only as a metabolic by-product but also as an ecological marker and potential driver of microenvironments that favor CRC-associated taxa.

Given that *Methanobrevibacter* species rely on bacterial fermentation end products (H_2 and CO_2) for energy metabolism, their ecological function cannot be assessed individually. Therefore, we integrated archaeal and bacterial data to examine how *M. smithii* may influence CRC-associated bacterial taxa beyond methanogenesis and potentially contribute to colorectal carcinogenesis through microbe–microbe and potential host–microbe interactions.

While the loss of co-occurrence between commensal archaea and bacteria has been reported in CRC, *M. smithii* has shown positive co-occurrence associations with known CRC-associated taxa, such as *F. nucleatum*, *B. fragilis*, and *E. coli* in previous studies[22,35], a pattern we also observe by correlation analysis as well as presence/absence analysis in our study. Consistent with these associations, a tissue-based study detected archaea (including *M. smithii*) together with bacteria, such as *F. nucleatum* in CRC tumor biopsies[47].

These bacteria are known to promote carcinogenesis by inducing DNA damage, inflammation, and activating oncogenic pathways, suggesting that CRC-enriched archaea and bacteria may synergistically contribute to CRC[91]. On the other hand, previous studies have reported significant co-exclusion patterns between CRC-enriched archaea and CRC-depleted bacteria, including butyrate-producing species, such as *Clostridium beijerinckii* and *Clostridium kluyveri*, implying a potential antagonistic interaction in colorectal tumorigenesis[91].

An interesting finding of our study based on metabolic modeling was the universal export of succinate by all CRC-associated bacterial partners and its predicted uptake by *M. smithii*, highlighting succinate as a key cross-fed metabolite. Additionally, *M. smithii* was predicted to export riboflavin in all archaeal-bacterial pairings and to import several CRC-associated amino acids, such as asparagine, glutamine, leucine, and arginine. These metabolic exchanges suggest potential cooperative networks that could influence both microbial ecology and host disease processes, beyond H_2 exchange.

Experimental co-culture experiments validated our in silico findings. *M. smithii* growth was significantly enhanced only in the presence of *B. fragilis*, while *F. nucleatum* and *E. coli* showed archaeon-induced early growth acceleration. In these conditions, the archaeon did not show a significant growth increase in return, indicating only mild commensal benefits or fully unidirectional support.

In all co-cultures, succinate levels were higher than in mono-cultures, supporting predictions from genome-scale metabolic models and confirming succinate as a shared cross-feeding metabolite. However, the overall changes in metabolism differed between bacterial partners. The *F. nucleatum*–*M. smithii* pairing showed the most extensive changes, with increased production of short-chain fatty acids (acetic, lactic, propionic, and butyric acids) and several amino acids (alanine, valine, isoleucine, leucine, phenylalanine, proline, and glycine), many of which have been linked to CRC[64,65,67].

Untargeted mass spectrometry-based metabolomics of supernatants further confirmed these findings, showing not only elevated levels of these CRC-related amino acids but also their modified forms, such as N-acetylated derivatives (e.g., N-acetyl-tyrosine, N-acetylvaline, and N6-acetyl-L-lysine).

Other detected metabolites are potentially directly connected to cancer-related pathways. For instance, arginine derivatives (N-α-acetyl-L-arginine, N-acetyl-arginine, and N-δ-acetylornithine) feed into nitric oxide and polyamine synthesis, both involved in CRC progression[67]. Interestingly, genes encoding cancer-related metabolites like polyamines have been shown to be more prevalent and diverse in gut and oral samples, affiliated with Euryarchaeota, especially methanogenic archaea[92]. Hypoxanthine, a purine compound known to affect gut function and tumor development, and I3P, an oncometabolite that supports tumor growth under tryptophan-starved conditions[63,72–74], were also found in the supernatant.

The co-cultures also showed significantly high abundance of some compounds likely impairing tumorigenesis. These compounds included γ-linolenic acid, which can trigger ferroptosis in tumor cells; 4E,8Z-sphingadiene, known to promote cancer cell death; apicidin F, a histone deacetylase inhibitor; and phenazine derivatives with strong anticancer activity[78,79,81–83]. Two of these compounds (γ-linolenic acid and 4E,8Z-sphingadiene) were significantly enriched in pure *M. smithii* cultures, indicating archaeal origin.

Our findings position *M. smithii* as a potentially active metabolic participant in CRC-associated microbial networks. Through both cooperative and asymmetrical metabolic interactions, *M. smithii* has the potential to modulate the abundance and function of key bacterial taxa and to actively contribute to a chemically rich microenvironment that includes metabolites with tumor-promoting and tumor-suppressive potential. Understanding how host factors like immune status affect the balance of these interactions, including the archaea-metabolome, will be key to determining their role in CRC development and therapy. Additionally, future in situ imaging and spatial-omics studies will be needed to validate these associations and clarify mechanistic roles.

Methods

Dataset collection

Relevant metagenomic investigations were identified through targeted keyword searches for diseases previously linked to gut methanogens[1–8,93], specifically CRC, IBD, T2D, MS, AD, SCZ, and PD (Supplementary Data 1). A systematic PubMed search was performed for English-language observational studies and meta-analyses published from 2000 until August 30, 2024. The search query used was: ("disease of interest") AND ((gut AND metagenome AND microbiome) OR fecal OR shotgun OR microbiota OR "whole genome"), with "disease of interest" encompassing CRC, IBD, PD, AD, T2D, MS, and SCZ. Additionally, reference lists from the identified articles and related meta-analyses were screened to identify additional studies. Additionally, the NCBI BioProjects database was screened for sequencing datasets using disease-specific terms (e.g., "CRC gut"), with filters applied for the "metagenome" data type and the human organism.

Studies employing shotgun metagenomic sequencing were considered. Only fecal shotgun metagenomic datasets were included, while studies with fewer than 20 case subjects or those involving participants under 18 years were excluded. Case subjects were defined as individuals with explicit disease diagnoses provided in the study metadata or NCBI BioProject records, whereas control subjects were those clearly described as healthy or designated as controls. Controls were defined as samples from individuals without a positive disease diagnosis. Thus,

it should be noted that controls do not necessarily present healthy individuals, but rather individuals without a specific diagnosis. Furthermore, studies were required to report metadata on sex, age, and/or BMI, or to have used case-control matched cohorts on at least two of these covariates. Studies that would have required additional ethical approvals or had restricted data access were omitted.

For CRC investigations, only samples from patients with confirmed CRC diagnoses were incorporated, excluding those with small or large adenomas. CRC staging information, based on the American Joint Committee on Cancer (AJCC) classification, was available for the Zeller et al.[41], Yachida et al.[45], Vogtmann et al.[46], Feng et al.[34], Wirbel et al.[42], and Gupta et al.[38] cohorts, which were therefore included in stage-specific analyses. In contrast, for the Hannigan et al.[94], Thomas et al.[37], and Yu et al.[33] datasets, staging information could not be identified from the available metadata. In the Yachida et al.[45] dataset, stage 0 samples were retained; however, in the other datasets, stage 0 groups comprised fewer than five samples or were not represented and were consequently excluded from stage-specific analyses in these cohorts. For the Wirbel et al.[42], Gupta et al.[38], and Feng et al.[34] datasets, the number of samples within individual stages fell below ten after case-control matching. To maintain statistical robustness, these datasets were analyzed only in overall case-control comparisons, without stage stratification. For analysis, stage I and II CRC cases were grouped as stage I/II, while stage III and IV CRC cases were grouped as stage III/IV. Consequently, CRC staging was taken into consideration for the Yachida et al.[45], Zeller et al.[41], and Vogtmann et al.[46] cohorts, where sufficient information and sample sizes were available. When matching CRC stages with controls, individual control samples were allowed to be reused across different stage groups. In the case of MS, inclusion was limited to two cohorts (from San Francisco, USA, and Edinburgh, Scotland) that consisted of treatment-naïve individuals and met the required sample size threshold, since treatment in these patients affects the abundance of the archaeome[26]. For AD, only pre-AD samples were considered, given the limited number of diagnosed cases. Sequence data were further limited to paired-end read libraries, thereby excluding datasets that combined single-end and paired-end reads. When available, sample covariates were extracted from the original study metadata, and for individuals with multiple SRA accessions, only the first available metagenome sample was used. Finally, any samples lacking accessible metadata from either the NCBI BioProject records or the published article were excluded.

Following these criteria, a total of 3243 samples from 19 studies across 12 countries were identified (Supplementary Table 1). Further details on study selection and the number of studies considered are provided in Fig. 1 and Supplementary Fig. 1.

Data retrieval and processing

Raw sequencing data were retrieved from the NCBI Sequence Read Archive using SRA Toolkit (v3.1.0). Human-derived sequences were removed by aligning the raw reads to the GRCh38 human reference genome using *removehuman.sh* within the BBMap suite (v39.01) with default parameters. Read quality filtering, adapter trimming, base correction, and removal of low-complexity sequences were conducted concurrently using fastp (v0.23.4) with the following parameters: *--average_qual 20*, *--detect_adapter_for_pe*, *--correction*, *--overrepresentation_analysis*, and *--low_complexity_filter*. Unpaired reads resulting from trimming or filtering were corrected using BBMap (*repair.sh*), ensuring synchronization of read pairs for downstream analyses.

For microbial taxonomic profiling, we employed a Kraken2 and Bracken approach, which has been shown to outperform marker gene-based methods in recent benchmarking studies[95]. Taxonomic classification of the stool samples was carried out using Kraken2[96] (v2.1.2) with the unified human gastrointestinal genome (UHGG v2.0.1) database, which comprises a total of 4644 prokaryotic species, including 4616 bacterial species and 28 archaeal species, and enables identification of human gut archaeal species with high resolution[26,97,98]. For the CRC tumor and biopsy samples, the remaining metagenomic reads (i.e, after stringent filtering against the human reference genome (GRCh38) and quality control) were classified with Kraken2 using the Standard Database, which includes RefSeq bacterial, archaeal, and viral genomes, the human genome, and UniVec_Core sequences, to minimize false positives from host contamination. To improve classification accuracy and minimize incorrect lowest common ancestor (LCA) assignments, a confidence threshold of 0.3 was applied. Species-level abundance estimates were refined using Bracken (v2.7) (https://ccb.jhu.edu/software/bracken/) with read length 150. The resulting taxonomic profiles were merged into a comprehensive microbial abundance table for downstream analyses.

For diseases represented by multiple cohorts (CRC, pre-AD, and PD), datasets were subsequently analyzed in pooled form. For this purpose, batch effects across studies were mitigated using the adjust_batch() function from the MMUPHin (v1.23) R package[99], which applies a mixed-effects model to estimate and remove study-specific offsets. To ensure stringency, given the variability in sequencing depth, read length, preprocessing methods, sample collection, and DNA extraction protocols across publicly available datasets, each dataset was also processed independently with the same workflow, including identical quality control procedures, human-read removal, and taxonomic profiling.

Archaeome and bacteriome community analyses

Shannon diversity indices were calculated separately for archaeal and bacterial communities. Species-level abundance tables were processed in R using the phyloseq package (v1.44.0). For each dataset, samples were rarefied to the 10th percentile of library sizes to normalize sequencing depth. Shannon diversity was estimated from rarefied data using the estimate_richness() function, and comparisons between case and control groups were performed using the Wilcoxon rank-sum test. To assess beta-diversity, principal coordinate analysis (PCoA) was performed based on Bray–Curtis distance on species-level abundance profiles after normalization of counts by total sum scaling. Sample clustering patterns were visualized in two-dimensional PCoA plots, with ellipses representing group dispersion (variability of samples within a group). To statistically evaluate differences in beta-diversity, we applied permuted multivariate analysis of variances (PERMANOVA) with 999 permutations.

Machine learning analyses

Machine learning analyses were performed in Python (v3.10) using the *scikit*-learn (v1.5) and *shap* (v0.44) libraries. Prior to model training, all features were subjected to a three-step preprocessing pipeline to reduce noise and ensure comparability across features.

First, near-zero variance features were removed using the VarianceThreshold function (threshold = 1×10^{-5}). Second, as feature values represented proportions ranging from 0 to 1, an arcsine square root transformation was applied to stabilize variance. Third, the resulting features were standardized (mean = 0, standard deviation = 1) using the StandardScaler function to ensure equal weighting in the model. The dataset was randomly partitioned into a training set (80%) and an independent validation set (20%).

A Random Forest classifier (RandomForestClassifier, scikit-learn) was trained using 2000 estimators with class weighting set to balanced and a fixed random seed (random_state = 42) to account for potential class imbalance and ensure reproducibility. Model performance was evaluated using stratified k-fold cross-validation (n_splits = 5, shuffle = true), which preserves class distribution across folds. For each fold, a ROC curve was generated, and the mean ± standard deviation of the AUC was reported to summarize model performance stability.

Feature importance was estimated using two complementary approaches. First, permutation importance (permutation_importance, *scikit-learn*) was computed on the independent test set with 1000 repetitions (n_repeats = 1000, n_jobs = −1), providing the mean and standard deviation of the importance score for each feature. Second, SHAP (SHapley Additive exPlanations) values were computed to derive model-agnostic and directionally interpretable estimates of feature contributions. The top-ranked features were visualized based on mean permutation importance, and SHAP summary plots were used to confirm the robustness and interpretability of the model outputs.

Selection of CRC bacterial markers

To identify CRC-associated taxa, we conducted a PubMed search using the keywords "CRC AND bacteria AND gut AND biomarkers" for studies published until August 30, 2024. After screening relevant publications and cross-referencing additional sources, we focused on bacterial CRC biomarkers at the species level. All identified bacterial taxa were incorporated into our metabolic modeling analyses alongside *Methanobrevibacter smithii* and CRC-associated bacterial markers.

Metabolic modeling

Draft metabolic models were generated using gapseq (development version of 1.4.0, commit acb9647) on the genomes of all CRC biomarkers namely, *Segatella copri* (formerly *Prevotella copri*) (GenBank ID GCA_020735445.1), *Mediterraneibacter torques* (formerly *Ruminococcus torques)* (GenBank IDGCA_000210035.1), *Otoolea symbiosa* (formerly *Clostridium symbiosum* (GenBank ID GCA_008632235.1), *E. coli* (GenBank ID GCA_000025745.1), *Prevotella intermedia* (GenBank ID GCA_001953955.1), *Gemella morbillorum* (GenBank ID GCF_900476045.1), *Peptostreptococcus stomatis* (GenBank ID GCA_000147675.2), *Porphyromonas asaccharolytica* (GenBank ID GCA_000212375.1), *Akkermansia muciniphila* (GenBank ID GCA_009731575.1), *Fusobacterium nucleatum* (GenBank ID GCA_003019295.1), *Parvimonas micra* (GenBank ID GCA_900637905.1), *Bacteroides fragilis* (GenBank ID GCA_000025985.1), as well as *M. smithii* (GenBank ID GCA_000016525.1). The gut medium formulation used in this study followed previously established protocols[100,101]. Subsequently, the initial metabolic models were gap-filled utilizing this specified medium. To simulate co-culture interactions, community metabolic models were constructed for each pair of organisms using PyCoMo[50] version 0.2.7. The corresponding gut medium was applied to each model. The simulations included calculations of community growth dynamics, metabolite exchanges, and cross-feeding interactions between *M. smithii* and CRC-associated bacterial biomarkers, employing PyCoMo's default settings.

For the three CRC biomarkers with validated relevance[68,] *F. nucleatum*, *E. coli*, and *B. fragilis,* co-cultures with *M. smithii* were also simulated on relevant culture media. For this, in addition to the gut medium, the MS + BHI medium formulation was incorporated for gap-filling procedures and subsequent PyCoMo simulations, as previously detailed in our previous study[69] (full medium composition available in the referenced publication, and deposited also in the GitHub repository indicated in the Data availability section). Metabolite exchanges and cross-feeding patterns were computed by scaling the flux bounds from flux variability analysis based on the relative abundances of *M. smithii* and the CRC-associated bacteria, as determined by qPCR analysis performed on co-cultures. The resulting cross-feeding interaction profiles, highlighting metabolites produced by one organism and utilized by the other within each co-culture, were visualized using ScyNet[102] integrated into the Cytoscape[103] software (version 3.10.0).

E. coli isolation and confirmation

To isolate the *E. coli* strain originally designated as *E. coli*_D based on the UHGG v2.0.1 taxonomy, and now classified as *E. coli* without the "_D" designation according to GTDB release 226 and subsequent updates (https://gtdb.ecogenomic.org/), we utilized a fecal sample from a previous study in which the co-occurrence of *M. smithii* and *E. coli*_D was confirmed through both cultivation and sequencing methods[69]. Specifically, 1 ml of the fecal sample from patient 51 (P51) of the aforementioned study was streaked onto CHROMagar™ *E. coli* medium. After incubation at 37 °C for 24 h, colonies displaying a characteristic intense blue coloration were selected for downstream processing.

Genomic DNA was extracted from the selected colonies using the PureLink™ Microbiome DNA Purification Kit (Invitrogen, Thermo Fisher Scientific, USA), following the manufacturer's protocol. To confirm the identity of the isolate as *E. coli*, two sets of primers were employed: one targeting the universal *E. coli* 16S rRNA gene (EC_F: 5′–CCAGGCAAAGAGTTTATGTTGA–3′, EC_R: 5′–GCTATTTCCTGCCGA TAAGAGA–3′)[104], and the other targeting the *adk* housekeeping gene (adkF: 5′–ATT CTG CTT GGC GCT CCG GG–3′, adkR: 5′–CCG TCA ACT TTC GCG TAT TT–3′)[105].

PCR amplification was performed as described previously[104], with small modifications. Briefly, PCR amplification of the *adk* gene was performed with an initial denaturation at 95 °C for 2 min, followed by 35 cycles of 95 °C for 1 min, 54 °C for 1 min, and 72 °C for 2 min. For the 16S rRNA gene, the protocol included an initial denaturation at 95 °C for 5 min, then 35 cycles of 92 °C for 1 min, 57 °C for 1 min, and 72 °C for 30 s. Both reactions concluded with a final extension at 72 °C for 5 min. PCR products of the expected size 212 bp for the 16S rRNA gene and 583 bp for *adk* were verified via 1.5% agarose gel electrophoresis. PCR products were subsequently purified using the Purification Kit (SolGent Co. Ltd., Daejeon, Republic of Korea), according to the manufacturer's instructions. The identity of the isolates was confirmed by direct Sanger sequencing of the purified PCR products.

Co-culturing assays

We selected three CRC-associated bacterial strains, *F. nucleatum* (DSM 15643), enterotoxigenic *B. fragilis* (DSM 2151), and *E. coli* strain D (updated to *E. coli* in GTDB r226), for co-cultivation with *M. smithii* DSM 2375 (=ALI), due to their CRC-relevant virulence[68]. The experimental layout is illustrated in Supplementary Fig. 12.

Standard archaeal medium (MS medium) was prepared under anaerobic conditions as previously described[106]. Briefly, the MS culture medium was prepared per liter of distilled water and consisted of 0.45 g NaCl, 5 g $NaHCO_3$, 0.1 g $MgSO_4{\cdot}7H_2O$, 0.225 g KH_2PO_4, 0.3 g $K_2HPO_4{\cdot}3H_2O$, 0.225 g $(NH_4)_2SO_4$, and 0.060 g $CaCl_2{\cdot}2H_2O$. In addition, 2 ml of a 0.1% (w/v) $(NH_4)_2Ni(SO_4)_2$ solution, 2 ml of a 0.1% (w/v) $FeSO_4{\cdot}7H_2O$ solution prepared in 0.1 M H_2SO_4, and 0.7 ml of a 0.1% (w/v) resazurin solution were included. The basal medium was supplemented with 1 ml each of 10× Wolfe's vitamin solution and 10× Wolfe's mineral solution.

Brain heart infusion (BHI) broth was prepared under anaerobic conditions in anaerobic chamber following standard protocols and flushed with nitrogen (100%). Subsequently, 10 ml of BHI broth and 20 ml of MS medium were combined in 100 ml serum bottles under anaerobic conditions. The medium was deoxygenated with nitrogen gas, supplemented with 0.75 g/l L-cysteine under anaerobic conditions, and adjusted to pH 7.0 if necessary. The 30 ml aliquots were sealed in 100-ml serum bottles with rubber stoppers and aluminum caps, pressurized with H_2/CO_2 (4:1), and sterilized by autoclaving at 121 °C for 20 min. Before use, 0.001 g/ml yeast extract and 0.001 g/ml sodium acetate were added under anaerobic conditions.

Time point designations were standardized relative to the initial inoculation of *M. smithii* ALI: t(−1) corresponds to the time of *M. smithii* ALI inoculation (0 h); t(0) denotes 24 h post−*M. smithii* ALI inoculation, or the point where bacterial mono-cultures in BHI + MS are initiated; t(0 +) denotes the point bacterial strains are introduced to 24 h post−*M. smithii* ALI inoculation (initiation of co-cultures); t(1)

represents 48 h post–*M. smithii* ALI inoculation (24 h post-bacterial inoculation for co-cultures); and t(2) indicates 96 h post–*M. smithii* ALI inoculation (72 h post-bacterial inoculation).

Cultures of *M. smithii* ALI (5 ml) were initiated at t(−1) in BHI + MS medium for further co-culturing with a bacterium, to avoid the overgrowth of bacteria due to higher incubation period for archaea and lower log phase time, with a parallel *M. smithii* ALI mono-culture prepared under identical conditions. The optical densities (OD) of *M. smithii* ALI master cultures in each experiment set used to inoculate in the mono- and co-cultures at t(−1) were: 0.07 ± 0.007 for *F. nucleatum* co-cultures, 0.05 ± 0.008 for *B. fragilis* co-cultures, and 0.47 ± 0.09 for *E. coli* co-cultures. At t(0), 0.2 ml of each bacterial strain pre-cultured overnight in BHI medium (*F. nucleatum* (OD = 0.82 ± 0.05), *B. fragilis* (OD = 0.90 ± 0.04), and *E. coli* (OD = 2.12 ± 0.02)), was separately inoculated into the *M. smithii* ALI culture to establish co-cultures, while bacterial mono-cultures were concurrently initiated in BHI + MS medium.

Optical density measurements were performed on 0.6 ml samples collected from *M. smithii* ALI mono-cultures and co-cultures at t(−1), t(0), t(1), and t(2), and from bacterial mono-cultures at t(0), t(1), and t(2). For metabolomic analyses, 1 ml samples were collected from *M. smithii* ALI mono-cultures, co-cultures, and bacterial mono-cultures at t(0), t(1), and t(2). For DNA extraction and subsequent qPCR analysis, 1 ml samples were collected from *M. smithii* ALI mono-cultures at t(2), from bacterial mono-cultures at t(1) and t(2), and from co-cultures at t(0), t(1), and t(2). At t(2), endpoint analyses were conducted on both co-cultures and *M. smithii* ALI mono-cultures to assess methane production, detect F_{420}-positive cells, and scanning electron microscopy was also conducted at t(2) for *M. smithii* ALI mono-cultures, co-cultures, and bacterial mono-cultures.

Blank BHI and BHI + MS media were incubated in triplicate for contamination monitoring, as well as for metabolomics experiments, while all inoculated cultures were performed in five biological replicates. All cultures were maintained at 37 °C with continuous shaking at 80 rpm throughout the experiments. DNA was extracted from cultures by using the PureLink™ Microbiome DNA Purification Kit (Invitrogen, Thermo Fisher Scientific, USA) according to the manufacturer's protocols. DNA extracts were stored at −80 °C for further analysis. Culture samples for metabolomics were also stored at −80 °C until further analysis.

CH_4 measurement and fluorescence microscopy

To evaluate whether methane (CH_4) production by *M. smithii* ALI was increased during co-cultivation, CH_4 concentrations were measured in the gas phase of the culture bottles with the CH_4 sensor BCP-CH4 (BlueSens gas sensor GmbH, Germany) following the manufacturer's instructions. Measurements were performed for both mono-cultures and co-cultures at the end of the incubation period.

Additionally, the presence and proliferation of *M. smithii* ALI were confirmed through the detection of the characteristic autofluorescence of coenzyme F_{420} with maximum emission wavelength of 480[107]. Fluorescence imaging was performed using a Zeiss Axio Imager A1 microscope (Carl Zeiss AG, Germany) equipped with a fluorescence module. Observations were carried out using Zeiss filter set 05, comprising a BP 395–440 excitation filter, an FT 460 beam splitter, and an LP 470 emission filter, in combination with a 100× Plan-NEOFLUAR objective.

Scanning electron microscopy

The cell morphologies of the mono-cultures and co-cultures were examined using a Zeiss Sigma 500 V7P scanning electron microscope (Carl Zeiss AG, Germany). For sample preparation, 2 ml of culture (including supernatant) were immediately transferred on ice to the Core Facility Ultrastructure Analysis at the Medical University of Graz (Austria) for scanning electron microscopy (SEM), where cell pellets were prepared by centrifugation at 4000 × *g* for 10 min and processed as previously described[69]. Briefly, cells were deposited onto coverslips and chemically preserved in 0.1 M phosphate-buffered saline (pH 7.4) containing 2% paraformaldehyde and 2.5% glutaraldehyde. Samples were dehydrated through a graded ethanol series, followed by post-fixation with 1% osmium tetroxide for 1 h at room temperature, and subsequently subjected to a second ethanol dehydration sequence spanning 30–100% (vol/vol). Final drying was performed using hexamethyldisilazane (HMDS), after which the coverslips were mounted on aluminum stubs with conductive double-sided carbon tape. Imaging was carried out on a Sigma 500 VP field-emission scanning electron microscope (Zeiss, Oberkochen, Germany) equipped with a secondary electron detector, operating at an accelerating voltage of 5 kV.

qPCR

Quantification of the absolute copy numbers of bacterial 16S rRNA and archaeal *mcrA* genes in the samples was conducted using a quantitative real-time PCR (qPCR) method with SYBR Green dye as previously described[9]. Briefly, each qPCR reaction mixture consisted of one microliter of DNA template combined with SYBR Green Supermix (Bio-Rad). The bacterial 16S rRNA genes were amplified using the primer pair 331F (5′-TCCTACGGGAGGCAGCAGT-3′) and 797R (5′-GGACTACCAGGGTATCTAATCCTGTT-3′)[108]. The thermal cycling protocol for bacterial amplification involved an initial denaturation step at 95 °C for 15 s, followed by 40 cycles consisting of denaturation at 94 °C for 15 s, annealing at 54 °C for 30 s, and extension at 73 °C for 40 s. For the detection and quantification of *M. smithii* ALI, primers M1F (5′-GCAATGCAAATTGGTATGTC-3′) and M1R (5′-TCATTGCGTAGTTAGGRTAGT-3′) were used, specifically targeting the *mcrA* gene (single-copy gene). The thermal cycling conditions included an initial denaturation at 94 °C for 3 s, followed by 40 cycles of denaturation at 94 °C for 45 s, annealing at 56 °C for 45 s, and elongation at 72 °C for 30 s.

The quantification cycle (Cq) values were analyzed using the regression method available in Bio-Rad CFX Manager Software (version 3.1). The absolute gene copy numbers for bacterial 16S rRNA and methanogenic *mcrA* genes were determined based on Cq values and corresponding amplification efficiencies derived from standard curves. These standard curves were established according to previously described protocols[9] based on standard curves from defined DNA samples of *E. coli* for bacterial 16S rRNA genes and the *mcrA* gene from the *M. smithii*[109,110].16S rRNA gene copy numbers were normalized using species-specific values from the rrnDB database (*F. nucleatum* = 5 copies, *B. fragilis* = 6 copies, and *E. coli* = 7 copies). The detection thresholds were established using the mean Cq values obtained from non-template control reactions. All qPCR assays were performed in three technical replicates, with each assay replicated across five independent biological replicates of both mono and co-cultures.

Metabolite quantification using nuclear magnetic resonance

In order to gain initial insights into the consumption/production of amino acids, the metabolic activity of *M. smithii* ALI was investigated by nuclear magnetic resonance (NMR) spectroscopy using *M. smithii* ALI cultures previously described in an earlier study[106]. Measurements were performed in triplicate for *M. smithii* ALI at 72, 168, and 240 h post-inoculation in MS medium supplemented with yeast extract, following the experimental protocol outlined in the same reference.

Metabolomic profiling of mono- and co-culture samples (cell + supernatant) collected for this study at different timepoints (Supplementary Fig. 12) was also conducted through NMR spectroscopy. For this purpose, samples were initially treated using protein precipitation by the addition of methanol to give a methanol–water mixture at a 2:1 ratio. After centrifugation, supernatants were collected and subsequently dried by lyophilization. The lyophilized extracts were then

reconstituted in a sodium phosphate-buffered solution supplemented with an internal NMR reference standard, 4.6 mM 3-trimethylsilyl propionic acid-2,2,3,3-d4 sodium salt, before being transferred into NMR sample tubes.

Spectral acquisition was performed using a Bruker Avance Neo 600 MHz spectrometer, equipped with a triple resonance inverse probe, operated at a controlled temperature of 310 K. Data were captured utilizing the Carr–Purcell–Meiboom–Gill pulse sequence over 128 scans, with acquisition and initial processing conducted via Topsin 4.5 software (Bruker GmbH, Rheinstetten, Germany). Post-acquisition data treatment, involving spectral alignment and probabilistic quantile normalization (PQN), was executed using MATLAB software (version 2014b, MathWorks, Natick, MA, USA).

For the precise quantification of metabolites displaying significant enhancement in signal intensities within co-cultured samples compared to mono-culture controls, integration of targeted metabolite peaks from the aligned spectra was conducted following baseline correction utilizing trapezoidal integration methods. Subsequent normalization against the proton number, specific J-coupling characteristics, and the integral of the internal standard allowed for accurate determination of metabolite molar concentrations.

Metabolite determination using mass spectrometry

The blank MS + BHI medium ($n = 3$ replicates), as well as supernatant of the co-culture of *M. smithii* ALI and *F. nucleatum* ($n = 3$ replicates) were measured using the Elute PLUS LC system (Bruker, Bremen, Germany) coupled to a timsTOF Pro 2 mass spectrometer (Bruker, Bremen, Germany) with a vacuum-insulated probe heated electrospray ionization (VIP-HESI) source in both reverse phase (RP) and hydrophilic interaction (HILIC) modes. System suitability of the LC-MS setup was confirmed by use of weekly measurements of the QSee Performance Test setup from Bruker (Bremen, Germany), using a mixture of 8 synthetic compounds.

A pooled QC sample was prepared by combining 100 μL aliquots of each supernatant. The pooled QC was measured intercalating between samples to perform within-batch correction.

RP separations were conducted on an Intensity Solo 2 C18 Column (100 Å; 2.0 μm; 2.1 mm × 100 mm; #BRHSC18022100, Bruker) with 0.1% formic acid (ROTIPURAN® ≥99%, LC-MS Grade, Carl Roth, Karlsruhe, Germany) in MilliQ water as mobile phase A and 0.1% formic acid in 9:1 (v:v) acetonitrile: MQ water (≥99.9%, HiPerSolv CHROMANORM® for LC-MS, VWR, Darmstadt, Germany) as mobile phase B. A 5 μl injection of each sample was used. The separation was carried out at a flow rate of 0.6 ml/min with a column temperature maintained at 50 °C. The following gradient was applied: 0–2 min, 5% B; 2–10 min, 5-40% B; 10–11 min, 40–98% B; 11–13 min, 98% B; 13–13.1 min, 98-5% B; 13.1–15.5 min, 5% B.

HILIC separations were performed on an ACQUITY UPLC BEH Amide column (130 Å, 1.7 μm, 2.1 mm × 150 mm; #186004802, Waters) with 10 mM ammonium formate and 0.1% formic acid in MilliQ water as mobile phase A and 10 mM ammonium formate and 0.1% formic acid in acetonitrile as mobile phase B. Injection volume was set to 5 μl, the flow rate of 0.5 ml/min and the column temperature at 40 °C. The gradient was as follows: 0–1 min, 100% B; 1–6 min, 100–90% B; 6–10 min, 90–75% B; 10–11 min, 75–60% B; 11–12 min, 60% B; 12–12.1 min, 50–100% B; 12.1–21 min, 100% B.

The VIP HESI source was set to default conditions: endplate offset 500 V; capillary 4500 V; nebulizer gas 2.0 bar; dry gas 8.0 l/min; dry temp 230 °C; sheath gas 4.0 l/min; sheath gas temperature 400 °C. The probe head was put at minimum distance to the front-end assembly for maximum intensity. LC-MS/MS data were acquired in both positive and negative DDA-PASEF modes, for a mass range of m/z 20–1300. Default Bruker PASEF acquisition parameters for MS/MS acquisition were used: 2 ramps (12 precursors each) per cycle; resulting cycle time 0.69 s; Intensity threshold 100 counts; target Intensity 4000 counts (signals below that threshold will be scheduled for MS/MS fragmentation more often); active exclusion activated (0.1 min; reconsider if intensity increase is at least 2-fold). Data acquisition was performed using Bruker software timsControl® and Compass HyStar® software. Quality control (QC) samples were run every ten injections in HILIC mode, and every five injections in RP mode, and blank samples were analyzed at the beginning and the end of each batch using H_2O for RP and methanol for HILIC.

Raw data were processed using MetaboScape® (version 2024b, Bruker, RRID:SCR_026044) with four-dimensional (4D) feature extraction, capturing mass-to-charge ratio (m/z), isotopic pattern quality, retention times, MS/MS spectra, and collision cross-section (CCS) values. Feature extraction was performed using the T-ReX® 4D algorithm (RRID:SCR_026044), followed by annotation through the Bruker Human Metabolome Database (HMDB, RRID:SCR_007712) and the NIST Mass Spectral Library (RRID:SCR_014668) as well as additional "target lists" derived from several CCS databases (Pacific Northwest National Laboratory, METLIN, MiMeDB), resulting in Level 2 annotation according to Sumner et al.[111]. Matching was performed using four parameters: m/z (accurate mass, error <5 ppm), mSigma (isotopic pattern, score <100), MS/MS match (score >600) and CCS accuracy (error <3%).

High-quality annotations for final analysis were selected through visual inspection of chromatogram and ion mobilogram peak quality and sufficient annotation scores (match for at least 2 of the 4 parameters). Duplicate annotations were resolved by removing annotations with (1) more missing values, (2) lower overall annotation quality and (3) lower CCS accuracy until only unique annotation remained.

Raw metabolite concentrations of 489 compounds (level 2 annotation) were processed with MetaboAnalyst Version 6 (www.metaboanalyst.ca). Missing values were replaced by LoDs (1/5 of the minimum positive value of each variable). Samples were normalized by PQN to account for different cell counts and dilution effects and log transformed (base 10).

Statistical analysis

All statistical analyses were conducted using R (version 4.3.1) in RStudio (version 2023.06.1 + 524). In datasets where case-control samples were not initially matched for potential confounding variables (age, sex, and BMI), additional control for these factors was applied where feasible. Specifically, case-control samples were matched within each dataset by sex, age (±5 years), and BMI (±3 units) to reduce potential bias (Supplementary Data 1).

Subsequent differential abundance analyses for both bacteria and archaea were carried out following centered log-ratio (CLR) transformation of the dataset, using the Wilcoxon rank-sum test, followed by Benjamini–Hochberg false discovery rate (FDR) correction for multiple testing. Following previously established criteria[112], provided that more than two datasets were available, a taxon was associated with a given disease if it demonstrated a statistically significant association (p-adjusted <0.05) in the same direction across at least two independent studies of the disease. Co-abundance networks of *M. smithii* with CRC-associated bacterial taxa in case samples were inferred using Spearman's rank correlation, and false discovery rate (FDR) correction was applied using the Benjamini–Hochberg method. Taxa were retained for analysis only if they were detected in at least 5% of case samples. Presence-absence matrices of *M. smithii* with CRC-associated bacterial taxa were generated from abundance tables by classifying values > 0 as "present." For each taxon and within each group (control or CRC), 2 × 2 contingency tables between *M. smithii* and the bacterial taxon were analyzed using Fisher's exact test to estimate odds ratios (OR), 95% confidence intervals, and Benjamini–Hochberg-adjusted p-values.

Two-sided Welch's t-test and two-sided Wilcoxon rank-sum test were used to compare co-cultures and mono-cultures across individual NMR metabolomic profiles, qPCR data, and methane measurements

based on the normal distribution of data. For NMR metabolomic data, multiple testing correction was applied using the Benjamini–Hochberg FDR method. Significant changes in metabolites measured with mass spectrometry in the co-culture of *M. smithii* ALI and *F. nucleatum* compared to the blank medium were determined by t-test with a threshold of *p*-adjusted <0.05 and minimum fold change threshold of FC > 1.5.

Reporting summary

Further information on research design is available in the Nature Portfolio Reporting Summary linked to this article.

Data availability

Raw sequencing data for stool samples All sequencing data analyzed in this study were obtained from previously published datasets and are publicly available from the European Nucleotide Archive (ENA) and the NCBI BioProject/SRA databases under the following accession numbers: PRJDB4176, PRJEB6070, PRJEB7774, PRJEB10878, PRJNA389927, PRJEB12449, PRJEB27928, PRJNA447983, PRJNA531273 and PRJNA397112, PRJNA400072, SRA045646 and SRA050230 [https://www.ncbi.nlm.nih.gov/sra/SRA050230], PRJEB32762, PRJEB47976, PRJNA798058, PRJEB29127, PRJNA834801, PRJNA743718, PRJEB53401, and PRJEB17784. The NMR raw data generated in this study are available in Zenodo at https://doi.org/10.5281/zenodo.16311518. The LC-MS raw data generated in this study are available in Zenodo at https://doi.org/10.5281/zenodo.16367666. All additional data generated and analyzed in this study, including Kraken2/Bracken outputs, gapseq outputs (including genome-scale metabolic models, gap-filled models, reaction and gene annotations, as well as pathway and transporter predictions), PyCoMo outputs (including flux variability analyses, metabolite secretion and uptake predictions, and community) are publicly available in our GitHub repository (https://github.com/CMElab-research/archaeome-disease-profiling/). Source data are provided with this paper.

References

1. Lecours, P. B. et al. Increased prevalence of *Methanosphaera stadtmanae* in inflammatory bowel diseases. *PLoS ONE* **9**, e87734 (2014).
2. Romano, S. et al. Meta-analysis of the Parkinson's disease gut microbiome suggests alterations linked to intestinal inflammation. *NPJ Parkinson's Dis.* **7**, 27 (2021).
3. Fumagalli, A. et al. Archaea methanogens are associated with cognitive performance through the shaping of gut microbiota, butyrate and histidine metabolism. *Gut Microbes* **17**, 2455506 (2025).
4. Jangi, S. et al. Alterations of the human gut microbiome in multiple sclerosis. *Nat. Commun.* **7**, 12015 (2016).
5. Scanlan, P. D., Shanahan, F. & Marchesi, J. R. Human methanogen diversity and incidence in healthy and diseased colonic groups using mcrA gene analysis. *BMC Microbiol.* **8**, 79 (2008).
6. Helen, T. et al. Gut microbiota composition and relapse risk in pediatric MS: a pilot study. *J. Neurol. Sci.* **363**, 153–157 (2016).
7. Bhute, S.S. et al. Gut microbial diversity assessment of indian type-2-diabetics reveals alterations in eubacteria, archaea, and eukaryotes. *Front. Microbiol.* **8**, 214 (2017).
8. Jia, L. et al. Metagenomic analysis characterizes stage-specific gut microbiota in Alzheimer's disease. *Mol. Psychiatry* **30**, 3951–3962 (2025).
9. Kumpitsch, C. et al. Reduced B12 uptake and increased gastrointestinal formate are associated with archaeome-mediated breath methane emission in humans. *Microbiome* **9**, 193 (2021).
10. Borrel, G., Brugère, J.-F., Gribaldo, S., Schmitz, R. A. & Moissl-Eichinger, C. The host-associated archaeome. *Nat. Rev. Microbiol.* **18**, 622–636 (2020).
11. Balch, W. E., Fox, G. E., Magrum, L. J., Woese, C. R. & Wolfe, R. S. Methanogens: reevaluation of a unique biological group. *Microbiol. Rev.* **43**, 260–296 (1979).
12. Nkamga, V. D., Henrissat, B. & Drancourt, M. Archaea: essential inhabitants of the human digestive microbiota. *Hum. Microbiome J.* **3**, 1–8 (2017).
13. Hoegenauer, C., Hammer, H. F., Mahnert, A. & Moissl-Eichinger, C. Methanogenic archaea in the human gastrointestinal tract. *Nat. Rev. Gastroenterol. Hepatol.* **19**, 805–813 (2022).
14. Ruaud, A. et al. Syntrophy via interspecies H2 transfer between *Christensenella* and *Methanobrevibacter* underlies their global cooccurrence in the human gut. *mBio* **11**, 10–1128 (2020).
15. Baradaran Ghavami, S. et al. Alterations of the human gut *Methanobrevibacter smithii* as a biomarker for inflammatory bowel diseases. *Microb. Pathog.* **117**, 285–289 (2018).
16. Schwiertz, A. et al. Microbiota and SCFA in lean and overweight healthy subjects. *Obesity* **18**, 190–195 (2010).
17. Pimentel, M. et al. Methane production during lactulose breath test is associated with gastrointestinal disease presentation. *Dig. Dis. Sci.* **48**, 86–92 (2003).
18. Laura, H. et al. Evaluating breath methane as a diagnostic test for constipation-predominant IBS. *Dig. Dis. Sci.* **55**, 398–403 (2010).
19. Ghoshal, U., Shukla, R., Srivastava, D. & Ghoshal, C. U. Irritable bowel syndrome, particularly the constipation-predominant form, involves an increase in *Methanobrevibacter smithii*, which is associated with higher methane production. *Gut Liver* **10**, 932–938 (2016).
20. Takakura, W. et al. A single fasting exhaled methane level correlates with fecal methanogen load, clinical symptoms and accurately detects intestinal methanogen overgrowth. *Am. J. Gastroenterol.* **117**, 470–477 (2022).
21. Madigan, K. E., Bundy, R. & Weinberg, R. B. Distinctive clinical correlates of small intestinal bacterial overgrowth with methanogens. *Clin. Gastroenterol. Hepatol.* **20**, 1598–1605 (2022).
22. Li, T. et al. Multi-cohort analysis reveals altered archaea in colorectal cancer fecal samples across populations. *Gastroenterology* **168**, 525–538 (2025).
23. Sun, Y., Liu, Y., Pan, J., Wang, F. & Li, M. Perspectives on cultivation strategies of archaea. *Microb. Ecol.* **79**, 770–784 (2020).
24. Mahnert, A., Blohs, M., Pausan, M.-R. & Moissl-Eichinger, C. The human archaeome: methodological pitfalls and knowledge gaps. *Emerg. Top. Life Sci.* **2**, 469–482 (2018).
25. Zhou, X. et al. Gut microbiome of multiple sclerosis patients and paired household healthy controls reveal associations with disease risk and course. *Cell* **185**, 3467–3486 (2022).
26. Woh, P. Y. et al. Reevaluation of the gastrointestinal methanogenic archaeome in multiple sclerosis and its association with treatment. *Microbiol. Spectr.* **13**, e02183-24 (2025).
27. Franzosa, E. A. et al. Gut microbiome structure and metabolic activity in inflammatory bowel disease. *Nat. Microbiol.* **4**, 293–305 (2018).
28. Wallen, Z. D. et al. Metagenomics of Parkinson's disease implicates the gut microbiome in multiple disease mechanisms. *Nat. Commun.* **13**, 6958 (2022).
29. de la Cuesta-Zuluaga, J. et al. Age- and sex-dependent patterns of gut microbial diversity in human adults. *mSystems* **4**, 10–1128 (2019).
30. Kuehnast, T. et al. Exploring the human archaeome: its relevance for health and disease, and its complex interplay with the human immune system. *FEBS J.* **292**, 1316–1329 (2025).
31. Mohammadzadeh, R. et al. Age-related dynamics of predominant methanogenic archaea in the human gut microbiome. *BMC Microbiol.* **25**, 193 (2025).
32. Jo, S. et al. Oral and gut dysbiosis leads to functional alterations in Parkinson's disease. *NPJ Parkinson's Dis.* **8**, 87 (2022).

33. Yu, J. et al. Metagenomic analysis of faecal microbiome as a tool towards targeted non-invasive biomarkers for colorectal cancer. *Gut* **66**, 70–78 (2017).
34. Feng, Q. et al. Gut microbiome development along the colorectal adenoma–carcinoma sequence. *Nat. Commun.* **6**, 6528 (2015).
35. Boktor, J. C. et al. Integrated multi-cohort analysis of the Parkinson's disease gut metagenome. *Mov. Disord.* **38**, 399–409 (2023).
36. Bedarf, J. R. et al. Functional implications of microbial and viral gut metagenome changes in early stage L-DOPA-naïve Parkinson's disease patients. *Genome Med.* **9**, 39 (2017).
37. Thomas, A. M. et al. Metagenomic analysis of colorectal cancer datasets identifies cross-cohort microbial diagnostic signatures and a link with choline degradation. *Nat. Med.* **25**, 667–678 (2019).
38. Gupta, A. et al. Association of *Flavonifractor plautii*, a flavonoid-degrading bacterium, with the gut microbiome of colorectal cancer patients in India. *mSystems* **4**, 10–1128 (2019).
39. Laske, C. et al. Signature of Alzheimer's disease in intestinal microbiome: results from the AlzBiom study. *Front. Neurosci.* **16**, 792996 (2022).
40. Ferreiro, A.L. et al. Gut microbiome composition may be an indicator of preclinical Alzheimer's disease. *Sci. Transl. Med.* **15**, eabo2984 (2023).
41. Zeller, G. et al. Potential of fecal microbiota for early-stage detection of colorectal cancer. *Mol. Syst. Biol.* **10**, 766 (2014).
42. Wirbel, J. et al. Meta-analysis of fecal metagenomes reveals global microbial signatures that are specific for colorectal cancer. *Nat. Med.* **25**, 679–689 (2019).
43. Misiak, B. et al. Associations of gut microbiota alterations with clinical, metabolic, and immune-inflammatory characteristics of chronic schizophrenia. *J. Psychiatr. Res.* **171**, 152–160 (2024).
44. Villette, R. et al. Integrated multi-omics highlights alterations of gut microbiome functions in prodromal and idiopathic Parkinson's disease. *Microbiome* **13**, 200 (2025).
45. Yachida, S. et al. Metagenomic and metabolomic analyses reveal distinct stage-specific phenotypes of the gut microbiota in colorectal cancer. *Nat. Med.* **25**, 968–976 (2019).
46. Vogtmann, E. et al. Colorectal cancer and the human gut microbiome: reproducibility with whole-genome shotgun sequencing. *PLOS ONE* **11**, e0155362 (2016).
47. Mira-Pascual, L. et al. Microbial mucosal colonic shifts associated with the development of colorectal cancer reveal the presence of different bacterial and archaeal biomarkers. *J. Gastroenterol.* **50**, 167–179 (2015).
48. Piccinno, G. et al. Pooled analysis of 3,741 stool metagenomes from 18 cohorts for cross-stage and strain-level reproducible microbial biomarkers of colorectal cancer. *Nat. Med.* **31**, 1–14 (2025).
49. Abdi, H., Kordi-Tamandani, D. M., Lagzian, M. & Bakhshipour, A. Archaeome in colorectal cancer: high abundance of methanogenic archaea in colorectal cancer patients. *Int. J. Cancer Manag.* **15**, e117843 (2022).
50. Predl, M., Mießkes, M., Rattei, T. & Zanghellini, J. PyCoMo: a Python package for community metabolic model creation and analysis. *Bioinformatics* **40**, btae153 (2024).
51. Maier, L. et al. Microbiota-derived hydrogen fuels *Salmonella typhimurium* invasion of the gut ecosystem. *Cell Host Microbe* **14**, 641–651 (2013).
52. Spinelli, J. B. et al. Fumarate is a terminal electron acceptor in the mammalian electron transport chain. *Science* **374**, 1227–1237 (2021).
53. King, A., Selak, M. A. & Gottlieb, E. Succinate dehydrogenase and fumarate hydratase: linking mitochondrial dysfunction and cancer. *Oncogene* **25**, 4675–4682 (2006).
54. Samuel, S. B. et al. Genomic and metabolic adaptations of *Methanobrevibacter smithii* to the human gut. *Proc. Natl. Acad. Sci. USA* **104**, 10643–10648 (2007).
55. Jiang, S.-S. et al. Fusobacterium nucleatum-derived succinic acid induces tumor resistance to immunotherapy in colorectal cancer. *Cell Host Microbe* **31**, 781–797 (2023).
56. Isar, J., Agarwal, L., Saran, S. & Saxena, R. K. Succinic acid production from *Bacteroides fragilis*: process optimization and scale up in a bioreactor. *Anaerobe* **12**, 231–237 (2006).
57. Yu, J. et al. Effect and potential mechanism of oncometabolite succinate promotes distant metastasis of colorectal cancer by activating STAT3. *BMC Gastroenterol.* **24**, 106 (2024).
58. Zhang, W. & Lang, R. Succinate metabolism: a promising therapeutic target for inflammation, ischemia/reperfusion injury and cancer. *Front. Cell Dev. Biol.* **11**, 1266973 (2023).
59. Takemoto, N., Tanaka, Y., Inui, M. & Yukawa, H. The physiological role of riboflavin transporter and involvement of FMN-riboswitch in its gene expression in *Corynebacterium glutamicum*. *Appl. Microbiol. Biotechnol.* **98**, 4159–4168 (2014).
60. Wang, H. et al. ^{1}H NMR-based metabolic profiling of human rectal cancer tissue. *Mol. Cancer* **12**, 121 (2013).
61. Shen, X. et al. Asparagine, colorectal cancer, and the role of sex, genes, microbes, and diet: a narrative review. *Front. Mol. Biosci.* **9**, 958666 (2022).
62. Mao, Z. et al. Prediagnostic serum glyceraldehyde-derived advanced glycation end products and mortality among colorectal cancer patients. *Int. J. Cancer* **152**, 2257–2268 (2023).
63. Liu, Y., Lau, H.C.-H. & Yu, J. Microbial metabolites in colorectal tumorigenesis and cancer therapy. *Gut Microbes* **15**, 2203968 (2023).
64. Avuthu, N. & Guda, C. Meta-analysis of altered gut microbiota reveals microbial and metabolic biomarkers for colorectal cancer. *Microbiol. Spectr.* **10**, e00013–e00022 (2022).
65. Xie, Z. et al. Metabolomic analysis of gut metabolites in patients with colorectal cancer: association with disease development and outcome. *Oncol. Lett.* **26**, 358 (2023).
66. Gao, R. et al. Integrated analysis of colorectal cancer reveals cross-cohort gut microbial signatures and associated serum metabolites. *Gastroenterology* **163**, 1024–1037 (2022).
67. Xu, S. et al. Intestinal microbiota affects the progression of colorectal cancer by participating in the host intestinal arginine catabolism. *Cell Rep.* **44**, 115370 (2025).
68. Slater, L. C., Fonseca-Pereira, D. & Garrett, W. S. Colorectal cancer: the facts in the case of the microbiota. *J. Clin. Investig.* **132**, e155101 (2022).
69. Duller et al. Targeted isolation of *Methanobrevibacter* strains from fecal samples expands the cultivated human archaeome. *Nat. Commun.* **15**, 7593 (2024).
70. Feng, T. et al. The arginine metabolism and its deprivation in cancer therapy. *Cancer Lett.* **620**, 217680 (2025).
71. Wu, G., Meininger, C.J., McNeal, C.J., Bazer, F.W. & Rhoads, J.M. Role of L-arginine in nitric oxide synthesis and health in humans 167–187 (Springer, 2021).
72. Lamaudière, M. T. F., Arasaradnam, R., Weedall, G. D. & Morozov, I. Y. The colorectal cancer microbiota alter their transcriptome to adapt to the acidity, reactive oxygen species, and metabolite availability of gut microenvironments. *mSphere* **8**, e00627-22 (2023).
73. Naes, S., Ab-Rahim, S., Mazlan, M., Hashim, N. A. A. & Abdul Rahman, A. Increased ENT2 expression and its association with altered purine metabolism in cell lines derived from different stages of colorectal cancer. *Exp. Ther. Med.* **25**, 212 (2023).
74. Grondin, J. A. & Khan, W. I. Emerging roles of gut serotonin in regulation of immune response, microbiota composition and intestinal inflammation. *J. Can. Assoc. Gastroenterol.* **7**, 88–96 (2024).

75. Venkateswaran, N. et al. Tryptophan fuels MYC-dependent liver tumorigenesis through indole 3-pyruvate synthesis. *Nat. Commun.* **15**, 4266 (2024).
76. Xiaojing, L., Binbin, Z., Yiyang, H. & Yu, Z. New insights into gut-bacteria-derived indole and its derivatives in intestinal and liver diseases. *Front. Pharmacol.* **12**, 769501 (2021).
77. Li, Q. et al. Gut barrier dysfunction and bacterial lipopolysaccharides in colorectal cancer. *J. Gastrointest. Surg.* **27**, 1466–1472 (2023).
78. Chen, Y. et al. γ-linolenic acid derived from *Lactobacillus plantarum* MM89 induces ferroptosis in colorectal cancer. *Food Funct.* **16**, 1760–1771 (2025).
79. Fyrst, H. et al. Natural sphingadienes inhibit Akt-dependent signaling and prevent intestinal tumorigenesis. *Cancer Res.* **69**, 9457–9464 (2009).
80. Niehaus, E.-M. et al. Apicidin F: characterization and genetic manipulation of a new secondary metabolite gene cluster in the rice pathogen *Fusarium fujikuroi*. *PLoS ONE* **9**, e103336 (2014).
81. Ueda, T., Takai, N., Nishida, M., Nasu, K. & Narahara, H. Apicidin, a novel histone deacetylase inhibitor, has profound anti-growth activity in human endometrial and ovarian cancer cells. *Int. J. Mol. Med.* **19**, 301–308 (2007).
82. Mueller, A.-L. et al. Bacteria-mediated modulatory strategies for colorectal cancer treatment. *Biomedicines* **10**, 832 (2022).
83. Song, S., Vuai, M. S. & Zhong, M. The role of bacteria in cancer therapy–enemies in the past, but allies at present. *Infect. Agents Cancer* **13**, 9 (2018).
84. Candeliere, F., Sola, L., Raimondi, S., Rossi, M. & Amaretti, A. Good and bad dispositions between archaea and bacteria in the human gut: new insights from metagenomic survey and co-occurrence analysis. *Synth. Syst. Biotechnol.* **9**, 88–98 (2024).
85. Mohammadzadeh, R., Mahnert, A., Duller, S. & Moissl-Eichinger, C. Archaeal key-residents within the human microbiome: characteristics, interactions and involvement in health and disease. *Curr. Opin. Microbiol.* **67**, 102146 (2022).
86. Pimentel, M. et al. Methane, a gas produced by enteric bacteria, slows intestinal transit and augments small intestinal contractile activity. *Am. J. Physiol. Gastrointest. Liver Physiol.* **290**, G1089–G1095 (2006).
87. Staller, K. et al. Chronic constipation as a risk factor for colorectal cancer: results from a nationwide, case-control study. *Clin. Gastroenterol. Hepatol.* **20**, 1867–1876 (2022).
88. Tito, R. Y. & Raes, J. Gut archaeal biomarkers in colorectal cancer prediction: a tale of opportunity and prudence. *Gastroenterology* **168**, 457–458 (2025).
89. Sieber, J. R., McInerney, M. J. & Gunsalus, R. P. Genomic insights into syntrophy: the paradigm for anaerobic metabolic cooperation. *Annu. Rev. Microbiol* **66**, 429–452 (2012).
90. Campbell, A., Gdanetz, K., Schmidt, A.W. & Schmidt, T.M. H2 generated by fermentation in the human gut microbiome influences metabolism and competitive fitness of gut butyrate producers. *Microbiome* **11**, 133 (2023).
91. Coker, O. O., Wu, W. K. K., Wong, S. H., Sung, J. J. Y. & Yu, J. Altered gut archaea composition and interaction with bacteria are associated with colorectal cancer. *Gastroenterology* **159**, 1459–1470 (2020).
92. Cai, M., Kandalai, S., Tang, X. & Zheng, Q. Contributions of human-associated archaeal metabolites to tumor microenvironment and carcinogenesis. *Microbiol. Spectr.* **10**, e02367-21 (2022).
93. Zengin, Ö.D. & Aydin, S. The hidden influence of methanogens in the gut microbiota. in *Methanogens-Unique Prokaryotes* (IntechOpen, 2025).
94. Hannigan, G.D., Duhaime, M.B., Ruffin, M.T., Koumpouras, C.C. & Schloss, P.D. Diagnostic potential and interactive dynamics of the colorectal cancer virome. *mBio* **9**, 10–1128 (2018).
95. Ye, H. S., Siddle, J. K., Park, J. D. & Sabeti, C. P. Benchmarking metagenomics tools for taxonomic classification. *Cell* **178**, 779–794 (2019).
96. Wood, D. E. & Salzberg, S. L. Kraken: ultrafast metagenomic sequence classification using exact alignments. *Genome Biol.* **15**, R46 (2014).
97. Chibani, C. M. et al. A catalogue of 1,167 genomes from the human gut archaeome. *Nat. Microbiol.* **7**, 48–61 (2021).
98. Almeida, A. et al. A unified catalog of 204,938 reference genomes from the human gut microbiome. *Nat. Biotechnol.* **39**, 105–114 (2021).
99. Ma, S.Y. et al. Population structure discovery in meta-analyzed microbial communities and inflammatory bowel disease using MMUPHin. *Genome Biology* **23**, 208 (2022).
100. Zimmermann, J., Kaleta, C. & Waschina, S. gapseq: informed prediction of bacterial metabolic pathways and reconstruction of accurate metabolic models. *Genome Biol.* **22**, 81 (2021).
101. De Bernardini, N. et al. pan-Draft: automated reconstruction of species-representative metabolic models from multiple genomes. *Genome Biol.* **25**, 280 (2024).
102. Predl, M., Gandolf, K., Hofer, M. & Rattei, T. ScyNet: visualizing interactions in community metabolic models. *Bioinform. Adv.* **4**, vbae104 (2024).
103. Shannon, P. et al. Cytoscape: a software environment for integrated models of biomolecular interaction networks. *Genome Res.* **13**, 2498–2504 (2003).
104. Lindsey, R. L., Garcia-Toledo, L., Fasulo, D., Gladney, L. M. & Strockbine, N. Multiplex polymerase chain reaction for identification of *Escherichia coli*, *Escherichia albertii* and *Escherichia fergusonii*. *J. Microbiol. Methods* **140**, 1–4 (2017).
105. Dahal, R. H., Choi, Y.-J., Kim, S. & Kim, J. Differentiation of *Escherichia fergusonii* and *Escherichia coli* isolated from patients with inflammatory bowel disease/ischemic colitis and their antimicrobial susceptibility patterns. *Antibiotics* **12**, 154 (2023).
106. Weinberger, V. et al. Expanding the cultivable human archaeome: *Methanobrevibacter intestini* sp. nov. and strain *Methanobrevibacter smithii* 'GRAZ-2' from human faeces. *Int. J. Syst. Evol. Microbiol.* **75**, 006751 (2025).
107. Ney, B. et al. The methanogenic redox cofactor F420 is widely synthesized by aerobic soil bacteria. *ISME J.* **11**, 125–137 (2017).
108. Nadkarni, M. A., Martin, F. E., Jacques, N. A. & Hunter, N. Determination of bacterial load by real-time PCR using a broad-range (universal) probe and primers set. *Microbiology* **148**, 257–266 (2002).
109. Probst, A. J., Auerbach, A. K. & Moissl-Eichinger, C. Archaea on human skin. *PLoS ONE* **8**, e65388 (2013).
110. Hales, B. A. et al. Isolation and identification of methanogen-specific DNA from blanket bog peat by PCR amplification and sequence analysis. *Appl. Environ. Microbiol.* **62**, 668–675 (1996).
111. Lloyd, W. S. et al. Proposed minimum reporting standards for chemical analysis. *Metabolomics* **3**, 211–221 (2007).
112. Duvallet, C., Gibbons, S. M., Gurry, T., Irizarry, R. A. & Alm, E. J. Meta-analysis of gut microbiome studies identifies disease-specific and shared responses. *Nat. Commun.* **8**, 1784 (2017).
113. Wickham, H. ggplot2: Elegant graphics for data analysis. https://ggplot2.tidyverse.org (Springer-Verlag New York, 2016).
114. Shuangbin, X. et al. Use ggbreak to effectively utilize plotting space to deal with large datasets and outliers. *Front. Genet.* **12**, 774846 (2021).

Acknowledgements

This research was funded in whole or in part by the Austrian Science Fund (FWF) [10.55776/P32697 (given to C.M.E.), excellence cluster "Microbiomes Drive Planetary Health" 10.55776/CoE7 (C.M.E., C.D., and G.G), and SFB ImmunoMetabolism 10.55776/F8300 (C.M.E.)]. C.M.E. has

received funding from the European Research Council (ERC) under the Horizon Europe research and innovation programme (Project ID 101199346, ERC-2024-ADG). T.M. is grateful to the Austrian Science Fund (FWF) for excellence cluster 10.55776/COE14, grants DOI 10.55776/P28854, 10.55776/I3792, 10.55776/DOC130, and 10.55776/W1226, the Austrian Research Promotion Agency (FFG) grants 864690 and 870454; the Integrative Metabolism Research Center Graz; the Austrian Infrastructure Program 2016/2017; the Styrian Government (Zukunftsfonds, doc.fund program); the City of Graz; and BioTechMed-Graz (flagship project). This project was funded in part by the FFG and the European Union (EFRE) under grant 912192. T.M. and H.H. acknowledge the Center for Medical Research for laboratory access. C.T. reports a research grant by Bruker Switzerland AG. For open access purposes, the author has applied a CC BY public copyright license to any author-accepted manuscript version arising from this submission. We gratefully acknowledge the computational resources provided by the MedBioNode at the Medical University of Graz, funded by the Austrian Federal Ministry of Education, Science, and Research through the Hochschulrat-Struktur Mittel 2016 grant within BioTechMed Graz. We also thank the ZMF Core Facility Computational Bioanalytics team at the Medical University of Graz for their support. We thank Claire Lamb for assistance with the provision of the *Bacteroides fragilis* strain. We thank Charlotte Neumann for her help in creating some illustrations for this study. R.M. was supported by the local PhD program MolMed.

Author contributions

R.M. designed the study, collected data, performed bioinformatics, data analysis, plotting, and drafted the manuscript. A.M. co-designed the study. T.Z. and L.W. performed sample cultivation. C.K. performed qPCR. K.F. assisted with plot preparation. P.M. performed *E. coli* isolation and confirmation. H.H. and T.M. performed NMR metabolomics. J.S. and C.T. performed MS metabolomics. D.P., K.H., and D.K. performed SEM. M.D performed the machine learning analysis. C.D. helped with data analysis. G.G. and A.L. assisted with sample preparation. G.G., C.T., C.D., and A.L. commented on and revised the manuscript. C.M-E. designed and supervised the study, and drafted and revised the manuscript. All authors reviewed and approved the final manuscript.

Competing interests

The authors declare no competing interests.

Additional information

Supplementary information The online version contains Supplementary material available at https://doi.org/10.1038/s41467-026-69711-7.

Correspondence and requests for materials should be addressed to Christine Moissl-Eichinger.

Peer review information *Nature Communications* thanks Sabina La Rosa and the other anonymous reviewers for their contribution to the peer review of this work. A peer review file is available.

Reprints and permissions information is available at http://www.nature.com/reprints

Publisher's note Springer Nature remains neutral with regard to jurisdictional claims in published maps and institutional affiliations.

Open Access This article is licensed under a Creative Commons Attribution 4.0 International License, which permits use, sharing, adaptation, distribution and reproduction in any medium or format, as long as you give appropriate credit to the original author(s) and the source, provide a link to the Creative Commons licence, and indicate if changes were made. The images or other third party material in this article are included in the article's Creative Commons licence, unless indicated otherwise in a credit line to the material. If material is not included in the article's Creative Commons licence and your intended use is not permitted by statutory regulation or exceeds the permitted use, you will need to obtain permission directly from the copyright holder. To view a copy of this licence, visit http://creativecommons.org/licenses/by/4.0/.

© The Author(s) 2026